PHD PROGRAM IN BIOROBOTICS

A MOLECULAR APPROACH TO BIOINSPIRATION: elucidating sensorial capabilities of octopus to drive robot design

TUTORS:

Andrea Degl'Innocenti, Ph.D.

Barbara Mazzolai, Ph.D.

SUPERVISOR:

Cecilia Laschi, Prof.

CANDIDATE:

Gabriella Meloni

Academic Year

2018/2019

INDEX

Collaboration statement

The biological work presented on this Ph.D. thesis has been developed in collaboration with Prof. Massimiliano Andreazzoli from "Unit of Cell and Developmental Biology" of the University of Pisa.

I would like to thank Prof. Andreazzoli who provided me the opportunity to join his team, and who gave access to the laboratory and research facilities. I would like to thank for his availability, his valid comments, but also for his technical and helpful questions which aided me to find solutions on my research.

My sincere thank also goes to Dr. Davide Martini, for the technical support, his encouragements and for our conversations that made long, hard-working days enjoyable in the laboratory.

UNIVERSITÀ DI PISA

Abbreviation list

1.	Ab	antibody
2.	bp	base pair
3.	CDS	coding-sequences
4.	CPG	central pattern generator
5.	DOF	degrees of freedom
6.	FIHC	fluorescent immunohistochemistry
7.	Gb	gigabase
8.	GDP	guanosine-5'-diphosphate
9.	GPCR	G-protein coupled receptor
10.	GTP	guanosine-5'-triphosphate
11.	IHC	immunohistochemistry
12.	ISH	*in situ* hybridization
13.	Mfp	mussel foot protein
14.	mfp-1	mussel foot protein-1
15.	MGR	metabotropic glutamate receptor
16.	MMP	matrix metalloproteinase-19
17.	NA	not available
18.	PBS	phosphate-buffered saline
19.	PCR	polymerase chain reaction
20.	PDMS	polydimethylsiloxane
21.	RACE	rapid amplification of cDNA ends
22.	RT	room temperature
23.	RT-PCR	reverse transcription polymerase chain reaction
24.	TAAR	trace ammine-associated receptor

Chapter 1: Outline of the thesis

1.1 Bioinspired robotics

As the Cambridge dictionary says, a robot is a machine controlled by a computer that is used to perform jobs automatically. In the past, it was easy to imagine something able to perform complex tasks independently as a human-like being, because we often regard humans as the highest expression of independent behavior. This assumption can be correct only considering specific capabilities of humans, like the ability to perform calculations or to walk on a street, but we cannot say that a person can walk on vertical surfaces, as instead the gecko does. In fact, locomotion is one of the critical points for the rise of biologically-inspired robotics, commonly called *bioinspired robotics*. In a sense, we can likewise say that humanoids are bioinspired robots as models of bipedal locomotion. Since the research on bipedal humanoid robots started, enormous progress has been made; for example, the iCub is a humanoid platform that shows optimized walking gait using a sophisticated whole-body control of motion (Tsagarakis et al. 2007). Nowadays, humanoids display optimization far beyond locomotion. iCub can grasp different objects with dexterity, even with learning capabilities. Bioinspiration in this sense becomes more than biological inspiration for locomotion. Rather, we can say that in general robotics is looking into natural behaviors, not only in terms of locomotion but also of perception and cognition. If we look only at robotic locomotion capabilities, we will have various categories (Fukuda, Chen, and Qing Shi 2018):

1. biped robots

2. quadruped robots
3. multi-legged robots
4. wheeled robots

As humans are the model for biped robots, it is easy to understand that tetrapods inspire quadruped robots; more specifically, the bioinspiration for this design comes from central pattern generators (CPGs). CPGs are neural circuits that produce rhythmic output while receiving only simple input signals, basically transforming a low-dimension input signal in a high-dimensional rhythmic signal output (Ijspeert 2008). This mechanism has been studied in the tetrapod *Salamadra salamadra*, demonstrating that a CPG model is fundamental for the modulation of velocity and the decision of the direction, and also that the limb oscillatory movements are indispensable to modulate velocity and coordinate movements of the entire body (Ijspeert et al. 2007; Ijspeert, Crespi, and Cabelguen 2005). The multi-legged robots are simply robots with more than four legs; this design aims to achieve increased stability with the ground. The behavior of a jumping spider inspires one example of this design; the robot has a kind of mechanical legs with four degrees of freedom. This spider-inspired robot can maintain stability while jumping and achieve an omnidirectional jump if remote control of the avoidance of obstacles is present (Zhu et al. 2018). The wheeled robots are not inspired by the morphology of animals, in fact in nature the wheel is basically used as a passive structure to carry objects, like in the case of *Geotrupes stercorarius*, the dung beetle that is also known as “roller”, or the pangolin *Manis temminckii*, in which the wheel is just a protective and defensive conformation, but without rolling. Even if it is not directly inspired by rotator locomotion present in nature, curiously wheeled robots found their bioinspiration from a biological process

called *germinal center reaction*, which is a site of lymph node where B-lymphocytes proliferate and develop. The control strategy of such omnidirectional wheeled robot uses a *germinal center optimization algorithm*, that hybridizes two modeling approaches (evolutionary computing and artificial immune systems) inspired by the model of the germinal center reaction of the immune system (Villaseñor et al. 2018).

In the case of quadruped robots or wheeled robots, bioinspiration was not necessarily connected with morphology, but with other mechanisms commonly present in nature. Bioinspiration does not mean just imitating the shape of biological beings, but it means to extract and to abstract particular principles occurring in nature and use them in robotics, not only to develop new solutions but even clarifying some aspects that might be unclear from a biological point of view. Just thinking of locomotion in robots we found four categories, but if we think on what nature can offer in terms of locomotion, we know that animals, or even plants, can walk and swim in different ways, jump, slide, climb, glide, crawl, or even fly. Behaviors in nature are plentiful, and many are the opportunities to be inspired from biology. One of the key points of a natural being is adaptation, *i.e.* the ability to adapt to an unknown environment and to select a winning strategy. In robotics, it is difficult to implement the concept of adaptation, but we can in some way predict the environment in which the robot will act, to decide which strategy to adopt. Modern technology enables robots to operate in different environments, even unstructured. Robotics is changing a lot in recent years because applications that were not contemplated at the beginning, now are becoming part of daily life, like the vacuum automatic cleaner which does not need to see where it is acting. Using a bioinspired approach allows the diversification of the already-known convectional strategy and study sensory-motor

coordination, that already is become commonly used, or to achieve stability, adaptation, and flexibility in manipulation and control.

1.2 Soft robotics

Traditional robots are mostly rigid, so that movements and locomotion are possible thanks to stiff joints that allow them to display a defined number of degrees of freedom (DOF). The more joints a hard robot has, the more flexible it is. However, the DOF reachable are limited, and if the number of these joints is too large, the control of the robots becomes difficult and hyper-redundant. Hence, engineers directed their attention to the problem of the limitation of the number of degrees of freedom, and instead of increasing the joints they started to change materials implemented in the design, eventually developing a new area of robotics: the soft robotics (Kim, Laschi, and Trimmer 2013). One of the problems of soft robotics is the control of these robots, because they have a continuum array of positions; oppositely, traditional and hard robots do not have this problem, and they can accomplish tasks within predefined spatiotemporal constrains. However, robots used for biomedical applications do not need only precision, but they also need to interact with biological tissues without damaging them. Moreover, in an unstructured environment it is useful to have a robot that can provide high dexterity as soft robotics can offer (Trivedi et al. 2008).

To solve the problem of control in soft robotics, robotics engineers look into natural strategies of soft-bodied animals such as worms, snakes, mollusks, and insect larvae. The mechanisms used in nature to vary stiffness, or to accomplish precise tasks when rigidity

is needed, can be classified in two different categories, and both examples can be found in invertebrates: animals with a rigid exoskeleton and animals that have hydrostatic muscles.

Animals usually have an exoskeleton to stabilize an otherwise soft body, protect it against predators or to accomplish complex tasks as in the case of lobster, the claws of which are optimized to cut (Boßelmann et al. 2007; Hadley 1986). A biomimetic robot lobster inspired is already present in nature, called *RoboLobster*, but this robot aims to investigate chemotaxis algorithms and understand the chemo-orientation strategy in the fluid environment of the animal (Grasso et al. 2000).

Hydrostatic muscles occur in invertebrates (but even in vertebrates), and is how they compensate for the lack of a skeleton, providing a dynamic mechanism to harden the body when needed. Invertebrates can also have a different mechanism, called hydrostatic skeletons. Usually, hydrostatic skeletons are cylindrical cavities, filled with a fluid (typically water), surrounded by a muscular wall reinforced with connective tissue (Chapman 1958; Kier 1992). Hydrostatic muscles are composed of muscle tissue mainly made of water. The main difference between these two structures is the presence of a cavity filled with water, in the case of hydrostatic skeletons, and in hydrostatic muscles, there is no cavity, but they rely on the same principle of the incompressibility of the water. Examples of these hydrostatic muscles are the elephant trunk, the tongues of many mammals and lizards and arms and tentacles, and even suckers, of cephalopod mollusks. Examples of these hydrostatic skeletons are the body of jellyfish, starfish, sea anemones, and common earthworm. With the hydrostatic mechanisms, worms can shorten the body and increase its diameter by contracting longitudinal muscles, whereas the contraction of

circumferential muscles decreases the diameter and elongates the body, in this way allowing for various movements.

In soft robotics, the hydrostatic skeleton has been studied to achieve the stiffness in particular designs, like the case of *Softworm*, a robot inspired by a caterpillar of Lepidoptera in which shape-memory alloy actuators are connected to micro-coils and tendons for the movement of the robotic platform (Umedachi, Vikas, and Trimmer 2016).

1.3 Octopus as a model in soft robotics

Octopus represents an ideal animal model for soft robotics in terms of the generation of the movements of its flexible arms and also in terms of control. Like other animals, the critical point of the various conformations is the presence of the hydrostatic muscles, in fact the octopus can achieve various tasks with its flexible arms. The octopus uses its arms for locomotion, hunting, foraging food, but also to manipulate objects in general.

The particularity of the octopus for soft robotic, as other invertebrate soft-bodied animals, is the lack of the internal skeleton, so they use muscles to stiffen and support their body or produce a movement alternately. The essential features studied in soft robotics is the presence of hydrostatic muscles in which a constant volume is maintained so that any change in one dimension causes compensation in another dimension (Kier and Smith 1985).

In general, the movements that an octopus can perform important for soft robotic inspiration are different:

1. Elongation
2. Shortening
3. Bending
4. Stiffening
5. Torsion

From a biomechanical point of view these movements are possible thanks to the conformation and the morphology of arm muscles (better described later), it seems that transversal muscles are responsible for elongation of the arms, the longitudinal musculature is responsible for shortening, the bending needs both transversal and longitudinal muscles, the stiffening is the results of a wave of contractions of longitudinal muscles, and the oblique muscle layers create torsion (Kier and Stella 2007).
Since volume is maintained constant, if there is a contraction in some muscles, there must be an elongation in other muscles to compensate for the pressure generated.

For soft robots in general, one of the challenges in the realization of a robot inspired to the octopus is the need to control a lot, or even an infinite, number of degrees of freedom. A robot with a high number of DOF is called a *continuum robot*, and it is usually characterized by flexibility and deformability relying on soft materials.
One of the first examples of continuum robots inspired by the octopus arm has been described by Immega and Antonelli (Immega and Antonelli 1995) in which they develop a hybrid system with limited DOF (*i.e.* six); they applied tendons in a pneumatic bellows structure for controlling the movement of a manipulator both for bending and extension.

Another strategy has been applied in the OCTARM (McMahan, Jones, and Walker 2005), in which the authors use a structure hose-in-hose with a more soft hose, the external, and a rigid one internal, but the rigidity present in the more internal part is a limitation, and again it represents a hybrid system. In recent years has become more frequent the use of shape-memory alloys: these are materials that can be deformed and then returned to their original shape by simply applying some physical forces, and in this sense, they "remember" their initial conformation. The possibility of use these particular materials for the design of soft robots has been exploited within the OCTOPUS project, in which they combine shape memory alloys with tendons inside a braided sheath, obtaining high softness and dexterity (Cianchetti et al. 2012; Laschi et al. 2012). Other strategies achieve deformability thanks to a network of chambers, located all along the arm, that presents elastomers with modifiable volume with the use of pressure and inflation (Martinez et al. 2013). Another smart solution inspired from octopus arms and its muscles distribution within the arm is the surgical manipulator STIFF-FLOPP. This manipulator presents different modules in which the change of stiffness is based on the use of granular jamming and a flexible fluidic actuator. The granular jamming is used for change stiffness just augmenting the attrite force between the granules inside the manipulator. The chamber inside the manipulator is used for the changing of stiffening, around this chamber there are three fluidic actuators that serve for the direction of the manipulator. The fluidic actuators are designed as three independent chambers with which is possible to obtain different movements by changing the pressure inside. They can obtain bending by increasing pressure in only one chamber, a torsion using two chambers at the same time and even an elongation activating three chambers at the same time. The STIFF-FLOP manipulator is an example of the octopus-inspired robotic system, in which the

hydrostatic skeleton of the muscle arrangement of the octopus arm drove a new robotic system (Cianchetti et al. 2013, 2014; Fraś et al. 2015).

From an engineering point of view, the main challenge of soft bio-inspired robotics is achieving an efficient control of flexible structures as an octopus arm. To study this complex behavior, engineers combine behavioral, kinematical, and modeling techniques. Movements like bending, rotations, torsions can be very complex, but the control strategies already developed aim to the restriction of the DOF to a limited number (Gutfreund et al. 1996; Sumbre et al. 2001). The key aspect of control of the octopus arm is a distributed sensory feedback system that needs to be understood to achieve a robotic replication. To understand the natural control strategy of the octopus, a kinematic study of the control of muscle activation was the first step. Gutfreund *et al.* (Gutfreund et al. 1998) measured the forces within the octopus arm *via* electromyogram, and found a correlation between peaks of acceleration and velocity in the prediction of the activation of muscles, in particular of the length of the extension of the segments of the arm.

Experiments conducted in arms of octopi disconnected from the brain by Sumbre *et al.* (Sumbre et al. 2001) reveals that the pattern of movements generated from the arms is comparable to the natural movements of the animal. Basically, it seems that the control of arm movements remains independent from the central brain and is locally exerted by the peripheral system within the arm. Trying to replicate this behavior in a robotic platform is very challenging. A widespread approach in robotics is to reduce the complexity present in nature. The reduction of the numbers of DOF is a valid strategy to obtain movements that are similar to the natural ones: in fact, this is what happens in the human arm, in which there are three-joint-points (called point-to-point); in a an octopus-like system, the softness of the material alone still enables complex movements.

1.4 An overview of octopus anatomy

1.4.1 General organization

The octopus body is divided into two main parts: the mantle cavity and the arms. The contents of the mantle cavity are the eyes, the brain, the tripartite heart, the gills, the kidney, the gonads, the gut, the anus and the funnel or siphon. *Octopus vulgaris* has eight arms covered of two rows of suckers, the four anterior arms are most frequently extended to anchor to substrates and the others are mostly used for crawling. A general schema is shown in Fig. 1.1.

1.4.2 Digestive and excretory system

The digestive system consists of different parts: the buccal mass with its beak, the pharynx and esophagus, the radula and the salivary glands. The beak is a chitinous hard organ with which food is pre-crashed; the radula is a muscular tongue-like organ supplied by rows of tiny teeth that helps again the crashing of food and the pushing into the esophagus. The food is then stored in the gastrointestinal tract, similar to a stomach, in which is digested from digestive gland and liver cells present in the membrane absorb the food; the waste accumulated (within the caecum) is then secreted and blown out of the funnel *via* rectum. Visceral nerves and sympathetic nerves converge to the gastric ganglion, the inferior buccal ganglion mainly controls the peristaltic movements of the oesophagus. Nerves fibers surround the apparatus; the upper part with paired buccal

ganglia constitutes the supraoesophagel brain, instead, the gastric ganglion together with the two brachial ganglion constitute the suboesophageal brain. The entire functioning of the digestive system control is not clearly understood, but the gastric ganglion seems an example of delocalized control without reference to the central nervous system.

1.4.3 Hearts and circulation

The enclosed circulatory system of octopus has a high number of capillaries lining arteries and veins. Octopus has two brachial hearts that pump blood into the gills, commonly also said gills hearts or branchial heart, and a systemic heart that serves blood to the rest of the body. The blood of the octopus contains hemocyanin, which transports oxigen thanks to two copper ions. The oxidated form of hemocyanin in arteries binds carbon dioxide (CO_2), which is then released in the veins forming carbonic acid. The deoxigenated hemocyanin in blood coming from the body goes to branchial hearts, and blood is then pumped across the gills to be oxygenated, finally flowing back to the systemic atrium for a new circle.

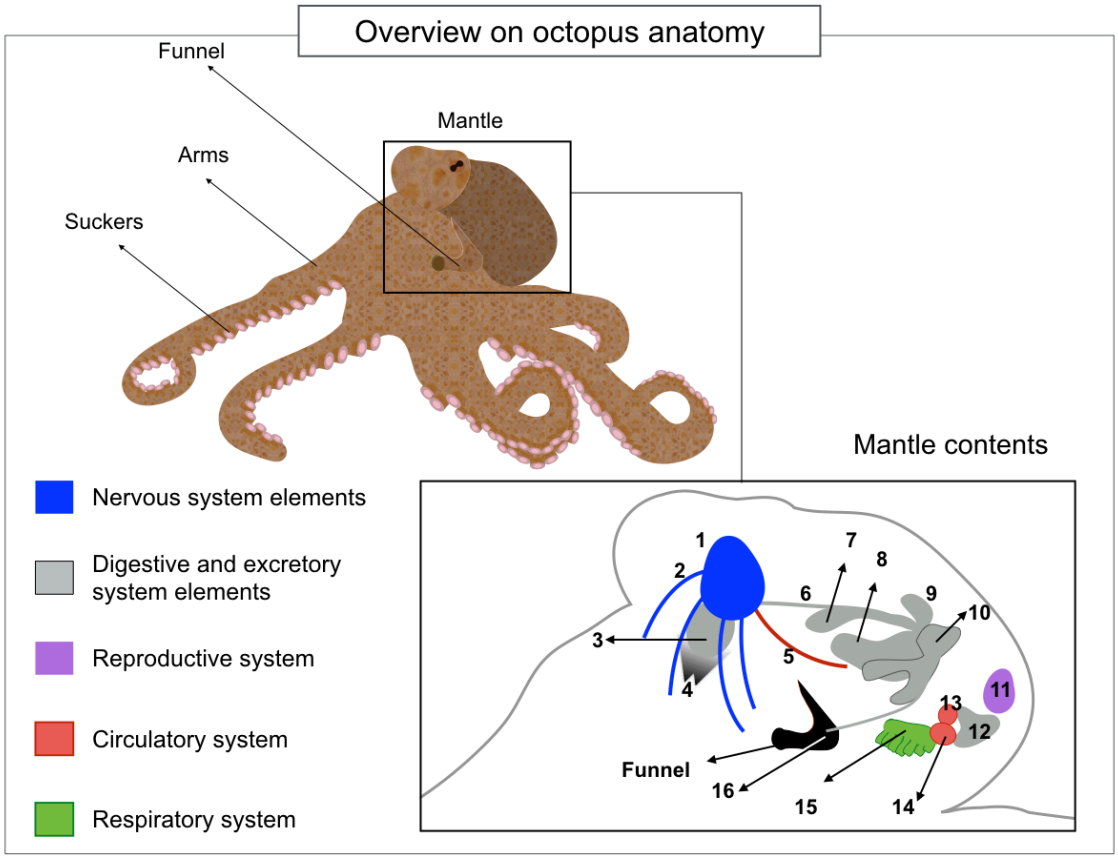

Fig. 1.1. Anatomy of octopus. Schematic representation of general anatomy of the octopus. In gray are pictured the digestive and excretory system elements, in blue elements of the peripheral nervous system, in red the circulatory system elements, in green the respiratory system, and in purple the reproductive system. Numbers indicates: 1, brain; 2, cerebrobrachial tract going to arms; 3, buccal mass; 4, beak; 5, cephalic vein; 6, esophagus; 7, gastrointestinal tract; 8, digestive gland; 9, stomach; 10, caecum; 11, gonad; 12, kidney; 13, systemic heart; 14, gill or branchial heart; 15, gill; 16, anus.

1.4.4 Respiratory system

The organs utilized for respiration are the gills, composed of brachial ganglia and a series of folded lamellae. The respiratory pigment is hemocyanin which is responsible for gaseous exchanges. The water moves over the gills within the lamellae, thanks to the rythmic contraction of the mantle cavity, and then pass through the funnel.

1.4.5 Nervous system

The nervous system of the octopus is one of the most fascinating for researchers thanks to its performances. The brain is considered large both between invertebrate and vertebrate standards, but it contains only about a third of the total neurons because the rest is located in arms.

The nervous system consists of three parts (Young 1971):

1. The central brain surrounding the esophagus (subdivided in supra and sub-esophageal brain) and situated inside a cartilaginous capsule.
2. The two optic lobes, in which are performed analysis of visual signals and also visual memory.
3. The peripheral nervous system, located within the arm and distributed in a chain of ca. 300 ganglia that constitutes the axial nerve cord. It also contains all the ganglia of suckers. The nerve system of the arm processes a large quantity of information coming from several sensory cells distributed all along the skin. It has also been experimentally shown that it controls entire movements of the arms.

1.4.6 Reproductive system

The octopus presents some sexual dimorphism. The male has a modified third right arm (called hectocotylus), which is specialized for mating; it has a tip and a flexible ciliated groove for the delivery of sperm coming from the spermatophores (Wells 2013). The females have a single ovary and two oviducts inside the mantle cavity. Males and females have almost the same size. Usually, males became senescent after mating and die a few

weeks later. Females lay thousands of eggs arranged in strings, attached to the rooves of their homes in the rocks, and stay there to brood them for about four to six weeks.

1.5 Anatomy of arms and suckers

To understand the organization of the central control of the octopus, it is crucial to deepen the analysis of the morphology of its arms and suckers.

Each arm has two paired rows of suckers along most of its ventral surface; all arms (eight in total) are similar, except for the third right arm of a male octopus, the hectocotylus.

The proximal part of the arm has only a single row of suckers; these are known as single suckers, and are present in a variable number. Their function is unclear (Tramacere, Beccai, M. J. Kuba, et al. 2013).

Each sucker can be divided into two different parts: the infundibulum and the acetabulum (Girod 1884; Kier and Smith 1990).

The infundibulum is the part of the sucker exposed to the external environment and deputed to the attachment. The acetabulum is a spherical cavity or cup-like bulge that ends in an orifice, and inside the acetabulum there is a protuberance called as acetabular protuberance. All along the surface of the infundibular part of the suckers, there are radial grooves that increase the friction force when adhering to object. Instead, the acetabular part surface is smooth. The acetabulum and infundibulum appear together as a single unit, and the cuticle is shed along with this two parts that are attached to the arm by a short muscular base (Nixon and Dilly 1977).

The infundibular part is covered by the rim, a dense loose epithelium (Kier and Smith 1990).

The arms of the octopus show an arrangement of muscle fibers that can be classified into four groups:

1. intrinsic musculature of the arms
2. intrinsic musculature of the suckers
3. extrinsic musculature
4. chromatophore-associated musculature

Along the length of the arm, the intrinsic musculature of the arm is complex, the longitudinal, circular and radial muscle allow the change on the length and the angle of the arm; twisting motions instead are possible thanks to oblique muscles along the periphery of the arm on the left and the right part, allowing the twist in both directions (Kier 1988).

The intrinsic musculature of the sucker can be subdivided into two sets, the longitudinal muscles that exhibit a radial orientation with respect to the external surface of a single sucker and the circular muscles just between the infundibulum and acetabular part of each suckers. These muscles surround the sphincter, and are in fact also known as sphincter muscles; they allow torsion.

The so-called extrinsic musculature is a series of muscle bundles that connects the suckers to the arm musculature and neighboring suckers. They originate on the connective tissue layer surrounding the arm's musculature and converge on the sucker at the level of the

sphincter muscles. Basically, these extrinsic muscles are those responsible to the bending of the external surface of the suckers and its orientation (Kier and Smith 1990).

Box 1. Camouflage, chromatophores and reflecting elements

One of the fascinating abilities of the octopus is camouflage. The camouflage in the octopus is the property to change color, in particular, in a fraction of second the octopus change color and skin texture. Camouflage is used by the octopus to protect itself from predators, together with the discharge of the black ink used for confusing hunters. As octopus is a hunting animal, camouflage also constitutes a mechanism to flush prey.

This remarkable ability is possible thanks to the presence of a specialized organ: the chromatophore. Basically, the chromatophore is a bag filled with granules of pigments and they can be four types: yellow, orange, red and black. The bag is surrounded by a single cell which appears as a series of folds in the contracted state. The cell is contained in radial muscles, each one itself containing a nerve covered in glia on its exposed surface. Each of these nerves contains axons that form a synaptic junction (Mirow 1972). The expansion of the chromatophores changes the color appearance.

Octopus also has reflecting structures lying beneath the chromatophores: the iridophores and the leucophores (Packard, Trueman, and Clarke 1988).

Iridophores are composed of series of platelets stacked of a chitinous material that reflects all colors in the environment around (Denton and Land 1971). Leucophores are located below iridophores with an irregular shape, filled with a guanine-like substance to reflect white light (Wells 2013).

The chromatophore-associated musculature is used to expand the chromatophores (the sac containing pigments) to vary skin texture for the camouflage, and it is not deputed to produce actions or movements (Packard and Sanders 1971).

In general, the interconnections between the muscular system and the nervous system in the arm are essential. In fact, even if a large bilaterally symmetrical brain is present, within the arm there is a significant nervous system and neurons in the arms are $3.5x10^8$ out of the total number of neurons in the whole body of the animal ($5x10^8$) (Graziadei 1971).

Concerning the nervous system, within the arm we can find four different parts:

1. central or axial nerve cord
2. ganglion of the sucker
3. group of ganglion cells situated above each sucker
4. intramuscular nerves cord

The axial nerve cord is also called ganglion of the arm, in fact it is a chain of linked ganglia all along the length of the arm extending down the length of the arm, with each ganglion is situated. In particular, the axial nerve cord is composed of ~300 interconnected ganglia (sometimes called as neuropil) and two cerebrobrachial (or axonal) tracts of ~30,000 nerve fibers running dorsally to the ganglia that carry sensory and motor information to and from the highly developed centralized brain, and must be considered as central nervous system instead of peripheral nervous system (Sumbre et al.

2001). Neuropil and cerebrobrachial tract are enveloped in the low part by an out layer of cell bodies (called as cellular layer or perikaryal layer, typical of invertebrates) with unclear function, that might be protection (Gutfreund et al. 2006). The high density of nerve cells of the axial nerve cord in correspondence to the suckers suggest the association with the activity of the suckers (Graziadei 1971).

The ganglion of the sucker is situated at base of each sucker, proximal to acetabular muscles, for this reason it is also called sub-acetabular ganglion (Rowell 1963). The sucker ganglion sends nerve fibers to and from the suckers and the axial nerve cord and *viceversa* (efferent and afferent), called ventral roots (Graziadei and Gagne 1976; Gutfreund et al. 2006). Most of neurons present in the sucker ganglia are described as motoneurons controlling the muscles of the suckers, and analyze chemosensory and mechanosensory input (Budelmann 1995; Young 1971). In particular, the sucker ganglion is composed of motoneurons that innervate the peduncle muscle of the suckers responsible of peripheral reflexes and bipolar and multipolar interneurons.

The intramuscular nerve cord are four longitudinal fibers all along the length of arms connected to the axial nerve cord with lateral nerves, supposedly to carry motor fibers to the intrinsic musculature and to the chromatophores, and sensory fibers from the arm periphery (Budelmann 1995). The intramuscular nerve cords are composed by internal fibers of monopolar elements, presumably motoneurons, surrounded by a layer of receptor cells that possess dendritic branches in the oblique muscles. The bundle of ganglion cells situated above each sucker serves to connect the sucker itself to the sucker ganglion and is situated in correspondence to the secondary sphincter of the acetabulum (Graziadei 1965). All described elements are represented in Fig. 1.2.

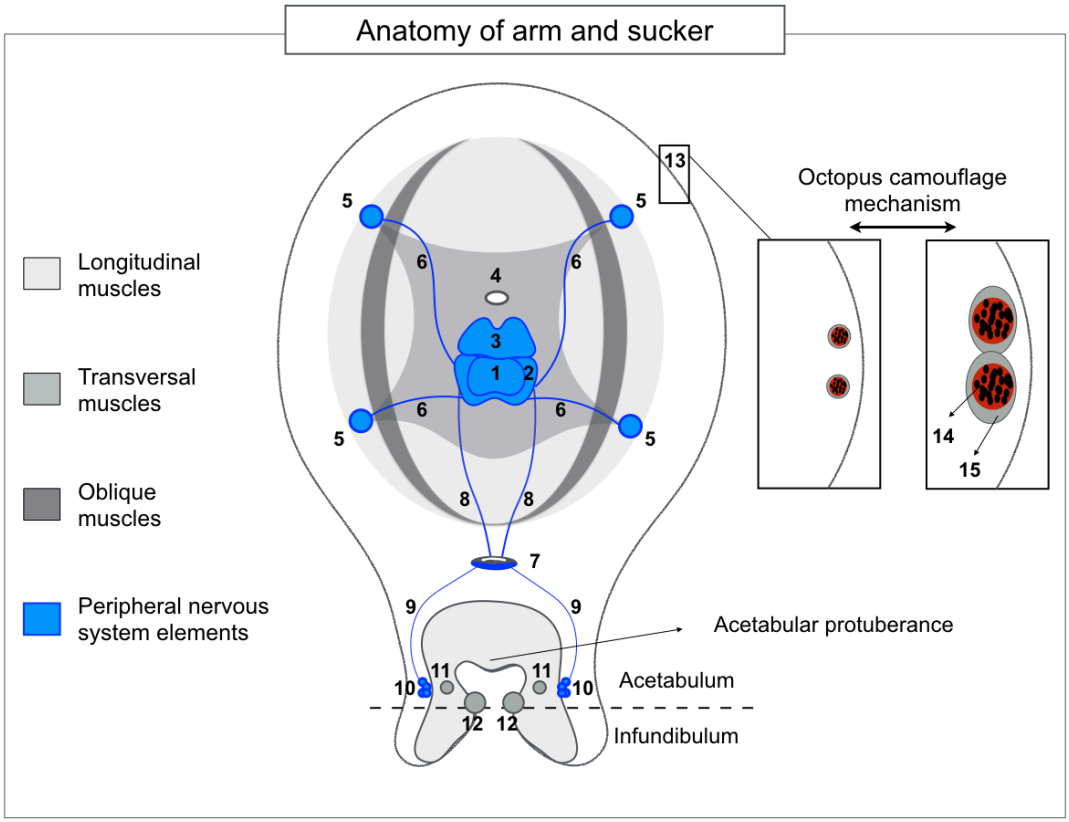

Fig. 1.2. Anatomy of arm and sucker. Schematic representation of a transversal section of the octopus arm. In gray are pictured the muscular elements: dark gray, oblique muscles, medium gray, transversal muscles, and light gray, longitudinal muscles. Elements of the peripheral nervous systems are represented in blue. Numbers indicates: 1, neuropil; 2, cellular layer; 3, cerebrobrachial tract; 4, brachial artery; 5, intramuscular nerve cord; 6, lateral roots; 7, sucker ganglion; 8, ventral roots connecting to axial nerve cord; 9, inferior ventral roots connecting to sucker ganglion; 10, bundle of ganglionic cells; 11, second sphincter; 12, primary sphincter; 13, skin; 14, chromatophore with pigment granules; 15, chromatophore-associated musculature. The two right boxes are a magnification of the skin, with a representation of the camouflage mechanism. Dotted line divides the acetabular portion of a sucker from the infundibulum.

1.6 Sensing capabilities within the arm and suckers

The anatomy of the octopus arm suggests the complexity of the control of its appendages, in particular the presence of high peripheral nervous system suggest that information coming from external environments are in some way elaborated locally to react immediately and appropriately to stimuli. It is not surprising that suckers have an effective mechanical and sensory system; in fact each sucker in both acetabular and infundibular parts is richly innervated by sensory cells.

The infundibulum of a sucker features radial grooves covered by a chitinous cuticle that is continuously renewed (Girod 1884; Nixon and Dilly 1977; Packard et al. 1988). The infundibulum is covered by a folded epithelium, the rim of the sucker, which includes cells rich of polysaccharides typical of molluscan mucus with staining characteristics (Kier and Smith 1990; Wells 2013).

The rim of the sucker is a soft and folded epithelium that surrounds the opening of the sucker, and is responsible for the first establishment of adhesion with external media, necessary for the activation of the vacuum. Therefore, the rim of the sucker is thought to be formed by a set of special nerve endings with a role in some kind of sensory perception. In fact, the rim of suckers presents a large number of sensory cells: a sucker of 3 mm of diameter has thousands of sensory cells, but in general the whole skin of the octopus is provided of $2.4x10^8$ sensory cells (Graziadei 1971).

In general, the epithelium of the sucker has a columnar aspect in section, and within this epithelium three type of receptor cells have been identified by Graziadei and Gagne (Graziadei 1964; Graziadei and Gagne 1976). This classification is based on morphology, as it is known different morphologies suggest different biological functions. The three

receptors found in suckers are conventionally called type1, type2 and type3; each element send their processes centripetally towards the ganglia.

Type1 receptors are irregular shaped sensory cells with numerous dendrites, usually located at the base of the epithelium. Type2 are pear-shaped sensory cells found in the lower half of the epithelium. Type3 are tapered sensory cells, very similar to the surface of the columnar epithelium; they are mainly located in the rim of the sucker, which lacks the cuticle. Their distal pole is contact with the external environment. The more external part of these sensory cells ends with microvilli (~ 30) of 1.3 μm length that appear arranged as a crown-like structures presenting a tuft of cilia. Type3 receptors are the most abundant, and due to their morphological resemblance with invertebrate chemoreceptors they are thought to be chemoreceptors as well. Type3 sensory cells are also directly connected to encapsulated nerve cells with their axons. Encapsulated nerve are egg-shape cells, with variable dimensions, mainly located below the epithelium lining the rim of the sucker, near the lateral side of the infundibulum and between the infundibular muscles. The function of encapsulated nerves is not clearly understood, but similar bodies are found in the inferior frontal system of the octopus brain. Encapsulated nerves present a synaptic axo-dendritic linkage between primary receptors, probably to reduce inputs from the thousands of primary receptors of the subjacent encapsulated nerve cells.

All these receptors and sensory cells with their axons and dendritic fibers represents the complex of general somatic sensory fibers, in accordance (Young 1971) with supposed specific functions of mechanoreception, chemoreception and nociception.

Box 2. General organization of nerve fibers

Young (Young 1971) divided into different groups all the nerve fibers that are afferent or efferent from the octopus brain:

1 - General somatic sensory fibers (usually located within, behind or nearby the epithelium and deputed to mechanoreception, chemoreception and nociception)

2 - Special somatic sensory fibers (associated to particular organs such as eyes, statocysts, olfactory organs and chemoreceptors of the lips)

3 - Proprioceptor fibers (located in the mantle, arm – as the four intramuscular nerve cords – and lips)

4 - Visceral sensory fibers (in the digestive system)

5 - General somatic motor fibers (directly connected to the muscles of the mantle from the central nervous system or peripheral ganglia)

6 - Chromatophore nerve fibers (efferent fibers from the chromatophores)

7 - Visceral motor fibers (a network of small and numerous fibers from peripheral ganglia)

8 - Vasomotor fibers (from the subesophageal mass to the walls of the blood vessels).

Some of these groups are multipolar fibers and other, like the chromatophore nerve fibers seem to be only afferent.

1.7 Recent efforts in omics on Octopus

Since the genome of *Octopus bimaculoides* has become available, researchers started to look into it to elucidate the sensing capabilities and its complex nervous system.

The octopus nervous system differs from other similar mollusks both in terms of size and organization, for the presence of circumesophageal brain, paired optic lobes and axial nerve cords in each arm.

The genome assembly of *Octopus bimaculoides* obtained from (Albertin et al. 2015) presents 97% of expressed protein-coding genes and 83% of the estimated 2.7-gigabase (Gb) genome size.

In general, the octopus genome turned out to be particularly interesting, also because actually, the size is not larger than other mollusks. All octopods, inside mollusks, has of 2n=60 chromosome, instead of 2n=92 of the neighboring sepioides, and even the distribution of the typology of chromosomes is different (Wang and Zheng 2017). These evident differences with similar taxa mean that octopus, in same way, diverges from them, and it is not surprising that behavior and complexity of function are so different from other mollusks. It also came out that nearly the 45% of the assembled genome is composed of repetitive elements, retrotransposons.

Box 3. Retrotransposons

In general, transposons are discrete elements in the genome that are mobile, so able to transport themselves in other locations amplifying themselves. Transposons are ubiquitous components of DNA of many eukaryotic and procariotic organisms. The mechanism that they adopt is “copy-and-paste”, and it derives from retrotransposons typical of retrovirus. The discovery of these elements dates back to 1940s from Barbara McClintock in the maize genome, *cf.* (Ravindran 2012). The mechanism of replication of these elements is very efficient because of the use of RNA that rapidly increases the copies and so the genome size. Retrotransposons can induce mutations as knock-out,

inserting within genes, or they can change the regulation of the genes inserting near to them. The mutations induced by retrotransposons are stable because they copy themselves to RNA and then back to DNA, by reverse transcriptase, that could be integrated into the genome.

The two main subclasses of retrotransposons are the long terminal repeat and the non-long terminal repeat retrotransposons.

In octopus, the presence of retrotransposons and their activity in somatic cells of the brain seem to confer increased neuronal plasticity and also can explain the distance from neighboring animals and the complexity of octopus behavior.

Another aspect that increases the complexity in octopus is the evidence of extensive mRNA editing by adenosine deaminases acting on RNA (ADARs). Albertin *et al.* (Albertin et al. 2015) found that of the predicted 33,638 protein-coding genes were found alternative splicing at 2,819 *loci*, even if no locus showed an unusually high number of splice variants; A-to-G discrepancies between assembled genome and transcriptome sequences were present. RNA editing must play an important role in complexation because mutations were found in many neural tissues in a high number of genes family, even housekeeping genes such as tubulins.

However, analyses on genomics and transcriptomics in octopus may be crucial in the understanding of sensing capabilities. Quantitative transcriptomic analysis on *Octopus bimaculoides* reveals a large presence of sensing receptors in skin and suckers (Albertin et al. 2015). In particular, the attention has been addressed to a particular class of receptors: G protein coupled receptors (GPCRs). GPCRs are also known as seven-transmembrane receptors, and they include chemosensory receptors (as odorant and taste-

like receptors), opsins (visual receptors) and adhesive receptors. This study might confirm the anatomical founding of receptors within the suckers and the skin of the suckers in *Octopus vulgaris* made by Graziadei and Gagne (Graziadei 1964, 1971; Graziadei and Gagne 1976).

1.8 General aim of the thesis project

The molecular knowledge on animals that are not classical models for biology remains comparatively scarce. Still, an increasing interest from engineers towards non-model species requires specific biological research. My thesis aims to overcome obstacles in the comprehension of the molecular aspects of sensing in *Octopus vulgaris* within its arms and suckers, starting from the *Octopus bimaculoides* genome. Are there any particular structures deputed to light detection within the arms? Are suckers used as a primary organ for foraging? To answer these questions, a first characterization of the expression pattern of genes involved in sensing is crucial. After a translation of biological and molecular mechanisms underlying the sensorial capabilities of octopus, the aspects implementable should be identified and transferred in new robotic solutions.

The innovation of my thesis is represented by its molecular approach, which is rarely used in bioinspired robotics. Namely, while it became quite frequent to look into nature to find innovative robotic solutions, but it is not equally common to implement molecular analyses. To answer biological questions, engineers typically utilize behavioral experiments; these can certainly provide great insight into the general understanding of an animal model, but a more in-depth biological analysis can yield a deeper

comprehension of natural phenomena. The nervous system of the octopus is particularly interesting for the delocalization of the control from the central brain: understanding how the sensorial capabilities are managed within the arm can drive new control strategies for robotics, in particular for soft robotics, in which control remains a primary issue.

1.9 Methods summary

The PhD work is divided in two main parts to achieve the purpose: a merely biological investigation and a robotic application.

The biological investigation has been further divided in two sections, one that handles genomic data *in silico* and a second one looking directly into tissue sections of arms and suckers. The genomic analyses include a gene screening of important sensory receptors selected for this study. Histological analyses discover where and how proteins and RNAs for the chosen genes are distributed.

The robotic application provides a method that might be implemented in the future using a sensing protein obtained from the biological investigation. The current application explores the aspect of adhesion of a sucker developing an adhesive device cured with a mollusk protein.

In Fig. 1.3 is outlined the general flow of the work.

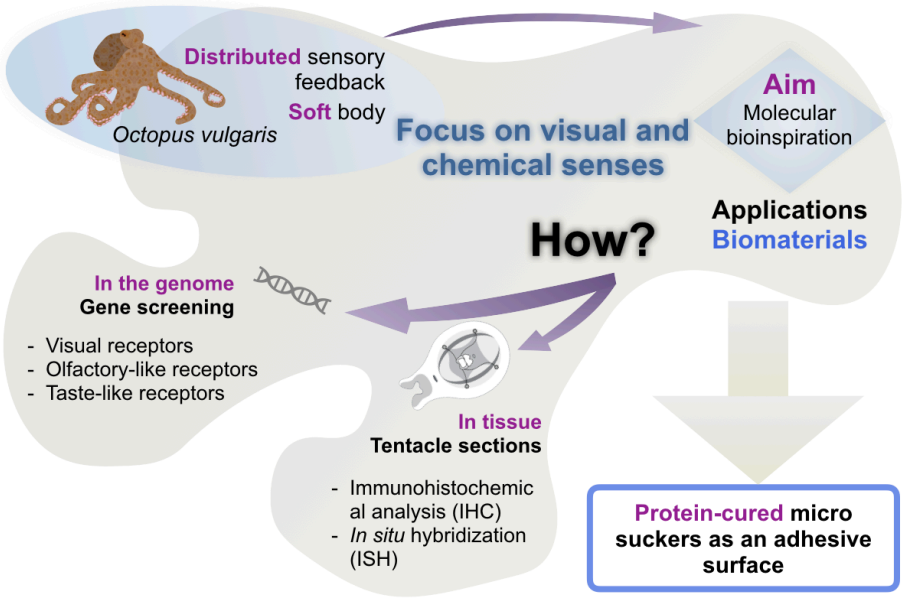

Fig. 1.3. Workflow. General schema of the work.

1.10 Results summary

We were able to characterize sensing capabilities of the octopus, as a photoreceptor, a taste-like receptor, and an odorant receptor, within the arm and suckers. In particular, we identify some structures, or at least cellular organizations, implicated in sensing in the peripheral nervous system. Results obtained can clarify the implications of these receptors and suggest a local control of the external stimuli perceived. For example, the presence of a photoreceptor within the arm suggests that this phenomenon might be implicated in the camouflage mechanism of the octopus.

The soft robotic device inspired by the octopus sucker adds a step on octopus-inspired robotics even laying the foundation of a more strictly match of biology and robotics. The implementations of animal proteins as added value in robotic designs must promote a

comprehensive overview of the possible solutions in robotics, also encouraging collaborations between these apparently different disciplines.

Our device serves in already applicable biomedical systems, and can be an example of a real match with biology in the meantime a more focused characterization in sensing will be available to be integrated into a similar system.

Chapter 2: Retrieval of selected genes relevant for sensory transduction in the sucker

Prologue

The word “bioinformatics” is referred to all the processes in which DNA, RNA and protein sequences are analyzed. Bioinformatics aims to understand the features, function, structures and even evolution and correlation between species. The common methodologies used involve the retrieval of genes (DNA), transcripts (RNA) or peptides (protein) sequences in databases, one of the most common is BLAST (an NCBI tool) in which are deposited sequences of any organism. To understand how evolution acts usually biologists look into similarities between compared sequences from the same organism or from different organism. To compare different sequences there are a number of diffused tools for sequence alignment, in this thesis has been used the software MacVector. Within the same organism if there a great percentage of similarities the sequences can be defined as homologue, when the comparison is between different organism these sequences are called orthologue, descending from the same ancestral sequence separated by a speciation (evolution event that generates different species). When looking to protein sequences the comparison might presume a conservation of the function.

2.1 Introduction:

2.1.1 Anatomical revision of sensing receptors within the sucker

The presence of particular receptors within the octopus suckers, or at least in the nearby skin, is documented in different papers. As revised before, three particular types of *O. vulgaris* receptors have been described by (Graziadei 1964, 1965, 1971; Graziadei and Gagne 1976) and classified based on their morphology and localization within the sucker. Type1 are irregular sensory cells, and they are located at the base of epithelium, type2 are bigger than type1, arranged in bud-like formation and located more externally, and type3 are flask-shaped receptors located in the rim of the sucker, and they are provided of cilia. Within these categories, other receptors have been identified. For example, among the type2 there are two different morphology: type2a is slender and spindle-shaped, type2b is irregular ovoid, both bipolar cells provided by cilia and they are also called "apical cluster". Type3 is a multipolar intraepithelial project looking to the surface of the epithelium and presents a spidery cell with a slender neck. Then another receptor, at first resembled to type2 were identified and has been called type4, a flask-shaped bipolar cell provided by a clump of apparently stiff, short cilia. Each element sends their processes centripetally towards the ganglia, but in some cases, they are also connected to interneuron to facilitate the signal process. The interneurons are ovoid with an irregular surface conformation, it is not reaching the surface of the epithelium, and its large axon extends from the basal lamina (between connective tissues and epithelium) across the connective tissue. A particular type of interneuron, called as "encapsulated cell" is located in two positions, in the connective tissue under the epithelium of the rim and within the infundibular muscle, and they are connected to type2 and type4 receptors.

In Tab. 2.1 are summarized these structures, their communications and the putative biological function (Graziadei 1964; Graziadei and Gagne 1976).

Classification	Receptor shape	Primary classification	Localization	Wiring	Supposed function
Type1	Ball shaped	Type1	Lateral epithelium	Encapsulated nerve cells below the epithelium that send their axons towards further synaptic contacts	Sensory receptor
Type2a	Ciliated fusiform	Type2	Marginal fold, rim	Encapsulated interneuron, or other basal interneurons, forming synaptic vesicles	Chemosensory receptor
Type2b	Fusiform with encapsulated cilia	Type2	Marginal fold, rim	Encapsulated interneuron, or other basal interneurons, forming synaptic vesicles	Olfactory receptor
Type4	Ciliated fusiform	Type2	Toothed cuticular epithelium	Directly to sucker ganglion	Mechanical receptor, tactile role
Type3	Multipolar, with electron dense material	Type3	Toothed cuticular epithelium	Directly to sucker ganglion	Stretch neuron (or proprioceptor) related to sucker deformation after adhesion, or related with rhabdomeres of light sensitive cells

Tab. 2.1. Sucker receptors. In table are listed all the receptors found in octopus sucker, the previous attributed name, the shape and the putative anatomic function.

The biological function of these receptors, for now is merely inferred from the anatomical shape and distribution of connections, based to similarities with other animals or with other similar sensory cell found in the olfactory organ or in the statocyst (organ deputed to orientation) of *O. vulgaris* (Emery 1975; Woodhams and Messenger 1974).

2.1.2 Molecular evidences of sensing receptors within the suckers

The molecular characterization of *O. vulgaris* receptors is still scarce, and the studies present are not related to the suckers or at least arms.

The revision of the present work already done in *O. vulgaris* receptors is summarized in Tab. 2.2.

Receptor gene	Presence in tissue	Role	Reference
Gonadotropin-releasing hormone receptor	Brain	Neurotransmitter involved in autonomic functions, feeding, memory and movements	(Kanda et al. 2006)
Estrogen Receptor	Brain, liver, kidney, gill, muscle, branchial heart, testis, ovary, oviduct, and oviducal gland	The receptor is widely expressed in both sexes, with the highest transcript levels in ovary; it may be important in female reproduction	(Keay, Bridgham, and Thornton 2006)
Oxytocin/vasopressin receptor	Central nervous system, peripheral nervous system, and reproductive tissues (as oviduct)	Oxytocin and vasopressin are neurohypophysial peptide hormones; receptors are implicated in endocrine functions for reproduction	(Kanda et al. 2005)

Tab. 2.2. Summary of *O. vulgaris* receptors. A summary of *O. vulgaris* receptors already characterized.

The molecular knowledge of *O. vulgaris* is scarce; by contrast, the studies on *O. bimaculoides* are more frequent. In particular, one of the works on *O. bimaculoides* transcripts has been done by Albertin et al. (Albertin et al. 2015). In this work they annotated the *O. bimaculoides* transcripts; in particular, they focused their attention on six family proteins that are expanded in relation to a neighbor as the squid in the octopus genome.

The family studied are: protocadherins, that are homophilic cell-adhesion proteins involved in cephalopod nervous system organization (Young 1971); the C_2H_2 zinc-finger proteins, that are transcription factor rich of C_2H_2 domains important for cell fate determination, early development and transposon silencing (Liu et al. 2014); the interleukin-17-like genes, a pro-inflammatory cytokine family that play a central player in the immune system; the chitinase, that are hydrolytic enzymes able to degrade chitin; the sialins that are involved in taste-like functions transporting glucuronic acid and free sialic acid; last, the G-protein-coupled receptors (GPCRs) family, known also as 7-transmembrane or serpentine receptors, that are a particular class of receptors that activates intracellular second messenger systems upon ligand binding. As the name says, GPCRs are coupled with G-proteins, they can activate a G-protein associated by exchanging the guanosine-5'-diphosphate (GDP) bound to the G-protein for a guanosine-5'-triphosphate (GTP). GPCRs detect a molecule outside of the cell (elicitor or ligand) and activate an internal signal transduction pathway.

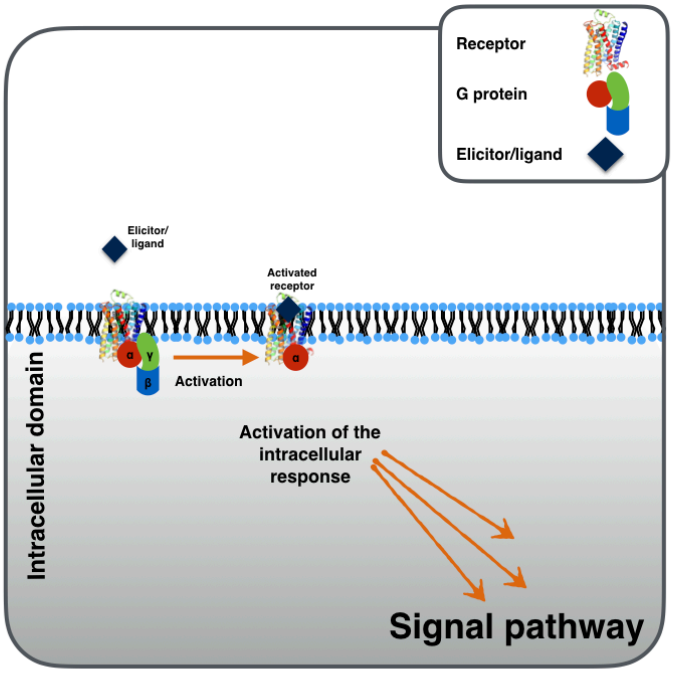

Fig. 2.1. Schema of function of GPCRs. Mechanism of GPCRs.

In Albertin et al. (Albertin et al. 2015), the GPCRs are subdivided in different classes: Class A includes opsins (photoreceptors), chemokine receptors, and the vertebrate olfactory receptors. Class B (the secretin-type) receptors include the adhesion GPCRs, calcitonin receptors, as well as several hormone receptors. Class C (glutamate-type) receptors consist of metabotropic glutamate receptors (taste-like receptors). Class F, the smallest class, includes the frizzled and smoothened genes involved in other neuronal pathways. They performed a quantitative analysis of these genes within different tissues, and GPCRs have been found in an appreciable quantity in suckers and skin. As is intuitable to find opsin in the retina, as they are photoreceptors, or taste-like receptors within the salivary organ or odorant receptors in the olfactory organ, it can be surprising to find them in peripheral tissues as arms, sucker, and skin in general.

Starting from this assumption, we aim to identify which sensory genes from GPCRs list of *O. bimaculoides* are expressed in peripheral tissues of *O. vulgaris*, and if particular structures are present.

2.2 Methods

2.2.1 Animals

Fresh dead animals were purchased as food from fish markets in Pisa or Empoli caught from Tyrrhenian Sea, and dissected immediately upon arrival to the laboratory. Arms and suckers were randomly chosen in different regions of the arm: proximal, medium and distal sections. Eyes were extracted from a single animal. Extractions were performed four times from different animals purchased in different periods of the year. For histological analyses, they were blocks of tissue/organs were embedded, sectioned ad stored at –80 ºC. For bioinformatic analyses, samples were prepared from skin and suckers, within which a sectorial portion of each sucker was kept, reaching up to 30 mg of total tissue.

2.2.2 Gene selection

Aiming to isolate sensory receptors in *O. vulgaris*, the list of GPCRs, a particular class of sensory receptors, in *O. bimaculoides* from (Albertin et al. 2015) were collected from the cladogram within the paper (specifically in figure S3 within Albertin *et al.* (Albertin et al. 2015)). All GPCRs were checked, and visual receptors (opsins) were found, but no

genes were explicitly annotated as odorant/olfactory/chemoreceptor. Visual receptors were then found using the keyword “opsin” in the *O. bimaculoides* transcriptome available at NCBI.

For odorant receptors, in the cladogram a gene from zebrafish (*Danio rerio*) is annotated as an odorant receptor, and it was clustered with other transcripts of *O. bimaculoides*, these genes were retrieved in the list of all GPCRs and via BLAST they were found to be annotated as glutamate receptors, and trace amine-associated receptors (TAARs) genes were also found. Finally, as for opsins, the keywords “TAAR” and “glutamate” were searched in the *O. bimaculoides* transcriptome available at NCBI.

2.2.3 Primer design

Primers were designed using two different platforms Primer3 and Net primer using targeting sequences of *Octopus bimaculoides* deposited on NCBI from (Albertin et al. 2015). When possible, primers were designed across splicing junctions to avoid genomic sequences. Primer parameters on Primer3 were set to 18-20 nucleotides in lengths, with a product size of 550-700 base pairs (bp) and melting point from 60 ºC to 70 ºC (with an optimum on 63 ºC). Then each putative primer couple was also analyzed in Net primer to evaluate the presence of forks inside a primer itself and primer-dimers that can reduce the efficiency of annealing. After evaluation and possibly avoiding these problems as mentioned above, the most promising primer couple was chosen and tested as putative amplicon in transcriptome of *O. bimaculoides* via NCBI Blast. After transcriptome test,

the putative amplicon was tested in the genome within Bio Linux via BLAST. The primers were obtained using the service Custom Primer Invitrogen.

2.2.4 RNA extraction

RNA extraction was performed using E.Z.N.A.® Mollusc RNA Kit (Omega Bio-Teck, D3373-01). A portion of 30 mg of tissue was homogenized with pestles in a 1.5 ml microcentrifuge Eppendorf tube, and then we followed the short protocol according to manufacturer instructions. RNA extracted was checked via UV absorption measurement (Nanodrop) to evaluate quality and quantity. RNA extracted was also run for ~ ten minutes at 150 V on 1 % agarose gel in TBE buffer with 1:20000 of Ethidium Bromide.

2.2.5 RT-PCR

Reverse transcription polymerase chain reaction (RT-PCR) is a polymerase chain reaction (PCR) combined with reverse transcription of RNA into DNA, called complementary DNA (cDNA).

Starting from RNA extracted the cDNA synthesis was performed using the SuperScript® First-Strand Synthesis System for RT-PCR (Invitrogen, 11904018) and a negative control sample (obtained without adding reverse transcriptase) was prepared to verify the absence of genomic amplifications.

Each amplification reaction was conducted in a volume of 50 µl containing: 2 µl of cDNA template, 2.5 µl of $MgCl_2$ 50 mM, 0.25 µl dNTPs ten mM, 5 µl of buffer 10X, 1 µl of each primer (20 µM), 0.2 µl of Taq DNA polymerase (BioLine, BIO-21040) and 38.05

µl of MQ water. The amplification cycles start with denaturation at 95 ºC (5 minutes), then 35 amplification cycles were carried out as follows: denaturation (95 ºC, one minute), annealing (56-58 ºC depending on primer couple, 1 minute), extension (72 ºC, two minutes). Finally, an extension cycle was carried out at 72 ºC for 10 minutes and stored at 4 ºC. Genomic contaminations were excluded introducing a non retrotranscripted sample, general contaminations using a negative control (water instead of cDNA). These three amplifications were performed in parallel each time.

The PCR products obtained were run for ~ one hour at 100 V on 1 % agarose gel in tris borate EDTA buffer with 1:20000 of ethidium bromide and detected. The expected bands were isolated and DNA purification from gels (this time in tris acetate EDTA buffer) was performed by centrifugation using Wizard® SV Gel and PCR Clean-Up System (Promega, A9281).

2.2.6 Transformation of competent bacteria

The purified DNA was inserted into the pGEM-T vector (Promega) using 50 or 100 ng of purified DNA with 50 ng (in some cases 100 ng) of pGEM-T, ten microliters of T4 ligase buffer 2X, one microliter of T4 ligase, and water up to reach 20 µl of volume; then, the solution obtained was incubated overnight at 4 ºC. The ligation sample obtained were transformed in chemically competent DH5-Alpha *Escherichia coli* cells using 3 or 7 µl of solution for 100 µl of cells. Transformation was performed with 45 s of heat shock at 42 ºC, and then cells were grown for an hour in 900 µl of liquid luria broth medium. After a gentle microcentrifugation, cells were plated on luria broth agar treated with isopropyl β-d-1-thiogalactopyranoside and X-gal (Termofisher) to perform the white/blue

screening to increase the successful probabilities of cloning. At least five independent putative positive clones were selected for plasmidic DNA extraction.

2.2.7 Plasmidic DNA extraction

Selected clones were grown in 3-4 ml of luria broth medium containing ampicillin (100 ng/µl), and for each sample a glycerol stock was prepared. The plasmidic DNA extraction, mini, was prepared according to an internal procedure. The internal procedure extracts plasmidic DNA with a first lysation of bacterial cells, denaturation of DNA. At first, bacterial cells were gently centrifugated in 1.5 ml Eppendorf tubes and supernatant was removed and 400 µl of solution one (S1: glucose 50 nM, TRIS-HCl 25 nM at pH 8, EDTA 10 nM at pH 8) were added allowing lysation. For denaturation, 400 µl of solution two (S2: Na(OH) 0.2 M, SDS 1 %) were added and tubes were gently inverted for three or four times. The same procedure was followed with solution three (S3: Potassium acetate 3 M at pH 5.3) to allow precipitation DNA and RNA. After five minutes at RT, sample were centrifugated for 15-20 min at 14000 rpm. Supernatants (~ 900 µl) were collected and 0.6 volumes of isopropanol at RT were added and gently mixed to obtain only plasmidic DNA. Tubes were again centrifugated for 15-20 min at 14000 rpm. Pellets obtained were washed with iced ethanol at 70 %, then let dry and resuspend in 20 µl of fresh MQ water.

All mini samples obtained were checked via PCR using the correspondent primer couple expected for each clone. Alternatively, clones were checked using the restriction enzyme Eco52I (ThermoFisher). Enzymatic reactions were performed overnight 37 ºC. Eco52I

excises the putative band inserted in pGEM-T vector (Promega), easily visible with electrophoretic ran.

Most promising clones were selected based on their closer size to the putative size of expected bands on *O. bimaculoides*.

Another plasmidic DNA extraction, midi, was performed following KitMidi (Qiagen) within the vacuum pump using an elution volume of 80 µl instead of 100 µl, as suggested on the protocol, to increase the efficiency of extraction. As for mini samples, the midi samples were checked via PCR and enzymatic restriction reaction.

2.2.8 Sanger sequencing

The midis were diluted to 95 ng/µl and a M13 forward primer 5 µM was used as GATC requires. The sequences obtained were analyzed using VecScreen software (NCBI) to discriminate bacterial DNA residues from *O. vulgaris* fragments. The identity of each insert was verified and confirmed via BLAST into the transcriptome of *O. bimaculoides*. Inserts obtained are meant to become *in situ* hybridization (ISH) probes for histological analyses.

2.2.9 Sequences analysis

Maps of vectors carrying our *O. vulgaris* sequences were prepared with MacVector software. Using MacVector, we aligned to reference all *O. vulgaris* inserts to their corresponding *O. bimaculoides locus* to find similarities between the two species.

Complete ISH-probe plasmid maps were prepared for selected clones. In addition, ISH-probe fragments were translated *in silico* into the putative proteins of *O.* vulgaris, generating a consensus sequence for each gene, via T-Coffee multi sequencing alignments via MacVector, using the "fast" alignment option. We compared each consensus sequence with the corresponding protein fragment of *O. bimaculoides*.

2.3 Results

2.3.1 Genes of *Octopus bimaculoides* selected

We designed a map for each gene we decided to implement the bioinformatic analysis. Maps are shown in Fig. 2.1 and feature mRNA, coding-sequences (CDS), forward and reverse PCR primers (FP and RP, respectively), and any possible amplicon on genome.

Tab. 2.3 is featuring the primer sequences and the length of putative *O. bimaculoides* fragments of transcripts.

We also checked the length of the *O. bimaculoides* genome to be sure to exclude genome amplification or to notice when the genomic amplification might be present in our investigation.

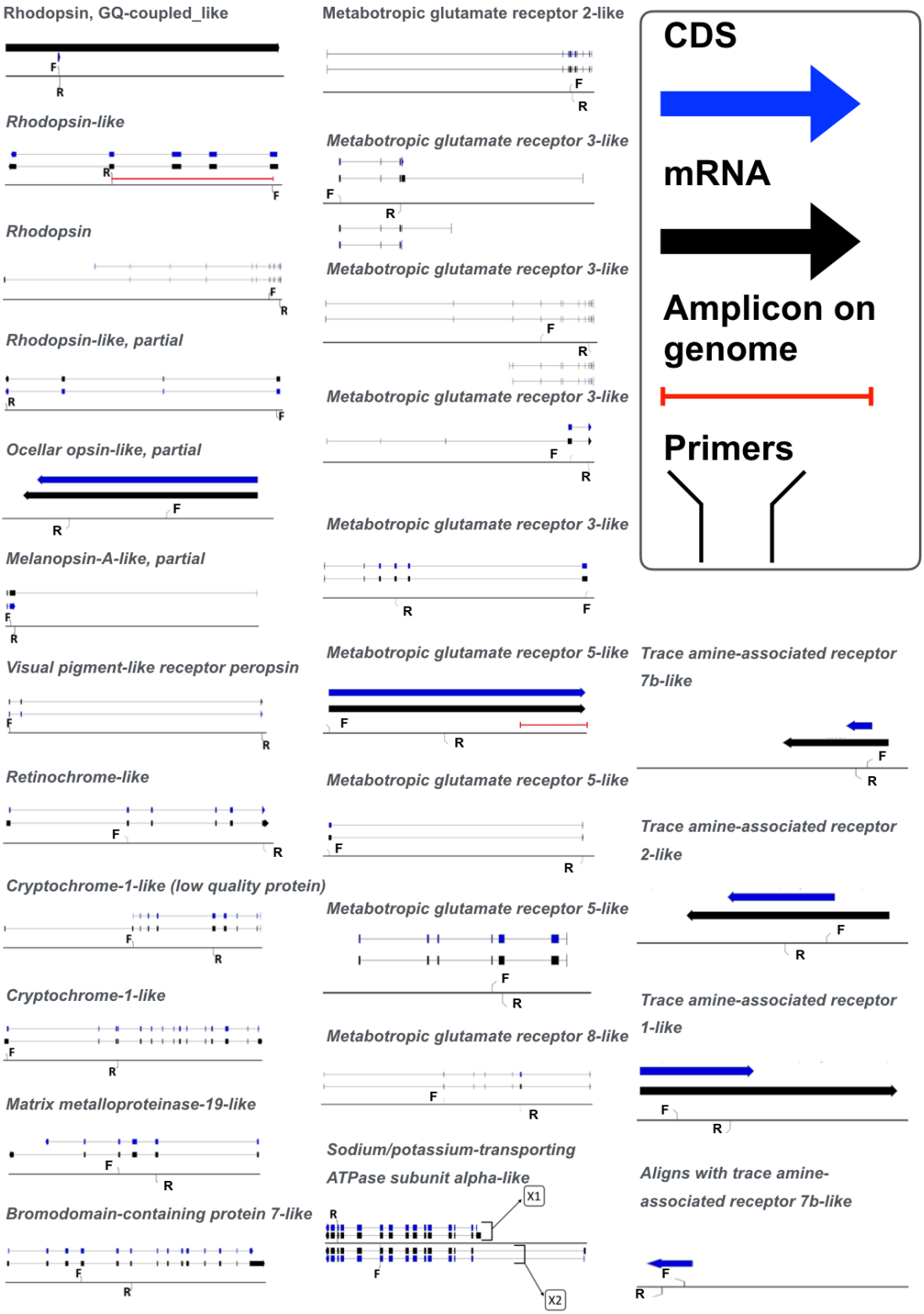

Fig. 2.2. Maps of the *O. bimaculoides* selected genes. The maps feature the CDS, mRNA, PCR primers and possible amplicons on genome. Introns are depicted as thin lines connecting exons (larger bars); arrows point to the 3' end of features.

Class		NCBI annotation referred to protein name	Forward primer sequence (5' - 3') Reverse primer sequence (5' - 3')	cDNA amplicon (bp)	Genome amplicon (bp)
Visual pigments	**Opsins**	rhodopsin, GQ-coupled-like	AGTTTGCCGTCCCACCAACT ACAAACGTGAAAGCAATCGTCTG	494	494
		rhodopsin-like	ACCAACTCCCTCACCACGCA TGACAACTGAAAGTGCTCCAGAC	776	5699
		melanopsin-A-like, partial	TCCAACATCGTGACGCCAGC TCATATCTTCATCGCACCTTTCCG	463	463
		visual pigment-like receptor peropsin, partial	GGATGTGTCTTTGTCTCTTCCCA TTCGCAGTTCCTCCTCCAGA	492	47440
		ocellar opsin-like, partial	ATTGCGAGCCAGTACCGACC CACCGCTACAAACCCCTGC	662	662
		rhodopsin	ACGCTGAAAGAAATGACGCCG AGCTGAGGGATGGGTTGGTCT	471	None
		rhodopsin-like, partial	GCGTAAAATGCGGAAGAAAATGAA ACCTTAGTCTCACCATCACCCA	303	12637
		retinochrome-like	GGCAAGGCAGAACACACAACC TTTGGACAGGAGAGGGGC	697	11845
	Others	cryptochrome-1-like *(low quality protein)*	CAGGACCCACACACAGGAATACC TTCCCACCGCCTCTGTCGTA	661	None
		cryptochrome-1-like	TGCGTACCACCGACGGAAAC GCTCTTCAATCTGCCAGCCA	535	None
Taste-like receptors		metabotropic glutamate receptor 2-like	CCCCTGTGGTAAAGGGCAATT GCTACGGCGTGTTGGTGGTA	648	1388
		metabotropic glutamate receptor 3-like isoform X1	ACTGGAAGGTTTGTTACTGCTGG ACGGTCAAATTGGATGGGGAC	691	42969
		metabotropic glutamate receptor 3-like	ACTCTGGTGTGGCTGGGACT AGTTCACCGTTAATGGGCGACA	571	88863
		metabotropic glutamate receptor 3-like	TGTTATTCTCTTCGTCCGCATCG CGCCGTACCCATCATAGAACGA	557	None
		metabotropic glutamate receptor 3-like	GTCAACGGAAGAAGGCGGAAGA CCGAATGGTGCAGGTAAGGAA	553	16341
		metabotropic glutamate receptor 5-like	TCAGCCCAACCTCAACCAGC CGTTGTGGTCGTCGAAGGCA	569	None

	metabotropic glutamate receptor 5-like	TCGACAAGCTAGCGTATCGGAC AAGGTGGGAGTCTTCAGTATGGA	635	None
	metabotropic glutamate receptor 5-like	GCTAACCTCACAGCCTGCCG CCAAGCCAGATCACACAAGTCGT	680	None
	metabotropic glutamate receptor 8-like	AGTGCCGTGACGATTCTTCCT AGCATAGCCAAGACCGCACG	564	49170
Odorant receptors	trace amine-associated receptor 7b-like	TGTTTGTCGTCATGCTGGCT ACTCCATCGTCGTTGAGCTTCA	569	569
	trace amine-associated receptor 2-like	GGGAAAGGCAAGACACAATGG GGCACAAATCCAAGAGCAGA	412	412
	trace amine-associated receptor 1-like	GCACTGTTGTAGCATGGACACC TGGTAAATGTGGGAAGAGTGGCA	570	570
	ALIGNS WITH trace amine-associated receptor 7b-like	TGTTTGTCGTCATGCTGGCTTG TCAACGGCTTCTACAGGTACA	631	631
Control markers	matrix metalloproteinase-19-like	CTCTCGGTCTCCTGGTTCAG ATTCTTTCGTGGCTGGATGG	677	3538
	bromodomain-containing protein 7-like	GTTTCTTCGCCTTCCCAGTT CTGTGCTTTCGGTTGTCTCA	537	4301
	sodium/potassium-transporting ATPase subunit alpha-like	GAGCGTGTACTAGGTTTCTGTGA ACACCAGTGACAATGGAGGC	638	None

Tab. 2.3. *O. bimaculoides* primers. The table lists all the genes selected with FP and RP sequences, the length of the expected *O. bimaculoides* amplicon, and the length of possible amplicons on genome.

2.3.2 Search of selected genes in suckers or skin

All the primers were checked via RT-PCR using sucker and skin cDNA as templates. The summary is indicated in Tab. 2.4. As shown in the table, seven out of ten visual pigments were found within the suckers and/or within the nearby skin; in particular, six of these visual pigments are GPCRs (opsins) and just one is a cryptochrome. Within the others GPCRs, one out of nine was present in sucker or skin, and one out of four for TAARs. As expected, all our control pan-expressed markers were found in our samples.

Class		NCBI annotation referred to protein name	Found in suckers or skin
Visual pigments	***Opsins***	rhodopsin, GQ-coupled-like	Yes
		rhodopsin-like	Yes
		melanopsin-A-like, partial	No
		visual pigment-like receptor peropsin, partial	No
		ocellar opsin-like, partial	Yes
		rhodopsin	Yes
		rhodopsin-like, partial	Yes
		retinochrome-like	Yes
	Other	cryptochrome-1-like (low quality protein)	No
		cryptochrome-1-like	Yes
Taste-like receptors		metabotropic glutamate receptor 2-like	No
		metabotropic glutamate receptor 3-like isoform X1	No
		metabotropic glutamate receptor 3-like	No
		metabotropic glutamate receptor 3-like	No
		metabotropic glutamate receptor 3-like	Yes
		metabotropic glutamate receptor 5-like	No
		metabotropic glutamate receptor 5-like	No
		metabotropic glutamate receptor 5-like	No
		metabotropic glutamate receptor 8-like	No
Odorant receptors		trace amine-associated receptor 7b-like	Yes
		trace amine-associated receptor 2-like	No
		trace amine-associated receptor 1-like	No
		ALIGNS WITH trace amine-associated receptor 7b-like	No
Control markers		matrix metalloproteinase-19-like	Yes
		bromodomain-containing protein 7-like	Yes
		sodium/potassium-transporting ATPase subunit alpha-like	Yes

Tab. 2.4. Transcripts identified in *O. vulgaris* sucker or skin RNA. List of genes found to be expressed in the sucker and/or the surrounding skin.

2.3.3 Sequences obtained

We attempted molecular cloning of the obtained PCR amplicons, and we were successful in seven cases. Cloned *O. vulgaris* cDNA fragments were sequenced; resulting sequences are shown in Tab. 2.5.

Gene name
Sequence of the cloned *O. vulgaris* cDNA fragment (5'-3')
rhodopsin, GQ-coupled-like
ACAAACGTGAANGCAATCGTCTGATCGTTTCTTCGATTGTAAAATTCTTGCTTTCCACATCTTTCGGTATTAAAGACA AAATACAGAAAGGAGAGAAACTAAGTGCGAACAATGCAGTTATAGAAATTACTGTTCGATTTATCCGATGAAGTTTTC TGATATTTTTTCGTTTATCTTTATCCAGTTTAGATTCGTCGGGCATGTCTAAACGAAGAAAGTGGCGTCGTGCAGTAC GCCAAACTAAACAATAAAGAACGAAATTTACGATGAGATCTAACGAATAGCCAAGAAAAACGGCTGCAAAATAGATTC TCCAACTAACTGATGATTTAAATTCACAAGTACTTACGTTTAACTTATATTCAAAGTCTGGTGCGTCAATCCTTATTG CCCAAATAACTGGCAAGGAGAATGCAAGTGAGCAAAAATTGATTACAAATGTCAGGATTCTTCCTTGGAATTTAGAGA ACTGAAAGTTGGTGGGACGGCAAACT
cryptochrome-1-like
GCTCTTCAATCTGCCAGCCATTGCTGATCTTTTGGGTGAAAATACCATAATCATAACGGATACCATATCCGTAAGCAG CAAGGCCAAGAGTAGCCATTGAGTCCAAAAAGCATGCAGCAAGACGACCAAGGCCACCATTACCAAGACCAGCATCTT CTTCCACTTCTTCTAGTTCTTCAATATCAAGTCCAAGCTAGTACATGGCTTCATCGCAGGCATTCTGGATACCCAGGT TGACCATGGTGTTGGCCAGAGTTCTCCCCATGTAGAATTCCAGAGAGATATAGTAGATTCTCTTGGGATCTTTTTCAT AATAATATTGTTGGGTTCTAATCCAGCGGCCAACCAAGTGGTCTTTAATTGTGTGCGCCAGGGCAAAGAAGTAATCTC TTTGTGTCGCCACATTTCTGTCCTTCACCAGAGTGAAATGCAAATGTCTATTAAAACTCTTCTTTATGCCAGAAATAT TACCGACTTGCGCTAAACCACGAATTGTAATTTGCTTGCGAAGTTCTGTTTCCGTCGGTGGTACGCA
metabotropic glutamate receptor 3-like
GTCAACGGAAGAAGGCGGAAGAACAGAAACAGGAAACGAAGCTCAAATTCAAGATATATGAGTGACTTTGCAGTCCGT AGAAACTTCGTTATTGTCTCGGGTGACATTTATTTTGGAGCGTTAATACAAATTCACAATGGTGGAAGAAATGACATT TGTGGGAATTTATCTCATACGGCTATACTGGAACTTGAAGCTCTGCTATATACAGTGGAAATGATAAATATTCATACA TCTTTACTGCCGGGCATCAAATTGGGGGTTTATGTACGAGACACGTGTGCAGACCCGGATCATGCTTTAAAACAAGCC TTAACCATTATGGAGGGTCGCTACTCAGAGAGTCCGCGATGGTCATACCGATGTCGAGGTGGAGAAATCGCCAAGTCC TTGCTGCCGACCATTAATGGAATCATAACCAGCATCGACTCGCCGGCAGCCAACGTCCAAGCAGCGTCTTTACTGCAG TTATTCCGTCTCCCGCAGATCAATGCAAAATCTCGGAGCCCTTTACTTCGAACAGTCGGAAGGTTTCCTTACCTGCAC CATTCGG
trace amine-associated receptor 7b-like
TGTTTGTCGTCATGCTGGCTTGTGCTGATTTGATACTTTGTGCTGTTGTATCACCAACTCGCATTGTTCAAAATTTTT ACCCCATGATGACGACCTGGGATGCAATGTGCAAGAGCCATATGTGCTTATCTGTATTTGTAGGACTTTGTAACTGTG GGTTTCTAGTGGCCATTGCAACAGATAGATACAGAAAAGTATGCCATATGCTGAAACCTCAGATAACAATGAGAGCTG

CTAAAATTATTACGGTATTTATATTTGTTTTCTCCGCAATACAGGGAAGTATTGCTATTCTTTACTACGGAAGTATCC AAAAACCGACTAATTATCCTGGTATCTACAGCTATTCTTGCTCAGCAAAAAACTACAAGGAGCTTAACTATTATCAAC TTGGATTCTTCGCTTTCTATTTTCTCTTAACAATGTTAACGTTCATTTATCTCAGTATAGTTTACACCATAATTCTTC GAAAAATTAAAGTCAAGGAAGGAAACAGTATTGAATTACAACAGAGTCGGAAGAACATCAGAAGTGCCTTGTATCCTG ATGAAGCTCAACGACGATGGAGT
matrix metalloproteinase-19-like
ATTCTTTCGTGGCTGGATGGAACACCGCAGAAGAGACGTTGGCTGGTGCTTTCCGGAAAAGGGCTCTAATTTTTCGTC GTTTGATGTTAAAGGATGCCACCTCATAGATATATTCGTTTCGGAACGCATAGGTCTTGTTATTGAGTCCGTCTACAA CAGCATCAAACTTCAGGTGGCAGACCTTTTTCTTCACGTGGCCCGTTTCATTCCTGAGTAAAGAATAACTTGTTCCGT TTTCGTTGTCTTGGTTGTACTCTCCATCGACCTCATCACTCCCAGTGTTTCTCCTCTCTGATTTCTTCGACACTTTCT TGCTTTTATTCTTCTGCTTCTTGTTGTGCTTTCGCCTATTTTTGTCTGATTTACAGTTCTTCGTATTGCCGTGGCAAC GCTTCCTATCTGAGTTTTTCGTTCCTTCAGCAGTCGATGTCTCCGATGTCATCTCAGCTATTGTGCCGTTCAAATCTT CCAATGGGTCGCTCGTTACGGCAATTGTGGAAATGTTTAGACTGTTTGTGAGCGAAGAGATTGTCGAAGTGGACGTTA CAGTATTATTAATCTCCATGCGAGGATCGTTTTTGTATAGACTCTGGATGCCCTTAATATCGTCGGCGTGAAGGGTGA AGTTTTCATTGAATTCCTCAAAAAATGGGCTCATCACTGAACCAGGAGACCGAGAG
bromodomain-containing protein 7-like
GTTTCTTCGCCTTCCCAGTTAATGATGTCATTGCTCCCGGTTATTCAAGTATCATTCAAAAGCCCATGGATTTCAGCA CAATTCTTTCTAAAGTAGATGACGAAGAGTATGCTAGCACAAAAGAATTCAAAAAAGATTTTATTCTTATGTGTCAGA ACGCTATGATCTACAACAGACCTGAGACTATTTATTATAAAGAAGCGAGACGTTTACTCCACATGGGAGTAAAACAAT TGAGCAAGGAGAACCTCCTTGGTATGAAGCGTAACCTCGATTTTATGAATGAATTGACCATGGAGGAGCTTGGTCTGG AAGATGAAAGTGAAGATAACATTATCGGTGTCAATGATGATAATTTTGATTCCGTCACAGATGACCAGCATTCCAAAG AAAAGAAGCACAAAAAACAGAAAACAAGCTTGAGTCGATTCGAAGCGATTCCTGATAATATGACACCTGAAGAAATTT TGGCACAAGCTCGTGCTGCAGCTAAAGAAGCCGCTGATCTGCTAACTTTGAGACAACCGAAAGCACAG
sodium/potassium-transporting ATPase subunit alpha-like
GAGCGTGTACTAGGTTTCTGTGAGATACTCTTCCAACGGAATCATTCCCTCCTGGATTCCAGTTTGATGGAGATGAAT TTAACTTTCCTCTTACTGGCCTTCGATTTGTTGGTTTGATGTCTATGATAGATCCCCCCCCAGCTGCTGTACCTGATG CTGTCGGAAAATGCCGAACTGCTGGTATCAAAGTTATCATGGTCACTGTTGACCATCCTATTACTGCTAAGGCTATTG CTAAAGGTGTTGGTATTTTATCAGAAGGAAGCTAATCAGTGTAAGATCTCGCCGCAGAGCAAGGGGTTGCTGTAGATC AACTTAATCCAAGAGATGCAAAAGCAGCTGTCATCCATGGAAGTGACTTGAGAGACATGACTCCGGCTCAAATTGATG AAATCCTCCGCAATCATTCTGAAATTGTTTTTGCCCGTACCTCCCCACAACAAAAACTGATCATTGTAGAAGGCTGCC AGCGTCAGGGTCAAATTGTGGCAGTCACAGGTGATGGTGTAAATGATTCTCCAGCTTTGAAGAAAGCTGATATTGGTG TTGCAATGGGAATTGCTGGCAGTGATGTGAGCACACAAGCTGCTGATATGATCCTGTTAGATGACAATTTTGCCTCCA TTGTCACTGGTGT

Tab. 2.5. *O. vulgaris* cDNA fragment sequences. List of *O. vulgaris* sequences successfully cloned.

We performed pairwise alignments to visualize differences between deposited *O. bimaculoides* sequences and obtained *O. vulgaris* sequences. Data are reported in Tab. 2.6, with sequence alignments and percentages of identities.

Name	%
cDNA sequence of *O. vulgaris* vs. *O.bimaculoides*	
rhodopsin, GQ-coupled-like	94

X1 variant

```
1     ACAAACGTGAANGCAATCGTCTGATCGTTTCTTCGATTGTAAAATTCTTGCTTTCCACAT  60
1742  ..........A.........................T.............G.......  1683

61    CTTTCGGTATTAAAGACAAAATACAGAAAGGAGAGAAACTAAGTGCGAACAATGCAGTTA  120
1682  T...T..C.A.....................................................  1623

121   TAGAAATTACTGTTCGATTTATCCGATGAAGTTTTCTGATATTTTTTCGTTTATCTTTAT  180
1622  ..........................................................  1563

181   CCAGTTTAGATTCGTCGGGCATGTCTAAACGAAGAAAGTGGCGTCGTGCAGTACGCCAAA  240
1562  ..GT...........A.....................................G.  1503

241   CTAAACAATAAAGAACGAAATTTACGATGAGATCTAACGAATAGCCAAGAAAAACGGCTG  300
1502  ..........T.............................................AC  1443

301   CAAAATAGATTCTCCAACTAACTGATGATTTAAATTCACAAGTACTTACGTTTAACTTAT  360
1442  .........G.........T.A.....................................  1383

361   ATTCAAAGTCTGGTGCGTCAATCCTTATTGCCCAAATAACTGGCAAGGAGAATGCAAGTG  420
1382  T......A.GC...A......GTT...C..................A.............  1323

421   AGCAAAAATTGATTACAAATGTCAGGATTCTTCCTTGGAATTTAGAGAACTGAAAGTTGG  480
1322  .....................................C..G......T...........  1263

481   TGGGACGGCAAACT  494
1262  ..............  1249
```

X2 variant

```
1     ACAAACGTGAANGCAATCGTCTGATCGTTTCTTCGATTGTAAAATTCTTGCTTTCCACAT  60
1840  ..........A.........................T.............G.......  1781

61    CTTTCGGTATTAAAGACAAAATACAGAAAGGAGAGAAACTAAGTGCGAACAATGCAGTTA  120
1780  T...T..C.A.....................................................  1721

121   TAGAAATTACTGTTCGATTTATCCGATGAAGTTTTCTGATATTTTTTCGTTTATCTTTAT  180
1720  ..........................................................  1661
```

```
181   CCAGTTTAGATTCGTCGGGCATGTCTAAACGAAGAAAGTGGCGTCGTGCAGTACGCCAAA  240
1660  ..GT...........A.......................................G.  1601

241   CTAAACAATAAAGAACGAAATTTACGATGAGATCTAACGAATAGCCAAGAAAAACGGCTG  300
1600  ..........T.............................................AC  1541

301   CAAAATAGATTCTCCAACTAACTGATGATTTAAATTCACAAGTACTTACGTTTAACTTAT  360
1540  .........G.........T.A.....................................  1481

361   ATTCAAAGTCTGGTGCGTCAATCCTTATTGCCCAAATAACTGGCAAGGAGAATGCAAGTG  420
1480  T......A.GC...A......GTT...C..................A.............  1421

421   AGCAAAAATTGATTACAAATGTCAGGATTCTTCCTTGGAATTTAGAGAACTGAAAGTTGG  480
1420  .....................................C..G......T...........  1361

481   TGGGACGGCAAACT  494
1360  ..............  1347
```

cryptochrome-1-like	97

```
1     GCTCTTCAATCTGCCAGCCATTGCTGATCTTTTGGGTGAAAATACCATAATCATAACGGA  60
931   ........................A..T.............................  872

61    TACCATATCCGTAAGCAGCAAGGCCAAGAGTAGCCATTGAGTCCAAAAAGCATGCAGCAA  120
871   ............................................................  812

121   GACGACCAAGGCCACCATTACCAAGACCAGCATCTTCTTCCACTTCTTCTAGTTCTTCAA  180
811   ................G...........................................  752

181   TATCAAGTCCAAGCTAGTACATGGCTTCATCGCAGGCATTCTGGATACCCAGGTTGACCA  240
751   ..............G.............................................  692

241   TGGTGTTGGCCAGAGTTCTCCCCATGTAGAATTCCAGAGAGATATAGTAGATTCTCTTGG  300
691   ........A...................................................  632

301   GATCTTTTTCATAATAATATTGTTGGGTTCTAATCCAGCGGCCAACCAAGTGGTCTTTAA  360
631   ....................................T.......................  572

361   TTGTGTGCGCCAGGGCAAAGAAGTAATCTCTTTGTGTCGCCACATTTCTGTCCTTCACCA  420
571   .......T.............A........C..............................  512

421   GAGTGAAATGCAAATGTCTATTAAAACTCTTCTTTATGCCAGAAATATTACCGACTTGCG  480
511   ...................G................................A.......  452
```

```
481  CTAAACCACGAATTGTAATTTGCTTGCGAAGTTCTGTTTCCGTCGGTGGTACGCA  535
451  ...T.........................C..G.....................  397
```

metabotropic glutamate receptor 3-like	97

```
1    GTCAACGGAAGAAGGCGGAAGAACAGAAACAGGAAACGAAGCTCAAATTCAAGATATATG  60
114  ............................................................  173

61   AGTGACTTTGCAGTCCGTAGAAACTTCGTTATTGTCTCGGGTGACATTTATTTTGGAGCG  120
174  ..................G.......................................  233

121  TTAATACAAATTCACAATGGTGGAAGAAATGACATTTGTGGGAATTTATCTCATACGGCT  180
234  .....G.............................C..................T..  293

181  ATACTGGAACTTGAAGCTCTGCTATATACAGTGGAAATGATAAATATTCATACATCTTTA  240
294  .....A.........................A..G.....................  353

241  CTGCCGGGCATCAAATTGGGGGTTTATGTACGAGACACGTGTGCAGACCCGGATCATGCT  300
354  ..............................G..........A.............  413

301  TTAAAACAAGCCTTAACCATTATGGAGGGTCGCTACTCAGAGAGTCCGCGATGGTCATAC  360
414  ..............................T.....................T..T  473

361  CGATGTCGAGGTGGAGAAATCGCCAAGTCCTTGCTGCCGACCATTAATGGAATCATAACC  420
474  ............................A........A........C.............  533

421  AGCATCGACTCGCCGGCAGCCAACGTCCAAGCAGCGTCTTTACTGCAGTTATTCCGTCTC  480
534  ......................T..................T..............A..  593

481  CCGCAGATCAATGCAAAATCTCGGAGCCCTTTACTTCGAACAGTCGGAAGGTTTCCTTAC  540
594  ..............................T.........................  653

541  CTGCACCATTCGG  553
654  .............  666
```

trace amine-associated receptor 7b-like	95

```
1     TGTTTGTCGTCATGCTGGCTTGTGCTGATTTGATACTTTGTGCTGTTGTATCACCAACTC  60
972   ...........................................................G..  1031

61    GCATTGTTCAAAATTTTTACCCCATGATGACGACCTGGGATGCAATGTGCAAGAGCCATA  120
1032  ..............G.........................T..........A.AT....  1091

121   TGTGCTTATCTGTATTTGTAGGACTTTGTAACTGTGGGTTTCTAGTGGCCATTGCAACAG  180
1092  ....T..............................T......A.............G.  1151
```

```
181   ATAGATACAGAAAAGTATGCCATATGCTGAAACCTCAGATAACAATGAGAGCTGCTAAAA  240
1152  ......................C.......................A...........  1211

241   TTATTACGGTATTTATATTTGTTTTCTCCGCAATACAGGGAAGTATTGCTATTCTTTACT  300
1212  ............................................................  1271

301   ACGGAAGTATCCAAAAACCGACTAATTATCCTGGTATCTACAGCTATTCTTGCTCAGCAA  360
1272  ............GG........................T...................  1331

361   AAAACTACAAGGAGCTTAACTATTATCAACTTGGATTCTTCGCTTTCTATTTTCTCTTAA  420
1332  ...T.......A................................................  1391

421   CAATGTTAACGTTCATTTATCTCAGTATAGTTTACACCATAATTCTTCGAAAAATTAAAG  480
1392  .......T...C......T....T..G............................G....  1451

481   TCAAGGAAGGAAACAGTATTGAATTACAACAGAGTCGGAAGAACATCAGAAGTGCCTTGT  540
1452  .........A.....................A.A.A....A.G...T.............  1511

541   ATCCTGATGAAGCTCAACGACGATGGAGT  569
1512  ............................  1540
```

matrix metalloproteinase-19-like 94

```
1     ATTCTTTCGTGGCTGGATGGAACACCGCAGAAGAGACGTTGGCTGGTGCTTTCCGGAAAA  60
982   ............................................................  923

61    GGGCTCTAATTTTTCGTCGTTTGATGTTAAAGGATGCCACCTCATAGATATATTCGTTTC  120
922   ...............................A.....T......................  863

121   GGAACGCATAGGTCTTGTTATTGAGTCCGTCTACAACAGCATCAAACTTCAGGTGGCAGA  180
862   ............T.....................T.........................  803

181   CCTTTTTCTTCACGTGGCCCGTTTCATTCCTGAGTAAAGAATAACTTGTTCCGTTTTCGT  240
802   T............A.....T..A............................T...A....  743

241   TGTCTTGGTTGTACTCTCCATCGACCTCATCACTCCCAGTGTTTCTCCTCTCTGATTTCT  300
742   ...........A..........A.....................................  683

301   TCGACACTTTCTTGCTTTTATTCTTCTGCTTCTTGTTGTGCTTTCGCCTATTTTTGTCTG  360
682   ..................T.G...G..T.......-..--..C..T..............  626

361   ATTTACAGTTCTTCGTATTGCCGTGGCAACGCTTCCTATCTGAGTTTTTCGTTCCTTCAG  420
625   ...................A...........T.......G......C.............  566
```

```
421  CAGTCGATGTCTCCGATGTCATCTCAGCTATTGTGCCGTTCAAATCTTCCAATGGGTCGC  480
565  T.........T..........C..................T...................  506

481  TCGTTACGGCAATTGTGGAAATGTTTAGACTGTTTGTGAGCGAAGAGATTGTCGAAGTGG  540
505  ......................A..C............................AC.....  446

541  ACGTTACAGTATTATTAATCTCCATGCGAGGATCGTTTTTGTATAGACTCTGGATGCCCT  600
445  ........T.CG..............TC.............................T.  386

601  TAATATCGTCGGCGTGAAGGGTGAAGTTTTCATTGAATTCCTCAAAAAATGGGCTCATCA  660
385  ..........C.....................................C..A.....T.  326

661  CTGAACCAGGAGACCGAGAG  680
325  ....................  306
```

bromodomain-containing protein 7-like	99

```
1    GTTTCTTCGCCTTCCCAGTTAATGATGTCATTGCTCCCGGTTATTCAAGTATCATTCAAA  60
569  ............................................................  628

61   AGCCCATGGATTTCAGCACAATTCTTTCTAAAGTAGATGACGAAGAGTATGCTAGCACAA  120
629  ............................................................  688

121  AAGAATTCAAAAAAGATTTTATTCTTATGTGTCAGAACGCTATGATCTACAACAGACCTG  180
689  ............................................................  748

181  AGACTATTTATTATAAAGAAGCGAGACGTTTACTCCACATGGGAGTAAAACAATTGAGCA  240
749  ..................................T.........................  808

241  AGGAGAACCTCCTTGGTATGAAGCGTAACCTCGATTTTATGAATGAATTGACCATGGAGG  300
809  ............................................................  868

301  AGCTTGGTCTGGAAGATGAAAGTGAAGATAACATTATCGGTGTCAATGATGATAATTTTG  360
869  .A..........................................................  928

361  ATTCCGTCACAGATGACCAGCATTCCAAAGAAAAGAAGCACAAAAAACAGAAAACAAGCT  420
929  ............................................................  988

421  TGAGTCGATTCGAAGCGATTCCTGATAATATGACACCTGAAGAAATTTTGGCACAAGCTC  480
989  ..........T...........C.....................................  1048

481  GTGCTGCAGCTAAAGAAGCCGCTGATCTGCTAACTTTGAGACAACCGAAAGCACAG  536
1049 ..........A.....................T..A.....................  1104
```

sodium/potassium-transporting ATPase subunit alpha-like	97

X1 variant

```
1     GAGCGTGTACTAGGTTTCTGTGA-GATACTCTTCCAACGGAATCATTCCCTCCTGGATTC  59
1750  ......................TT..................................  1809

60    CAGTTTGATGGAGATGAATTTAACTTTCCTCTTACTGGCCTTCGATTTGTTGGTTTGATG  119
1810  ..................G....T......................C.............  1869

120   TCTATGATAGATcccccccAGCTGCTGTACCTGATGCTGTCGGAAAATGCCGAACTGCT  179
1870  ..............A...AG.................................G....  1929

180   GGTATCAAAGTTATCATGGTCACTGTTGACCATCCTATTACTGCTAAGGCTATTGCTAAA  239
1930  ........................G.................................  1989

240   GGTGTTGGTATTTTATCAGAAGGAAGCTAATCAGTGTAAGATCTCGCCGCAGAGCAAGGG  299
1990  ............A..............A..A.....G.....................  2049

300   GTTGCTGTAGATCAACTTAATCCAAGAGATGCAAAAGCAGCTGTCATCCATGGAAGTGAC  359
2050  ..C............G.........................................  2109

360   TTGAGAGACATGACTCCGGCTCAAATTGATGAAATCCTCCGCAATCATTCTGAAATTGTT  419
2110  ..............................................C.............  2169

420   TTTGCCCGTACCTCCCCACAACAAAAACTGATCATTGTAGAAGGCTGCCAGCGTCAGGGT  479
2170  ..........................................................  2229

480   CAAATTGTGGCAGTCACAGGTGATGGTGTAAATGATTCTCCAGCTTTGAAGAAAGCTGAT  539
2230  ..................G.....................................  2289

540   ATTGGTGTTGCAATGGGAATTGCTGGCAGTGATGTGAGCACACAAGCTGCTGATATGATC  599
2290  ........................................A.................  2349

600   CTGTTAGATGACAATTTTGCCTCCATTGTCACTGGTGT  637
2350  .....G.............................  2387
```

X2 variant

```
1     GAGCGTGTACTAGGTTTCTGTGA-GATACTCTTCCAACGGAATCATTCCCTCCTGGATTC  59
1931  ......................TT..................................  1990

60    CAGTTTGATGGAGATGAATTTAACTTTCCTCTTACTGGCCTTCGATTTGTTGGTTTGATG  119
1991  ..................G....T......................C.............  2050
```

```
120   TCTATGATAGATccccccccAGCTGCTGTACCTGATGCTGTCGGAAAATGCCGAACTGCT  179
2051  ..............A...AG.................................G....  2110

180   GGTATCAAAGTTATCATGGTCACTGTTGACCATCCTATTACTGCTAAGGCTATTGCTAAA  239
2111  ........................G.................................  2170

240   GGTGTTGGTATTTTATCAGAAGGAAGCTAATCAGTGTAAGATCTCGCCGCAGAGCAAGGG  299
2171  ............A..............A..A.....G.....................  2230

300   GTTGCTGTAGATCAACTTAATCCAAGAGATGCAAAAGCAGCTGTCATCCATGGAAGTGAC  359
2231  ..C............G.........................................  2290

360   TTGAGAGACATGACTCCGGCTCAAATTGATGAAATCCTCCGCAATCATTCTGAAATTGTT  419
2291  ............................................C............  2350

420   TTTGCCCGTACCTCCCCACAACAAAAACTGATCATTGTAGAAGGCTGCCAGCGTCAGGGT  479
2351  ........................................................  2410

480   CAAATTGTGGCAGTCACAGGTGATGGTGTAAATGATTCTCCAGCTTTGAAGAAAGCTGAT  539
2411  ..................G.....................................  2470

540   ATTGGTGTTGCAATGGGAATTGCTGGCAGTGATGTGAGCACACAAGCTGCTGATATGATC  599
2471  ........................................A...............  2530

600   CTGTTAGATGACAATTTTGCCTCCATTGTCACTGGTGT  637
2531  .....G..............................  2568
```

Tab. 2.6. Transcript alignments. *O. vulgaris* cDNA fragments *vs.* they *O. bimaculoides* counterparts. Differences are indicated in red.

Putative protein sequences were obtained *in silico* via Sequence Manipulation Suite and a consensus sequence is reported in Tab. 2.7.

Name
Translated protein sequences of *O. vulgaris*
rhodopsin, GQ-coupled-like
VCRPTNFQFSKFQGRILTFVINFCSLAFSLPVIWAIRIDAPDFEYKLNVSTCEFKSSVSWRIYFAAVFLGYSLDLIVN FVLYCLVWRTARRHFLRLDMPDESKLDKDKRKNIRKLHRINRTVISITALFALSFSPFCILSLIPKDVESKNFTIEET IRRLSRL
cryptochrome-1-like
CVPPTETELRKQITIRGLAQVGNISGIKKSFNRHLHFTLVKDRNVATQRDYFFALAHTIKDHLVGRWIRTQQYYYEKD PKRIYYISLEFYMGRTLANTMVNLGIQNACDEAMY*LGLDIEELEEVEEDAGLGNGGLGRLAACFLDSMATLGLAAYG YGIRYDYGIFTQKISNGWQIEE
metabotropic glutamate receptor 3-like
VNGRRRKNRNRKRSSNSRYMSDFAVRRNFVIVSGDIYFGALIQIHNGGRNDICGNLSHTAILELEALLYTVEMINIHT SLLPGIKLGVYVRDTCADPDHALKQALTIMEGRYSESPRWSYRCRGGEIAKSLLPTINGIITSIDSPAANVQAASLL
trace amine-associated receptor 7b-like
FVVMLACADLILCAVVSPTRIVQNFYPMMTTWDAMCKSHMCLSVFVGLCNCGFLVAIATDRYRKVCHMLKPQITMRAA KIITVFIFVFSAIQGSIAILYYGSIQKPTNYPGIYSYSCSAKNYKELNYYQLGFFAFYFLLTMLTFIYLSIVYTIILR KIKVKEGNSIELQQSRKNIRSALYPDEAQRRWS
matrix metalloproteinase-19-like
SRSPGSVMSPFFEEFNENFTLHADDIKGIQSLYKNDPRMEINNTVTSTSTISSLTNSLNISTIAVTSDPLEDLNGTIA EMTSETSTAEGTKNSDRKRCHGNTKNCKSDKNRRKHNKKQKNKSKKVSKKSERRNTGSDEVDGEYNQDNENGTSYSLL RNETGHVKKKVCHLKFDAVVDGLNNKTYAFRNEYIYEVASFNIKRRKIRALFRKAPANVSSAVFHPATKE
bromodomain-containing protein 7-like
FFAFPVNDVIAPGYSSIIQKPMDFSTILSKVDDEEYASTKEFKKDFILMCQNAMIYNRPETIYYKEARRLLHMGVKQL SKENLLGMKRNLDFMNELTMEELGLEDESEDNIIGVNDDNFDSVTDDHSKEKKHKKQKTSLSRFEAIPDNMTPEEILA QARAAAKEAADLLTLRQPKA
sodium/potassium-transporting ATPase subunit alpha-like
ERVLGFCDYTLPTESFPPGFQFDGDEVNFPLTGLRFVGLMSMIDPPRAAVPDAVGKCRSAGIKVIMVTGDHPITAKAI AKGVGIISEGSKTVEDLAAEQGVAVDQVNPRDAKAAVIHGSDLRDMTPAQIDEILRNHSEIVFARTSPQQKLIIVEGC QRQGQIVAVTGDGVNDSPALKKADIGVAMGIAGSDVSKQAADMILLDDNFASIVTG

Tab. 2.7. Putative *O. vulgaris* translated cDNA fragments. List of putative protein sequences.

We performed translated transcripts alignments via BLAST to see differences between deposited *O. bimaculoides*. Data are reported in Tab. 2.8, with translated transcript sequences alignments and percentages of identities.

Protein name	**%**
Translated transcript sequences of *O. vulgaris* vs. *O.bimaculoides*	
rhodopsin, GQ-coupled-like	89
1 VCRPTNFQFSKFQGRILTFVINFCSLAFSLPVIWAIRIDAPDFEYKLNVSTCEFKSSVSW 60 131 .....I.TC.....VKL.V.H..N.....L.. 190 61 RIYFAAVFLGYSLDLIVNFVLYCLVWRTARRHFLRLDMPDESKLDKDKRKNIRKLHRINR 120 191 .L..G.....T..... 250 121 TVISITALFALSFSPFCILSLIPKDVESKNFTIEETIRR-LSRL 163 251 .....L..N.D....K.....L.... 294	
cryptochrome-1-like	98
1 CVPPTETELRKQITIRGLAQVGNISGIKKSFNRHLHFTLVKDRNVATQRDYFFALAHTIK 60 3 .....I..... 62 61 DHLVGRWIRTQQYYYEKDPKRIYYISLEFYMGRTLANTMVNLGIQNACDEAMY*LGLDIE 120 63 .....H.....V.....Q..... 122 121 ELEEVEEDAGLGNGGLGRLAACFLDSMATLGLAAYGYGIRYDYGIFTQKISNGWQIEE 178 123 180	
metabotropic glutamate receptor 3-like	97
1 VNGRRRKNRNRKRSSNSRYMSDFAVRRNFVIVSGDIYFGALIQIHNGGRNDICGNLSHTA 60 24 .....M.....S 83 61 ILELEALLYTVEMINIHTSLLPGIKLGVYVRDTCADPDHALKQALTIMEGRYSESPRWSY 120 84 .....E..... 143 121 RCRGGEIAKSLLPTINGIITSIDSPAANVQAASLL 155 144 178	
trace amine-associated receptor 7b-like	90
1 FVVMLACADLILCAVVSPTRIVQNFYPMMTTWDAMCKSHMCLSVFVGLCNCGFLVAIATD 60 69 .....S.....V.....S...N.....M..... 128 61 RYRKVCHMLKPQITMRAAKIITVFIFVFSAIQGSIAILYYGSIQKPTNYPGIYSYSCSAK 120 129 .....L.....K.....R..... 188	

```
121  NYKELNYYQLGFFAFYFLLTMLTFIYLSIVYTIILRKIKVKEGNSIELQQSRKNIRSALY  180
189  I..K.................F.L.F.CV........M....E.......N..S......  248

181  PDEAQRRWS  189
249  .........  257
```

matrix metalloproteinase-19-like 93

```
1    SRSPGSVMSPFFEEFNENFTLHADDIKGIQSLYKNDPRMEINNTVTSTSTISSLTNSLNI  60
100  ....................................S....TN....V...........  159

61   STIAVTSDPLEDLNGTIAEMTSETSTAEGTKNSDRKRCHGNTKNCKSDKNRRKHNKKQKN  120
160  ...................V......T......H.....................-H..H.Q  218

121  KSKKVSKKSERRNTGSDEVDGEYNQDNENGTSYSLLRNETGHVKKKVCHLKFDAVVDGLN  180
219  ......................F....D.R........D.......I.............  278

181  NKTYAFRNEYIYEVASFNIKRRKIRALFRKAPANVSSAVFHPATKE  226
279  ..............................................  324
```

bromodomain-containing protein 7-like 99

```
1    FFAFPVNDVIAPGYSSIIQKPMDFSTILSKVDDEEYASTKEFKKDFILMCQNAMIYNRPE  60
158  ............................................................  217

61   TIYYKEARRLLHMGVKQLSKENLLGMKRNLDFMNELTMEELGLEDESEDNIIGVNDDNFD  120
218  ............................................................  277

121  SVTDD-HSKEKKHKKQKTSLSRFEAIPDNMTPEEILAQARAAAKEAADLLTLRQPKA  176
278  .....Q.....................................................  334
```

sodium/potassium-transporting ATPase subunit alpha-like 100

X1 variant

```
1    ERVLGFCDYTLPTESFPPGFQFDGDEVNFPLTGLRFVGLMSMIDPPRAAVPDAVGKCRSA  60
556  ............................................................  615

61   GIKVIMVTGDHPITAKAIAKGVGIISEGSKTVEDLAAEQGVAVDQVNPRDAKAAVIHGSD  120
616  ............................................................  675

121  LRDMTPAQIDEILRNHSEIVFARTSPQQKLIIVEGCQRQGQIVAVTGDGVNDSPALKKAD  180
676  ............................................................  735

181  IGVAMGIAGSDVSKQAADMILLDDNFASIVTG  212
736  ................................  767
```

X2 variant

```
1    ERVLGFCDYTLPTESFPPGFQFDGDEVNFPLTGLRFVGLMSMIDPPRAAVPDAVGKCRSA  60
561  ............................................................  620

61   GIKVIMVTGDHPITAKAIAKGVGIISEGSKTVEDLAAEQGVAVDQVNPRDAKAAVIHGSD  120
621  ............................................................  680

121  LRDMTPAQIDEILRNHSEIVFARTSPQQKLIIVEGCQRQGQIVAVTGDGVNDSPALKKAD  180
681  ............................................................  740

181  IGVAMGIAGSDVSKQAADMILLDDNFASIVTG  212
741  ................................  772
```

Tab. 2.8. Proteins alignments. List of alignments of *O. vulgaris* putative proteins *vs. O. bimaculoides* proteins. Differences are indicated in red.

2.4 Discussion

In this bioinformatic analysis, we need to considerate the presence of some confounding effects. First of all, we obtained the sequences using different preparations of RNA and cDNA, deriving from different suckers and animals. This might have had an impact on sequencing results.

While most primers are positioned across a splicing junction, in a few instances this was not feasible, so that a genome amplification might be present. We mitigated this problem by implementing no-RT controls. A second possible issue is that samples were obtained from dead animals purchased from supermarkets; therefore, the freshness of RNA for extractions is not optimal.

Despite these limitations, in many cases we still obtained *O. vulgaris* RNA sequences that are close to the corresponding *O. bimaculoides* sequences. The vicinity of putative translated proteins of *O. vulgaris* obtained with *O. bimaculoides* protein sequences confirms the validity of our approach, and we were able to proceed with histological analysis.

To enrich our analysis, in the future we might evaluate other GPCR genes, or study the expression pattern of G proteins, which are also useful to track sensory transduction cascades.

Chapter 3: Histological characterization

Prologue

The word “histology” indicates the study of the microscopic anatomy of the biological tissue, in this case the octopus tissues with particular regards to arm and suckers. Usually, the tissues for histological analyses are fixed and embedded in a medium that allows the possibility to perform a series of sections for microscopic observation.

There are several techniques used in histology, and some of them aim to selectively color some tissues instead of others to increase the contrast and to identify a specific tissue (as muscles, connective tissue, epithelium or neurons).

In this context, we used antibodies for proteins or specific probes directed to RNA. The detection of the signal is possible thanks to a conjugation with a secondary antibody that reveals if the primary ligand has been attached to the target. These techniques enable us to characterize the pattern of expression of the targets, which means to describe where and how the targets can be found in the anatomical tissues.

3.1 Introduction

As revised before, some studies have been performed in *O. vulgaris* tissues to understand the anatomy of receptors, but anatomy is not enough to understand how these receptors work and how they communicate, and also which is their specific biological function. Histological techniques are required to give a more functional insight into these receptors. In *O. vulgaris* histological investigations are still rare, but in recent years a number of analyses have been performed.

In particular, tissues of *O. vulgaris* have been analyzed via immunohistochemistry (IHC)

Tab. 3.1 features a list of antibodies (Ab) already tested in *O. vulgaris* tissues.

Product name	Product code	Antigen	Tissue tested	Reference
Acetylated alpha-tubulin, ascites fluid	Sigma, T6793	Axoneme assembly	Gastric ganglion	(Baldascino et al. 2017)
Acetylated alpha-tubulin	Sigma, T7451	Axoneme assembly	Mantle skin	(Ramirez and Oakley 2015)
Anti-Rhodopsin	CosmoBio, LSL-LB-5509	Rhodopsin	Mantle skin	(Ramirez and Oakley 2015)
Anti-Serotonin	Sigma, S5545	Serotonin-containing fibers	Arm	(Ponte and Fiorito 2015)
Anti-Neurofilament	Sigma, N 5389	Neurofilament	Palliative nerve	(Imperadore et al. 2017)
Monoclonal Anti-phospho-Histone H3 (pSer28)	Sigma, H9908	Phosphorylated serine-28	Palliative nerve	(Imperadore et al. 2017)
Neuronal nuclear antigen	Millipore, ABN78C3	Neuronal nuclei	Gastric ganglion	(Baldascino et al. 2017)
Corticotropin Releasing Factor	BMA BIOMEDICALS, T-4037	Corticotropin-Releasing Factor	Optic lobe; gastric ganglion	(Baldascino et al. 2017; Suzuki, Muraoka, and Yamamoto 2003)
FMRFamide	Immunostar, 20091	FMRF-amide	Retina; gastric ganglion	(Baldascino et al. 2017; Di Cristo et al. 2002)
Tyrosine Hydroxylase	Millipore, AB152	Tyrosine hydroxylase	Gastric ganglion	(Baldascino et al. 2017; Ponte and Fiorito 2015)
Noradrenaline	GemacBio, AP006	Noradrenalin	Gastric ganglion	(Baldascino et al. 2017;

				Ponte and Fiorito 2015)
Octopamine	GemacBio, AP007	Octopamine	Gastric ganglion	(Baldascino et al. 2017; Ponte and Fiorito 2015)
Common type of Choline Acetyltransferase	Not available (NA)	Choline acetyltransferase	Supra/suboesophageal masses; gastric ganglion	(Baldascino et al. 2017; Casini et al. 2012; Sakaue et al. 2014)

Tab. 3.1. Summary of antibodies used in *O. vulgaris*. The table reviews all antibodies used in *O. vulgaris* IHC.

Concerning *in situ* hybridization (ISH), in *O. vulgaris* tissues a few studies have been performed. These are listed in Tab. 3.2.

Probe tested	Tissue tested	Reference
Gonadotropin-Releasing Hormone	Central nervous system (supraesophageal part, subesophageal part, the optic lobe); heart, oviducal gland, and oviduct	(Iwakoshi-Ukena et al. 2004)
Acetylcholinesterase	Arm of embryos	(Fossati et al. 2015)

Tab. 3.2. Summary of ISH probes. A summary of *O. vulgaris* derived probes for ISH.

The scarce presence of ISH studies offers a window of opportunity to deepen our molecular knowledge of octopus, but on the other hand increases difficulties because of the lack of specific protocols.

The aim of performing histological analyses is to characterize the pattern of expression of particular receptors. Using fluorescent immunohistochemistry (FIHC) we were able to have an idea of receptors, with ISH we could appreciate the specific localization of selected RNAs of receptors.

3.2 Methods

3.2.1 Sample preparation

Tissues samples were fixed by immersion in a solution containing 4 % paraformaldehyde in phosphate-buffered saline (PBS) for an overnight at 4 ºC, then placed in PBS containing 30 % sucrose for at least 24 h. Samples were then frozen in optimal cutting temperature compound and cut in a cryostat into 12-µm-thick sections, placed onto starfrost® slides, let to dry for about two hours at RT and then stored at -80 ºC until used for histological analyses. Before usage, samples were dried at RT for one hour.

3.2.2 FIHC

For FIHC, sections were incubated for 24 hours with a primary antibody at 4 ºC and then washed three times with PBS for ten minutes each time. Primary antibodies used were anti-octopus rhodopsin (LSL- LB-5509, CosmoBio) and acetylated tubulin (T7451, Sigma-Aldrich). After washing, sections were incubated for two hours with a secondary antibody and then again washed three times with PBS for ten minutes each time. Second

antibody used were Goat anti-Rabbit, Oregon Green 488 (ThermoFisher) and Goat Anti-Mouse, Alexa Fluor 594 (ThermoFisher) at 1:4000 in PBS/0.1 % Tween-20 for both. Nuclei coloration was performed with 1:3000 Hoechst treatment with incubation of ten minutes, and subsequently washed three times with PBS for ten minutes each time. Slides were mounted with about a few drops of Aqua PolyMount mounting medium.

3.2.3 Probe preparation

Antisense probes (plus a control sense probe for rhodopsin) were prepared after plasmidic DNA extraction. Our plasmidic vectors containing inserts were previously linearized using two different restriction enzymes depending on their orientation, with either NotI or SphI (Termofisher). About 1 µg of linearized plasmid was used for reaction by using digoxigenin RNA Labeling Kit SP6/T7 (Roche) following the manufacturer suggestions. Then the retrotranscription reaction was blocked using ethylenediaminetetraacetic acid and RNA precipitation was obtained using isopropanol and ammonium acetate for overnight stored in – 80 ºC. After centrifugation at 4 ºC, obtained RNA was washed with ethanol and then resuspended. After spectrophotometric and electrophoretic quantification, the RNA probe obtained was diluted in zebrafish hybridization buffer (50 % formamide, 5X saline-sodium citrate buffer, 5mM EDTA at pH 8, 0.1% Tween-20, 0.1% CHAPS detergent (3-((3-cholamidopropyl) dimethylammonio)-1-propanesulfonate), 50 µg/mL heparin, 1 mg/mL torular RNA and water up to volume).

3.2.4 ISH

Probes were denatured at 70 ºC for ten minutes and put it on ice, then an aliquot of ~200 µl for each slide was added, covered with coverslips and incubated in a humid chamber at 65 ºC overnight. A series of washes were performed in a slide rack, the first with washing solution for 15 min at 65 ºC to remove the coverslips, then three washes with washing solution for 30 min at 65 ºC and subsequently two washes with maleic acid buffer containing Tween 20 (MABT) 1X for 30 min at room temperature (RT). Then, 1 ml per slide of blocking solution was added, and they were stored for about two hours at RT in a humid chamber. On each slide, 200 µl of anti-digoxygenin antibody (1:2500 in blocking solution) were added and after coverslips were applied, they were incubated overnight at RT in a humid chamber. The day after, slides were washed in the slide rack with MABT for 30 minutes at RT. On each slide, 200 µl of the chromogenic solution were added; this contains 5-bromo-4-chloro-3-indolyl phosphate and nitro blue tetrazolium, ready to use, Sigma) and left for detection at RT (or 14 ºC for slow detection) as needed. Once a clear signal was detected, the chromogenic reaction was stopped, washing slides tree times for five minutes in PBS. Nuclei coloration was performed with 1:3000 Hoechst treatment with incubation of ten minutes and subsequently washed three times with PBS for ten minutes each time. Slides were mounted with a few drops of Aqua PolyMount mounting medium.

3.2.5 ISH+FIHC

In particular cases, ISH was followed by FIHC primary described. FIHC was performed after a clear ISH signal was detected. At the end, slides obtained were treated with Hoechst coloration as previously and mounted.

3.3 Results

3.3.1 FIHC

In Fig. 3.1 are summarized the expression features found within octopus arm sections. We identified six types of expression feautres. A and B types are globular structures; the first one is clearly innervated and found in correspondence with intramuscular nerve cord, with rhodopsin staining present as a ring of cells and acetylated tubulin signal colocalizing with some cells. Type B is a glomerular structure found in arrays, roughly organized in lines beneath the sucker; they diffusely co-express rhodopsin and acetylated tubulin. Type C is present beneath chromatophores. In particular, such signal is associated to chromatophores positive to acetylated tubulin. Type D is associated with the axial nerve cord, strongly stained for both acetylated tubulin and rhodopsin, sometimes with some overlap, and marking a thick nerve that proceeds towards the sucker. Isolated cells and neuritis for rhodopsin and acetylated tubulin constitute type E, found in the infundibulum; a few of them colocalize. Type F represents the sucker ganglion, in which the half section looking towards the sucker is positive to acetylated tubulin with colocalization of rhodopsin.

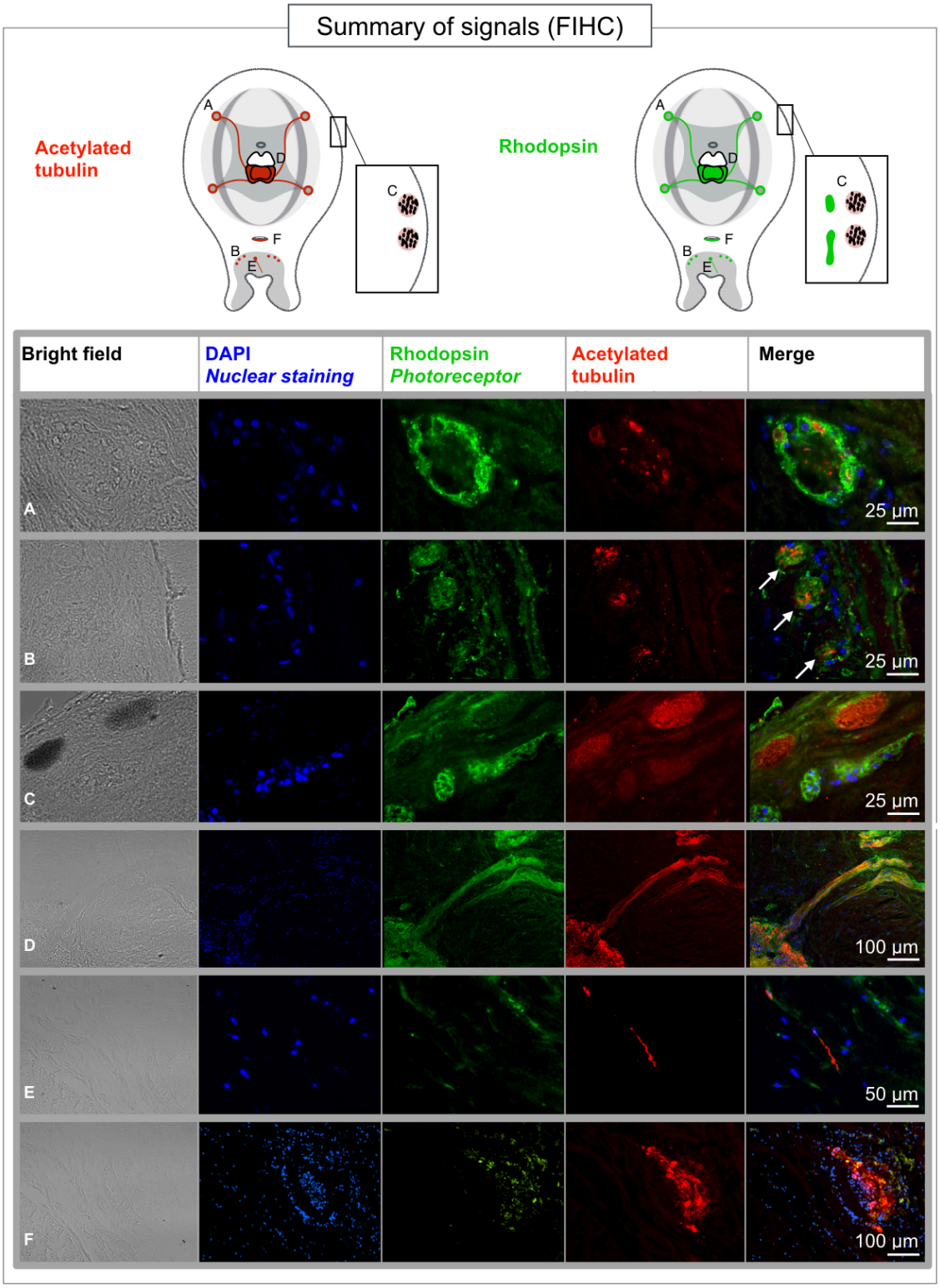

Fig. 3.1. FIHC signals summary. Expression features for each antibody within the octopus arm are summarized on top, red for acetylated tubulin and green for rhodopsin; letters indicate the position from which micrograph were taken.

In micrographs, DAPI is in blue, acetylated tubulin in red and rhodopsin in green, yellow showing colocalization of rhodopsin and acetylated tubulin, and magenta highlighting colocalization of DAPI and acetylated tubulin. White arrows highlight expression features when needed.

3.3.2 ISH

The expression features found with ISH and ISH+FIHC are subdivided according to the probe used for histological analysis. When we performed ISH+FIHC the ISH signal visible in the bright field was turned in green in the merged micrographs.

Fig. 3.2 summarizes expression features found for matrix metalloproteinase (MMP) probe, our control.

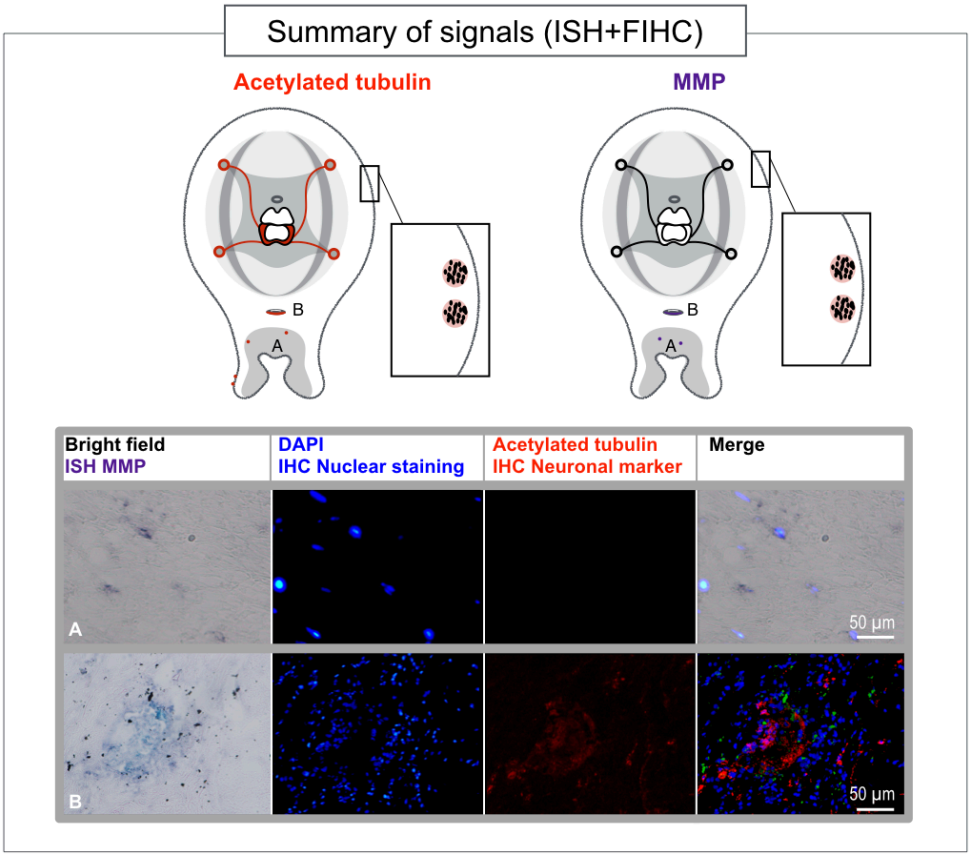

Fig. 3.2. MMP signals summary (ISH, ISH+FIHC). On top are summarized the expression features within the octopus arm section for MMP probe (ISH), red for acetylated tubulin (FIHC), letters indicate the position from which micrographs were taken.

In micrographs DAPI is shown in blue, acetylated tubulin in red and MMP is visible in the bright field in purple; for the merge, in row A the colors are purple for MMP and blue for DAPI, and in row B the MMP is green, yellow showing colocalization of MMP and acetylated tubulin, magenta highlighting colocalization of DAPI and acetylated tubulin.

Feature A shows isolated cells found within the acetabular and infundibular part of a sucker. Acetylated tubulin was not tested, but a clear colocalization for DAPI is present. Feature B represents a sucker ganglion with MMP signal, with no obvious colocalization with acetylated tubulin.

Fig. 3.3 summarizes the expression features found for rhodopsin probe.

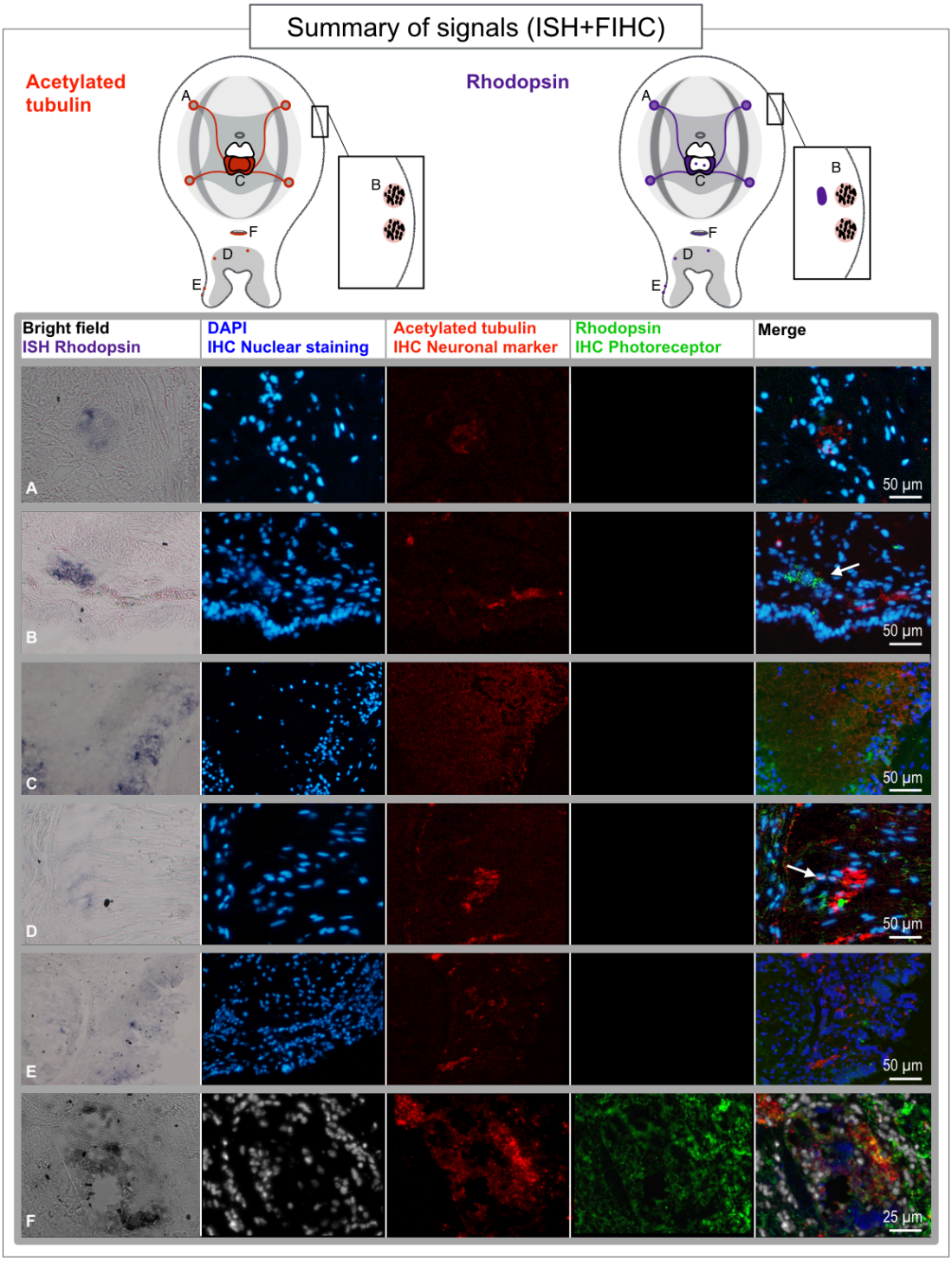

Fig. 3.3 Rhodopsin signals summary (ISH+FIHC). On top are summarized the expression features within the octopus arm section for rhodopsin probe (ISH), red for acetylated tubulin (FIHC), letters indicate the position from which micrographs were taken.

In micrographs DAPI is shown in blue (in raw F in gray), acetylated tubulin in red and rhodopsin is visible in the bright field in purple (in raw F in black), within the merge the rhodopsin is green, yellow show colocalization of rhodopsin and acetylated tubulin, magenta e colocalization of DAPI and acetylated tubulin. In row F we maintained the same color of single micrographs, except for ISH rhodopsin that has been turned on blue. White arrows highlight expression features when needed.

We identified six types of expression features. The A is a globular feature within the intramuscular nerve cord, and no colocalizations with acetylated tubulin are present. Type B is a chromatophores-associate signal beneath chromatophores positive to acetylated tubulin. Type C is associated with the axial nerve cord, in particular in the cellular layer toward the sucker, but some isolated cells are present even in the neuropil. Isolated cells are shown in type D and they are found in the acetabulum; colocalizations are not visible. Type E is a diffused signal located within the epithelium, the rim of the sucker. Type F is the signal present in the sucker ganglion, colocalization with acetylated tubulin is diffusely present; the signal of anti-rhodopsin antibody (FIHC) seems disturbed.

In Fig. 3.4 are summarized the expression features found for metabotropic glutamate receptor (MGR) probe, our taste-like receptor.

Expression features are three typologies. Type A corresponds to the intramuscular nerve cord, and there are no colocalizations with acetylated tubulin, even if it is clearly innervated. Type B is associated with the axial nerve cord, in particular in the cellular layer towards the sucker. Type C is present within the sucker ganglion, more intensely in the half section facing the sucker.

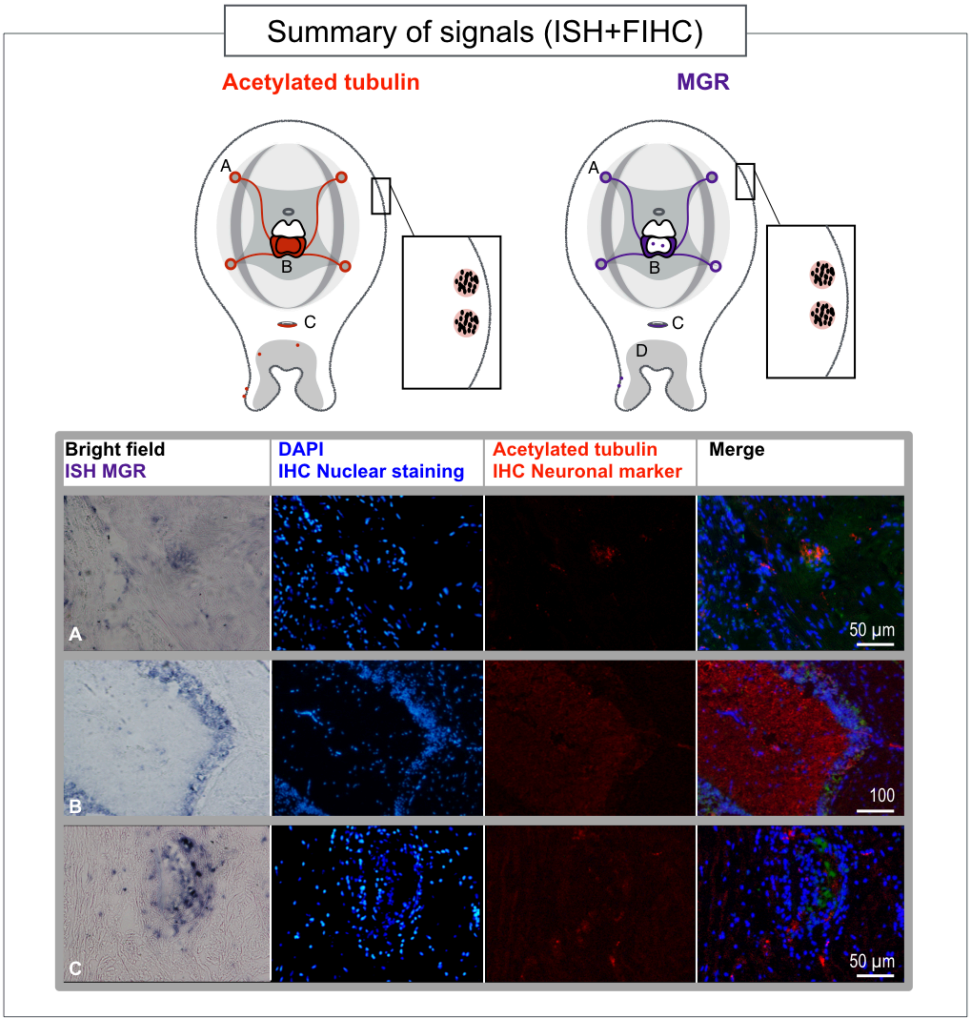

Fig. 3.4 MGR signals summary (ISH+FIHC). On top are summarized the expression features within the octopus arm section for MGR probe (ISH), red for acetylated tubulin (FIHC), letters indicate the position from which micrographs were taken.

In micrographs DAPI is shown in blue, acetylated tubulin in red and MGR is visible in the bright field in purple, within the merge the MGR is green, yellow show colocalization of MGR and acetylated tubulin, magenta e colocalization of DAPI and acetylated tubulin.

In Fig. 3.5 are summarized the expression features found for TAAR probe, our odorant-like receptor.

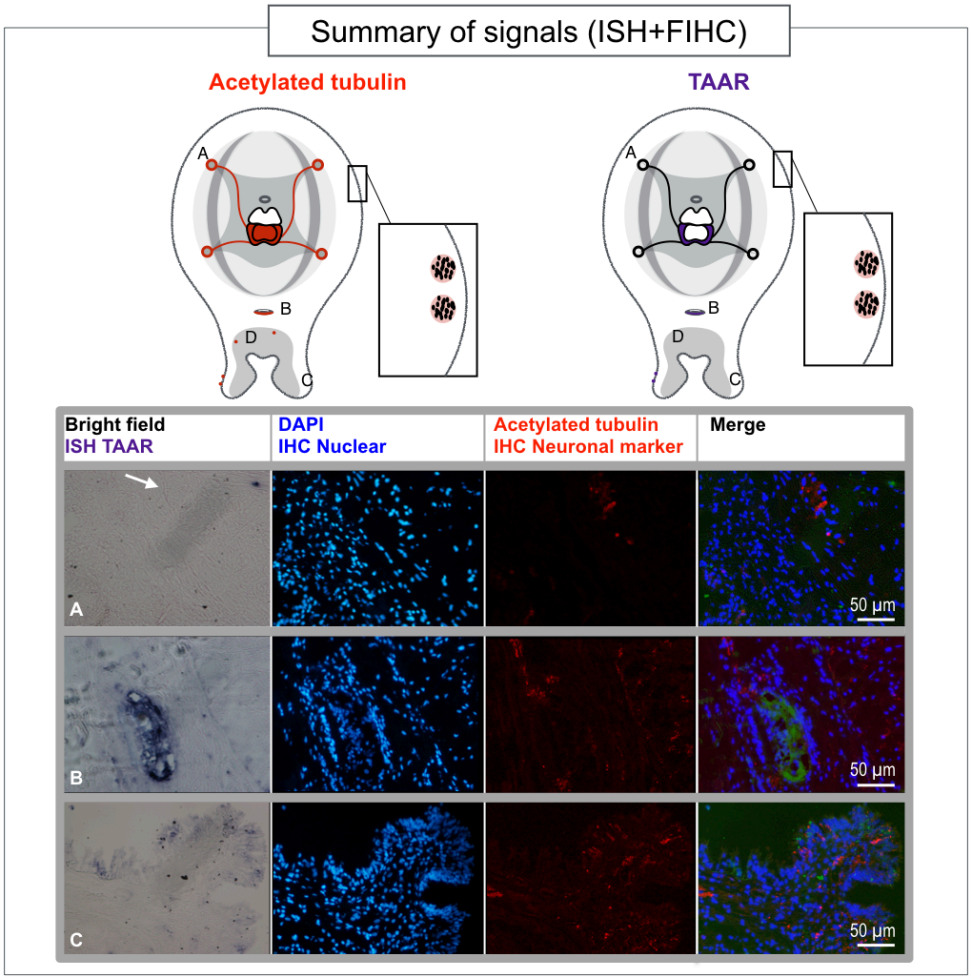

Fig. 3.5 TAAR signals summary (ISH+FIHC). On top are summarized the expression features within the octopus arm section for TAAR probe (ISH), red for acetylated tubulin (FIHC), letters indicate the position from which micrographs were taken.

In micrographs DAPI is shown in blue, acetylated tubulin in red and TAAR is visible in the bright field in purple, within the merge the TAAR is green, yellow show colocalization of TAAR and acetylated tubulin, magenta e colocalization of DAPI and acetylated tubulin.

3.4 Discussion

Some expression features obtained with ISH are not persuasive, because they recur for the vast majority of tested probes. For example, all of our probes stained the sucker ganglion, and this might be related to the particular composition of this structure. Moreover, almost all probes present a diffused signal within the epithelium of the sucker, the rim; in this case, the tissue is particularly folded, so that chromogens may tend to be accumulated within the folds, and the presence of a mucus rich in mucopolysaccharides might increment this interaction. Another common observation is the presence of staining within the cellular layer of the axial nerve cord; this feature is not characterized in literature, and its function and composition are still unclear.

However, it must be considered that the genes selected for the analysis are all GPCRs, and for this reason they might share metabolic and histological characteristics.

Moreover, we were not able to identify a convincing colocalizations between acetylated tubulin signal (FIHC) and our probes (ISH), probably because the antibody was not able to rich the target if the chromogen was already on sections.

We mainly focused our attention on rhodopsin, for which we could implement FIHC because anti-octopus rhodopsin was commercially available. The features observed with FIHC were in some cases confirmed with the ISH analysis, even if with a lower resolution that at times alters the gross appearance of some structures. With both techniques, we observed signal within the intramuscular nerve cord: in FIHC, it was clearly a ring of more external cells, whereas in ISH it was inside the cord and more diffused. Similarly, we found a chromatophore-associated signal in the presence of chromatophores positive to acetylated tubulin, even if we observed that the morphology of chromatophores was

altered by ISH procedures. The ISH process requires high temperatures, and for this reason the pigments might have been damaged. Fortunately, we were still able to identify them. Both ISH and FIHC stain the sucker ganglion within the half section looking towards the sucker, the innervated one. We observed a signal within the axial nerve cord distributed in the neuropil for FIHC; in contrast, ISH signal was more concentrated within the cellular layer around the axial nerve cord, and some cells inside were also expressing rhodopsin. At last, we were even able to identify signals present in some isolated cells within infundibulum and acetabulum of the sucker.

We believe that, after excluding some artifacts that we found, there might be a chance for photoreceptors being directly connected to the peripheral nervous system. The presence of rhodopsin within the sucker and/or the skin may be significant, possibly serving for extraocular photoreception, and also the presence of the signal to different tissues suggests a photoreceptive function. Moreover, our results are consistent with other studies that hypothesize an extraocular photoreception mediated by the skin of cephalopods (Kingston and Cronin 2016; Ramirez and Oakley 2015). In the future, it would be interesting to implement and compare our results with other analyses on the transient receptor potential (TRP) gene. TRP has been found within the eyes of drosophila with a role of phototransduction, and it responds to rhodopsin-associated signal (Montell 2005).

Chapter 4: Robotic applications

Prologue

Octopus have inspired many technological innovatiotions from a robotic point of view. For the sucker, we can distinguish two different types of bioinspiration: one is merely based on morphology, and looks into sucker anatomy to translate its design into artificial adhesive solutions; the other looks into sucker sensing and composition to find evidence of particular receptors and how they are organized, aiming in develop new bioinspired materials. We were able to develop arrays of artificial suckers cured with an adhesive patch using a mollusk protein; this might be useful for biomedical applications. Based on our histological screening, eventually we might be able to implement octopus-based innovative materials, possibly useful as bioinspired sensors or optoelectronics depending on the molecule used.

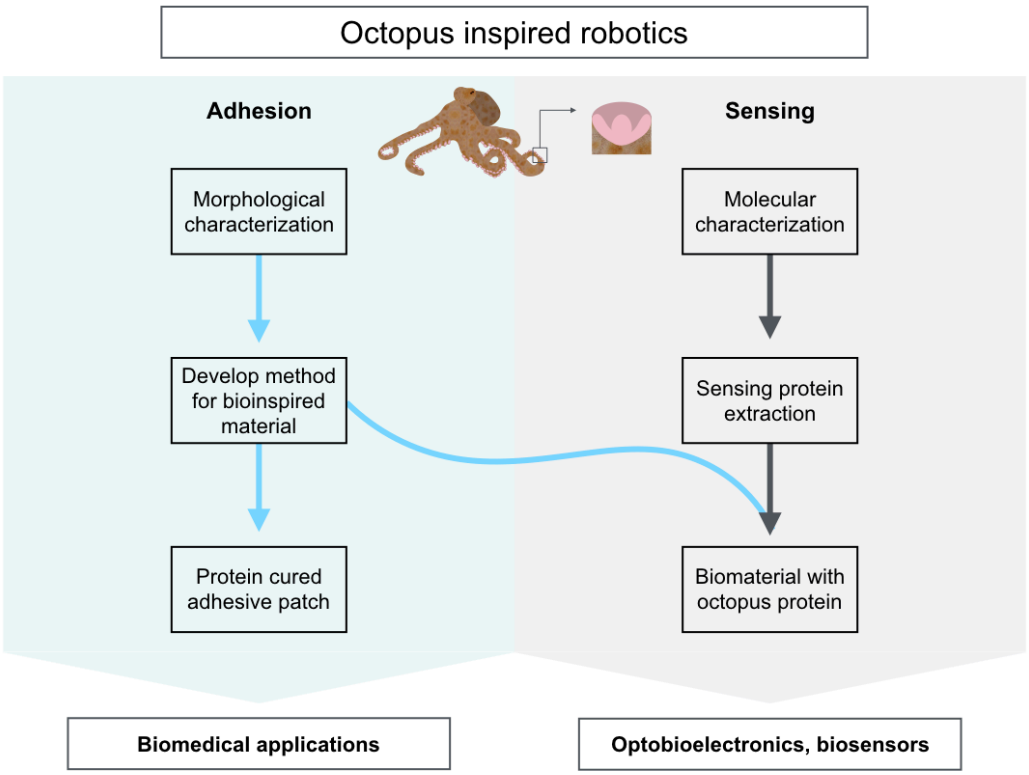

Fig. 4.1. Octopus-inspired robotic application. A schema of possible applications of octopus-inspired devices.

Since the molecular characterization of octopus sensing receptors is a long process, we focused our primary attention on the adhesion mechanism of a sucker to bring forward sucker-inspired devices by combining them with a mollusk protein. For this application, we used a mussel protein that is involved in the adhesion mechanism of the animal to obtain a device with increased adhesion, laying the foundations of a curing method that in future might feature octopus-derived proteins. In Fig. 4.1 we schematize this concept.

A number of devices inspired by the octopus sucker already exist in the literature. However, they lack a satisfactory standardization of the manufacturing process, or allow only non-reversible adhesion.

We summarized the state of the art about devices inspired by the octopus suckers in table 4.1, evidencing each aspect relevant for our analysis, such as resistance to underwater environments, materials, dimensions, target surface and the possibility to reverse the adhesion.

Our robotic application is presented in this chapter formatted as a scientific manuscript because we are preparing for publishing.

Reference	Description	Material	Sucker dimensions	Preloads tested	Maximum adhesion achieved	Tested in water	Surface tested	Standardized fabrication	Reversibility
(Tramacere et al. 2012)	One single sucker tested for pull-off with imposed suction	Dragon-Skin, Ecoflex 00-30	1.5 cm diameter for the acetabulum, 2 cm diameter for the infundibulum	NA	8 N (loading)	Yes	Aluminum, Delrin®, Plexiglas®	Yes	Stopping vacuum
(Follador, Tramacere, and Mazzolai 2014)	Dielectric elastomer actuator connected to a passive suction sucker	Acrylic (VHB 4905) and Dragon-Skin	NA	NA	Yes	NA	Yes	NA	NA
(Tomokazu et al. 2015)	Vacuum powered gripper	Silicone	Gripper with a diameter of 60 mm, which has 21 suckers with a diameter of 6 mm	NA	640 gf	Yes	Aluminum	Yes	Stopping vacuum
(Tramacere et al. 2015)	One sigle sucker tested for pull-off with imposed suction	Ecoflex 00-30, Ecoflex 00-50, and Dragon Skin 10; Smooth	Different morphology of grooves in sucker surfaces	NA	9.8 N (loading)	Yes	NA	Yes	Stopping vacuum
(Baik et al. 2017)	1*1 cm patch with internal suckers tested for pull-off	Polyurethane-acrylate-based polymer	15 µm, 50 µm, 150 µm or 500 µm in diameter	10–35 kPa	160 kPa	Yes	Silicon wafer	No (obtained with trapped liquid droplets)	Peeling-off
(Chen and Yang 2017)	1*1 cm patch with external suckers tested for pull-off	Polydimethylsiloxane (PDMS)	250 nm	NA	3 N	No	Glass, porcine (pig) heart	No (obtained with silica colloidal crystals)	NA
(Sareh et al. 2017)	One single sensorized sucker for anchoring with vacuum	Ecoflex 00 – 30/Dragon Skin 00 – 10, quantum tunneling composite	NA	NA	1.09 N (loading)	No	Aluminum, wood	Yes	NA
(Baik et al. 2018)	1*1 cm patch with external suckers tested for pull-off	NA	15, 50, and 500 µm in diameter	10–35 kPa	12 N/cm^2	Yes	Silicon wafer, hairy skin	No (obtained with trapped liquid droplets)	Peeling-off (up to 15 mJ)

(Chun et al. 2019)	1*1 cm patch sensor with micro-suckers	Graphene -coated PDMS	100 µm in diameter	NA	4 N/cm^2	Yes	Silicon wafer, skin	No (obtained with silica colloidal crystals)	NA

Tab. 4.1. Summary of octopus-inspired sucker devices. List of existing devices inspired by the octopus sucker.

4.1 A protein-cured micro-sucker patch inspired by the octopus sucker

Gabriella Meloni[1,2]*, Omar Tricinci[3], Andrea Degl'Innocenti[3], Barbara Mazzolai[1]*

[1] Center for Micro-BioRobotics; Istituto Italiano di Tecnologia; Viale Rinaldo Piaggio 34; 56025; Pontedera (Pisa); Italy

[2] The BioRobotics Institute; Scuola Superiore Sant'Anna; Viale Rinaldo Piaggio 34; 56025; Pontedera (Pisa); Italy

[3] Smart Bio-Interfaces; Istituto Italiano di Tecnologia; Viale Rinaldo Piaggio 34; 56025; Pontedera (Pisa); Italy

4.2 Abstract

In medical robotics, micromanipulation becomes particularly challenging in the presence of blood and secretions. Nature offers many examples of adhesion strategies that can be divided into two macro-categories: morphological optimizations and chemical mechanisms. This paper analyzes how two successful adaptations from different marine animals can converge into a single biomedical device usable in moist environments. Taking inspiration from the morphology of the octopus sucker and the chemistry of mussel secretions, we developed a protein-cured octopus-inspired micro-sucker device

that retains in moist conditions roughly 50% of its dry adhesion. From a robotic perspective, this study emphasizes the advantages of taking inspiration from specialized natural solutions to optimize standard robotic designs.

4.3 Introduction

In robotics, a fundamental aspect of grippers and micromanipulators is adhesion; improving adhesion capabilities of robotic devices can simplify the manipulation of compliant or slippery objects (Dejeu et al. 2009; Gauthier and Régnier 2011; Mishra et al. 2017; Zesch, Brunner, and Weber 1997). Adhesion is also a basic requirement for the locomotion of climbing robots (Chu et al. 2010; Grieco et al. 1998; Menon, Murphy, and Sitti 2004). In the last years, it became common to take inspiration from adhesive structures diffused in nature to develop artificial adhesion solutions. Several organisms are naturally provided with different strategies for adhesion, depending on their habitat and on the physiological function of the attachment (Bhushan 2009; Gorb 2008). *Galium aparine* is a climbing plant that anchors to substrates mechanically by leveraging its hooks; geckos exploit fibrillar matrices covering their pads to adhere to vertical or inverted surfaces (Hennebert et al. 2015). A high number of adhesive robots have been derived from biological models, suggesting a general validity for the method (Andrews and Badyal 2014; Baik et al. 2017; Fiorello, Tricinci, and Mishra 2012; Mahdavi et al. 2008; Murphy, Aksak, and Sitti 2009).

When looking at different natural strategies to implement adhesive artifacts, it is important to consider the characteristics of the environment in which one wants to

operate. An organ evolved for dry adhesion might be not as successful in wet conditions, and vice-versa. For biomedical applications, the challenge is often to develop new materials and devices that solidly interact with different tissues without causing damage.

In nature, adhesion strategies can be divided into two macro-categories: those depending on morphology and others based on chemical interactions. Among the natural solutions for wet adhesion relying on morphology, a remarkable example is the octopus sucker (here we refer in particular to *Octopus* spp.). This is a flexible organ deputed to the reversible adhesion to different materials, with a crucial role for sensing, grasping and body anchoring (Kier and Smith 2002; Tramacere et al. 2012; Wells 2013). A sucker is roughly composed by two distinct concavities: an external cup named *infundibulum* connected to an *acetabulum*, a more internal chamber with a central protuberance (Kier and Smith 2002; Wells 2013). To reach vacuum, at first infundibular muscles are contracted, maximizing the contact area between infundibulum and substrate. Then, acetabular muscles are contracted, both to push water inside the cup and to minimize space between the infundibulum and the acetabular protuberance, generating increased friction and a negative force (Smith 1991; Tramacere, Beccai, M. Kuba, et al. 2013). The key aspect for the adhesion of such a structure is conformability, which depends on a peculiar muscle distribution allowing the sucker to adapt to various objects and textures. Throughout the octopus skin, there is a kind of mucus that is not precisely described, but seems to be composed of mucopolysaccharides and glycoproteins, which may be involved in the mechanical reduction of friction to facilitate adhesion (Potts 1967; Wells 2013). Instances of artificial octopus-inspired suckers are already available, each one implementing different aspects of their biological counterpart. Some of these devices

focus on the morphology of a single sucker, the presence of grooves in the infundibulum, and the role of vacuum in the adhesion (Tramacere et al. 2012, 2015). The actuator developed by Follador *et al.* (Follador et al. 2014) exploits the passive deformation of a sucker for the activation of the device. Suckers are also present in a gripper proposed by Tomokazu *et al.* (Tomokazu et al. 2015), in which they ensure an excellent grasp of objects with different shapes. All these examples need an external vacuum pump either to activate the grabbing (Tomokazu et al. 2015) or just to maintain a stable internal pressure (Follador et al. 2013; Tramacere et al. 2012, 2015). Other devices only mimic the compliant design of an octopus sucker, as in the case of adhesive patches that rely solely on the deformation of miniaturized suckers when external pressure is applied (Baik et al. 2017, 2018; Chen and Yang 2017). Chun and colleagues (Chun et al. 2019) use this strategy to develop a sensorized wearable electronic gear for health monitoring. The aforementioned examples of octopus-mimicking designs confirm an increasing interest in octopus bioinspiration for new solutions in robotics and medical care.

Another mollusk, the mussel *Mytilus edulis*, utilizes a different mechanism to chemically adhere to submerged or moist substrates: the secretion of adhesive proteins. In mussels, adhesion is mediated by *byssus*, a coriaceous bundle of protein filaments that builds a plaque anchoring the mussel to various surfaces (Lee, Lee, and Messersmith 2007; Lee, Scherer, and Messersmith 2006; Lin et al. 2007). The adhesive proteins involved in the byssus formation are known as mussel foot proteins (mfps). The gluing power of these proteins is due to the presence of the amino acid 3,4-dihydroxy-L-phenylalanine, an unusual form of hydroxylated tyrosine residues (Hwang, Gim, and Cha 2008). There are different types of mfp; their capacity to adhere depends on the proportion of 3,4-

dihydroxy-L-phenylalanine residues, with the mussel foot protein-1 (mfp-1) being the stickiest mfp (Lin et al. 2007; Waite and Qin 2001). Byssus already influenced a few robotic applications, such as an adhesive inspired to the pads of geckos and coated with a molecule that imitates the sticky proteins of mussels (Lee et al. 2007). The mussel foot attachment has also been studied to develop new materials that aid the self-healing of wounds (Holten-Andersen et al. 2011; Lin et al. 2007).

With this work, we present a device that combines the morphology of the octopus sucker and the chemical properties of the mussel foot for reversible adhesion in wet conditions. Our product is composed of an array of micro-suckers cured with an mfp; it is soft and highly biocompatible, allowing a safe interaction with biological tissues. In comparison with previous wet-tolerant patches (Baik et al. 2017, 2018), our device may prove especially useful when a high level of reproducibility is desired, both between single micro-suckers in a given array and in terms of standardization of different fabrications.

Among other potential uses, wet-tolerant devices like the one we propose are helpful supplements for common medical robotic platforms, to provide reliable attachment to tissues when blood and secretions are present. Adhesive patches also promote the regeneration of wounds, and may become part of body sensors or drug delivery systems even in particularly moist locations, such as the eye (Chen and Yang 2017; Chun et al. 2019; Kong et al. 2019; Trujillo-de Santiago et al. 2019).

4.4 Results

4.4.1 Device fabrication

Millimetric square arrays of micro-suckers in polydimethylsiloxane (PDMS) were obtained from molds produced by direct laser lithography; each sucker is composed of a pillar harboring a spherical infundibulum-like bulge, as shown in Fig. 4.2. Flat PDMS surfaces served as negative controls for all downstream procedures.

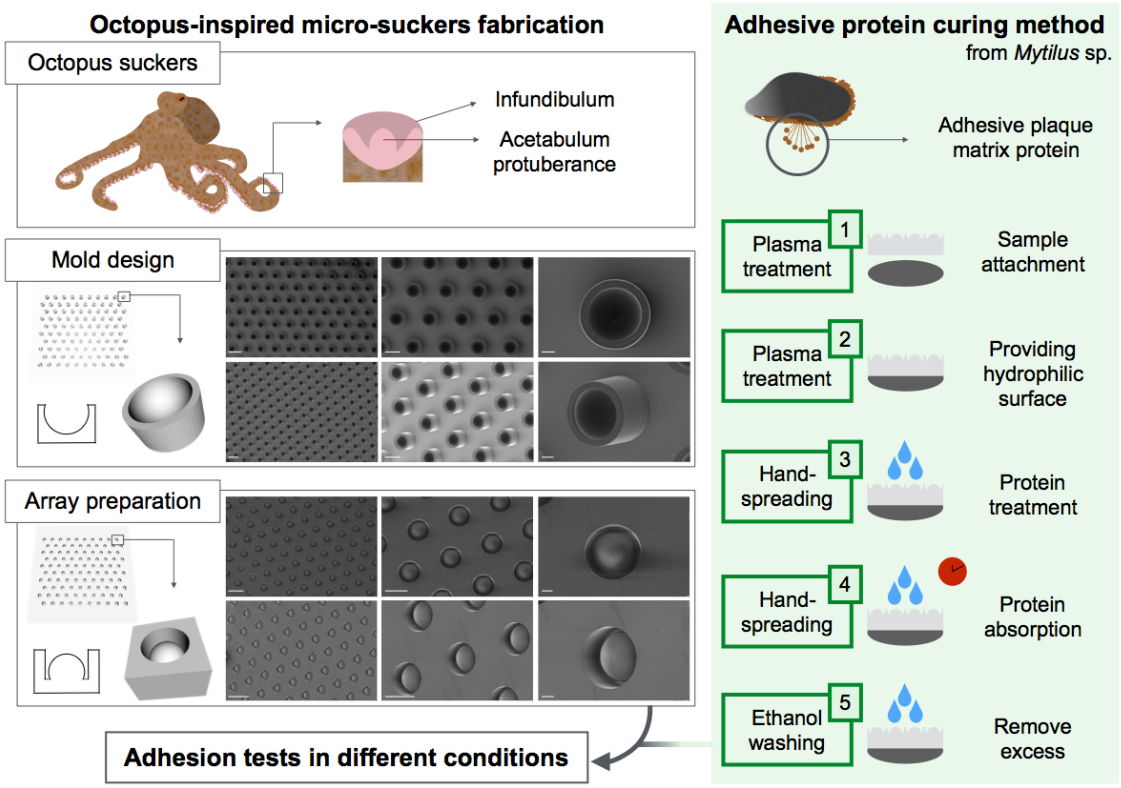

Fig. 4.2. General framework. Octopus arms with suckers; a magnified box shows a sucker section. Mold design box shows the mold array model, a magnified box shows a 3D model of a single mold-sucker, on left the simplified profile of a single cavity. SEM images show mold array in top lane is an orthogonal view, the bottom lane is oblique view; scale bar images are 200 µm on left, 100 µm on central and 20 µm on right. Array preparation box shows the final array model, a magnified box shows a 3D model of a single sucker-like structure and, on the left simplified profile of a single cavity. SEM images show PDMS array, top lane is an orthogonal view, the bottom lane is oblique view; scale bar images are 200 µm on left, 100 µm on central and 20 µm on right. The green box shows the outline of the curing method with adhesive plaque matrix protein.

4.4.2 Preliminary optimizations of protein coating

Samples were coated with an mfp-1 solution; some received instead a control treatment. We initially tested two different protein concentrations, and carried out adhesion tests (n=3, ten repetitions each, Fig. 4.3) in a dry environment, quantifying attachment as a function of imposed preloaded pressures.

In these conditions, adhesion is mildly enhanced in the presence of proteins, and this becomes more evident for micro-sucker arrays vs. control (flat) surfaces (Fig. 4.3). Best results were achieved with a 0.1 mg/ml mfp-1 coating solution. In turn, micro-suckers *per se* do not seem to have major effects under tested circumstances.

4.4.3 Adhesion tests in dry and wet environments

Further adhesion experiments (n=3, ten repetitions each, Fig. 4.3) were invariably performed in the presence of protein coating (coating solution 0.1 mg/ml mfp-1), again for micro-sucker arrays or flat PDMS surfaces as controls. Each sample was first tested in dry conditions; in order to probe protein coating stability, a second dry experiment was then performed. Two other tests served to assess adhesion properties when a drop of fluid was added: the first was carried with deionized water, the second one with a saline buffer at pH 7.5, closer to the natural marine environment (S. Kim et al. 2017).

Adhesion does not visibly decrease when an experiment in dry conditions is repeated. The two different wet experiments yield comparable results. Suckers do not seemingly offer particular advantages in dry circumstances under experimental settings. However,

when some moisture is added the system clearly needs suckers to retain relevant adhesive properties. This becomes particularly obvious regrouping data into two macro-categories,

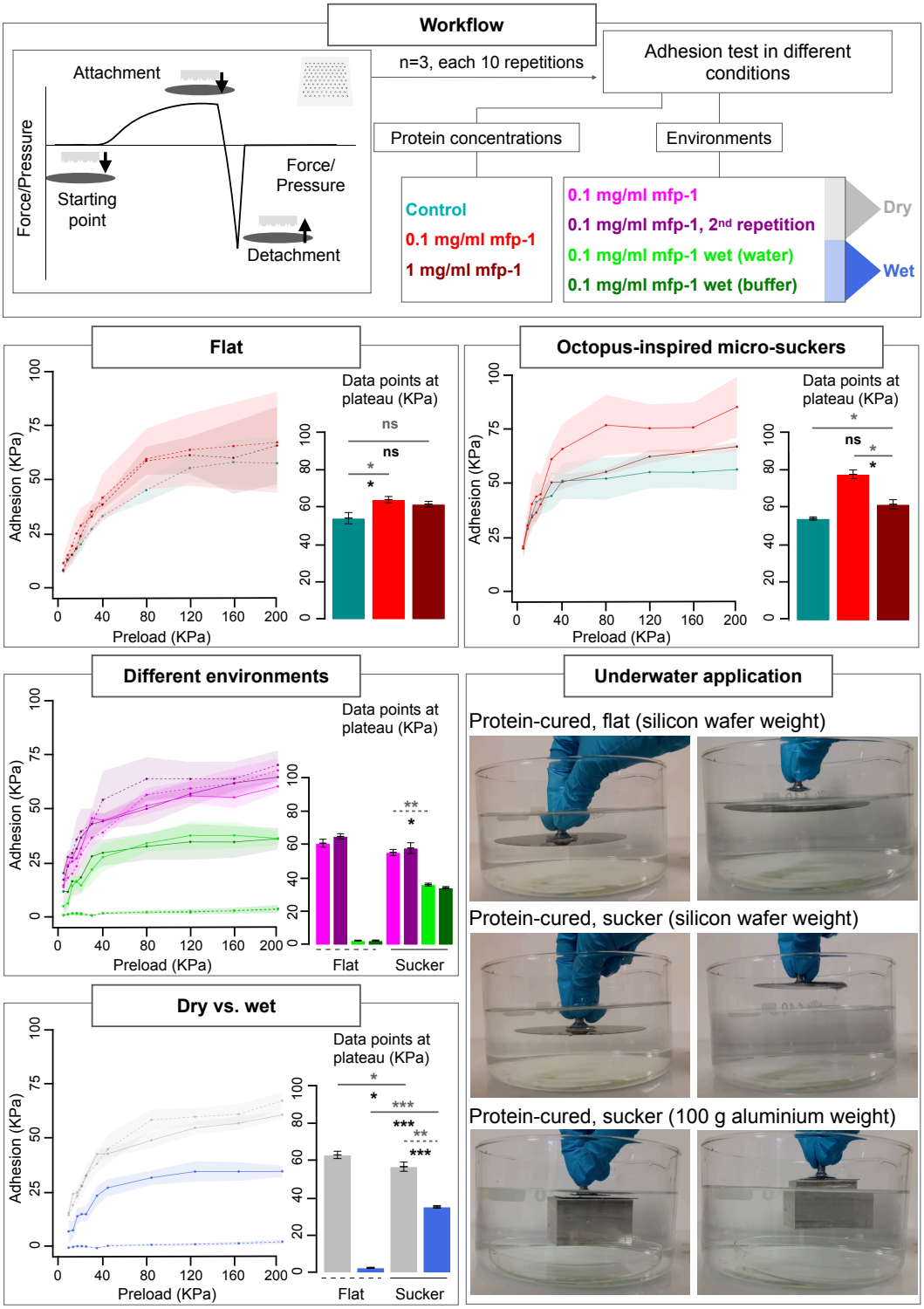

namely all dry and all wet experiments (Fig. 4.3).

Fig. 4.3. Adhesion tests in different conditions. The left top box shows a simplified graph of the measurement of force, in which the detachment moment is the adhesion force; the left top box lists all tested conditions, each one represented with different colors. Dotted line indicates control experiments with flat surface device. Continuous line indicates experiments with octopus-inspired micro-sucker device. Error bars report standard error of the mean. Bar plots represent the n=4 plateau points of curves. The significance level is specified by asterisks for different p-value thresholds (ns for $p > 0.05$, *for $p < 0.05$, **for $p < 0.01$, ***for $p < 0.001$); continuous lines indicate unpaired two-tailed T-test and dotted lines paired two-tailed T-test, gray asterisk are for T-test and black asterisks for two-tailed Mann-Whitney U-test; error bars report standard error of the mean. The right box represents the underwater application; images are screenshots from the demonstrative Supplementary Video S1.

4.4.4 Demonstrative application underwater

As a practical demonstration, we tested a wider array of protein-cured micro-suckers underwater. The array was attached to a grip, then pushed by hand against a submerged weight found in the bottom of a beaker, and slowly lifted vertically beyond the water surface; after that, the detachment was attempted by tilting the grip towards one side.

Our device was able to collect a silicon wafer, as well as a 100 g aluminum block; tilting the grip proved sufficient to achieve intentional detachment. An analogous flat device, tested in identical conditions, failed already to collect a silicon wafer, see Fig. 4.3 and Supplementary Video S1.

4.5 Discussion

The present work highlights the possibility to implement protein-cured octopus-inspired micro-suckers in robots and plasters to improve object adhesion in moist environments. Our device achieves underwater attachment by combining morphological adaptations of octopi with molecular features of mussels.

Confirming literature, we found the protein alone to display relevant adhesive properties. Micro-suckers do not offer particular advantages in the tested dry conditions. However, the protein coating becomes more effective when micro-suckers are present; one might think this is because suckers increase surface, but the most effective protein concentration was the lowest investigated, rather suggesting a synergy between the physical adhesion provided by suckers and the chemical stickiness attributable to mfp-1. Consistent with the idea that impurities might alter the functioning of a morphology-based adhesive, the decreased performance of the higher tested concentration vs. the lower one hints to an excess of protein cluttering suckers. An ideal protein concentration should trade off gluing effects against disturbance of the mechanical action of suckers. Fine tuning might enhance performances, and will also depend on final use. Adhesion stands multiple experiments, showing at least some robustness of the design. Unexpectedly, the use of a saline buffer instead of pure water was largely dispensable under our settings.

In a moist environment, protein plus micro-suckers are ~ 14 times more adhesive than a flat surface with protein; roughly fifty percent of the dry adhesion is retained when protein-cured micro-suckers are exposed to moisture. The adhesion of flat device in water drops instead to almost nothing even in the presence of mfp-1, and this is evident also in

practical demonstrations: a flat sample could not keep attachment when presented to minor disturbances, *i.e.* the reaching of the water surface.

Likely due to positional effects when placing samples, the use of a single sample for different experimental classes reduce data dispersion; this indicates that the direction of pressure is important, namely that pushing must be orthogonal to the surface. While this property might be a limitation for some applications, it might turn useful for others. For instance, at the end of our demonstrative video we intentionally detached the recovered objects.

Silicone materials have been widely used in medical applications. In particular, PDMS satisfies standard criteria for biocompatibility not causing irritation and sensitization when in contact with biological tissues. In fact, PDMS-based devices have also been approved for long-term usage implants, also thanks to the introduction of anti-bacterial treatments (Khorasani, Mirzadeh, and Sammes 1999; Kim et al. 2011; J. H. Kim, Park, and Seo 2017).

The proven biosafety of PDMS allows the deployment of our proposed protein-cured micro-sucker adhesive patch in different medical usage, such as long-term implants for drug delivery, wound regeneration and body sensors, or in robotic platforms for surgical procedures, particularly in moist or wet conditions rather than dry environments.

4.6 Methods

4.6.1 Fabrication

The design of a single octopus-inspired micro-sucker was modeled with Blender (Blender Foundation). It consists of a cylindrical cavity with a depth of 75 μm and a diameter of 100 μm. Inside the cavity, there is a spherical bulge of diameter 85 μm and height 65 μm. The design of the mold was obtained from the negative of the model of the sucker. Molds were fabricated in IP-S photoresist (Nanoscribe GmbH) on glass substrates, by means of direct laser lithography (Photonic Professional system, Nanoscribe GmbH). For every mold, the glass substrate was rinsed with isopropyl alcohol and deionized water, and the negative tone IP-S photoresist was cast on it. The writing configuration of the Photonic Professional system was with the objective (25x, NA 0.8) in immersion in the photoresist. The mold was fabricated by exposing the photoresist to a laser beam (Calman laser source) at a center wavelength of 780 nm, using a writing speed of 15 mm/s with a power of 68.4 mW. The sample was developed for 20 min in SU-8 Developer (MicroChem Corp) and rinsed in isopropyl alcohol and deionized water. The final result was a square array mold of microstructures following a hexagonal lattice pattern with a spacing of 200 μm between the centers of each sucker. The area measured 25 mm^2, except for those patches used for practical demonstrations, which had an area equal to 1 cm^2.

Each PDMS patch was produced by means of a micro-molding technique from the micro-fabricated mold. The mold was chemically functionalized by means of silanization in order to ensure an easy detachment of the PDMS: the surface was activated in air plasma for one minute at 50 W, and evacuated to 650 mbar below atmosphere together with 3 ml solution 0.3% v/v of Trichloro(1H,1H,2H,2H-perfluorooctyl)silane in cyclohexane. PDMS (monomer and reticulation agent in a 1:10 ratio) was cast onto the mold in a Petri

dish, reaching a thickness of 1 mm. The curing was carried out for 24 h at room temperature in vacuum. The sample for the adhesion tests was cut with a surgical blade under an optical microscope (Fig. 4.2). A 25 mm^2 PDMS array was totally composed of 168 micro-suckers. To verify the standardization of the fabrication process, micrographs of both molds and casts were taken with a scanning electron microscope (SEM).

For each sample, a flat control was cut from the same cast in a region without micro-suckers, in order to reduce fabrication variability between adhesive samples and relative controls. Each mold was used several times after rinsing and subsequent silanization.

To achieve a permanent and stable attachment of the PDMS patch to its support (a silicon wafer), a plasma treatment was performed on both ends. Plasma exposes hydroxyl groups on the silicon wafer and sinalon groups on PDMS, allowing the formation of a strong Si-O-Si covalent bond. As PDMS is a hydrophobic material, a second plasma treatment was performed to provide a hydrophilic surface. This method, known as *hydrophilic functionalization*, also increases biomolecular adsorption (Bhattacharya et al. 2005). Both treatments were carried out in an oxygen plasma system for 30 seconds, at a power of 30 W and a pressure of 20 mBar.

4.4.2 Protein curing

PDMS patches were coated with *Mytilus edulis* mussel foot protein 1, mfp-1, commercially available as Native Mussel Adhesive protein (ab155708 from Abcam); the stock concentration was 1 mg/ml in 1% of acetic acid. Two concentrations of protein

were chosen, namely 1 and 0.1 mg/ml, invariably with 1% acetic acid. A 1% acetic acid solution was used as a control. A low amount of liquid (20 µl for 25 mm^2 and 80 µl for 1 cm^2) was spread on the patch surface. Solutions were kept for ten minutes under a chemical hood, enabling the evaporation of the acetic acid. Afterward, surfaces were washed with absolute ethanol to remove excess protein (Fig. 4.2).

4.4.3 Adhesion tests

Adhesion experiments were conducted with a custom-built multi-axis measurement platform integrated with a loading cell (ATI, Nano17), at room temperature. Each sample was mounted by its support on a metal screw, and then orthogonally pushed against a silicon wafer with different preloads (4, 8, 12, 16, 20, 30, 40, 80, 120, 160, 200 kPa). When the imposed preload pressure is reached the loading cell starts the detachment. Within a single experiment, every preload pressure was tested ten times (Fig. 4.3).

We first performed a set of experiments in dry conditions, testing both protein concentrations. More precisely, we assessed adhesion for micro-suckers arrays and their flat controls in presence or absence of protein coating, in the latter case either at 1 or 0.1 mg/ml starting concentration. Different PDMS casts were used for each of three repetitions.

A second set of tests was conducted exclusively on protein-cured (0.1 mg/ml starting concentration) samples, namely micro-suckers arrays and their flat controls. For each of three repetitions, this time a single PDMS cast was used for all different experimental

classes: first, an experiment in dry conditions was performed twice; a third test was conducted after putting a 100 µl drop of deionized water on the area of the silicon wafer entering in contact with the sample. Finally, we added 100 µl of a saline buffer (0.1M acetate, 0.6M NaCl in PBS with a pH 7.5) were we previously place the water, and a further experiment was carried out.

4.4.4 Data analysis

Plots were obtained using a local R script using R. We produced line charts showing mean attachment pressures (± standard error of the mean) as a function of imposed preloaded pressures. Averaging the four highest mean attachment pressures for each curve, we also produced bar charts, reporting data dispersion as standard error of the mean. Two-tailed independent and dependent t-tests and Mann-Whitney U-test were performed when needed.

4.4.5 Demonstrative video

A crystallizer was filled with deionized water to demonstrate the ability to collect objects in water. A protein-cured flat device and a protein-cured micro-sucker device (each 1 cm^2 broad, with 0.1 mg/ml mfp-1 starting concentration) were mounted on a metal screw as a support holder. Both devices were tested by hand for the collection of a silicon wafer (3 inches of diameter, 380 µm of thickness) and a rectangular aluminum weight of 100 g (30x0x41 mm). In case the weight was successfully lifted beyond the water surface, the

detachment was attempted by tilting the support to one side. The procedure was taped for demonstration.

Chapter 6: Conclusion and future outcomes

This project for the first time looks into biology not only in a general overview as usually bio-inspired robotic does, but it gives a more insight individuating molecular aspects relevant in the sensing capabilities of the octopus. We believe that this study can constitute a milestone in molecular bio-inspiration for future steps.

The sensing receptors identified within this work seems strictly related to the peripheral nervous system, and even if additional functional studies are required, the results are sound. The method that we develop in the robotic application can be enforced with our octopus proteins.

6.1 Future steps on molecular biology

The next step in molecular biology will be the usage of the techniques of rapid amplification of cDNA ends (RACE); with RACE we will be able to clarify the regulation of genes studied deepening the tissue expression.

With RACE we will also be able to obtain the full-length sequences of our RNA transcripts. Once obtained the full-lengths, we can perform different analyses, one aiming to clarify the function of our genes or producing the proteins. For the first purpose, using the full-lengths genes we can express our genes in a different animal (*i.e.*, zebrafish) to understand if our genes can act in a different system. On the other hand, we will be able to produce the octopus proteins of studied genes building an expression vector to be used for protein synthesis. The proteins obtained can be purified and used as we did with

mollusk protein, or we can even produce crystals for performing structural biological analysis to study the molecular structure of the proteins and their interactions with other proteins or targets.

6.2 Future steps on biorobotics

Once obtained the purified proteins of selected genes from the molecular project, we will be able to use them, as we already did with the mollusk protein in the protein-cured adhesive device, developing new bio-inspired materials that can sense particular stimuli.

Chapter 7: Appendix

7.1 Introduction of collateral projects

During these three years, I have been involved in diverse collateral projects that allowed me to contextualize my work in a broader research environment.

The collateral projects in which I collaborated are three. For each one, I reported the abstract of the corresponding scientific productions:

1. Degl'Innocenti A., **Meloni G.**, Mazzolai B., & Ciofani G. (2019). A purely bioinformatic pipeline for the prediction of mammalian odorant receptor gene enhancers, *BMC Bioinformatics*. 20(1), 474.
2. Degl'Innocenti, A., Rossi, L., Salvetti, A., Marino, A., **Meloni, G.**, Mazzolai, B., & Ciofani, G. (2017). Chlorophyll derivatives enhance invertebrate red-light and ultraviolet phototaxis. *Scientific Reports*, *7*(1), 3374.
3. Mazzolai, B., **Meloni, G.**, & Degl'Innocenti, A. (2017). Can a robot grow? Plants give us the answer. In *Bioinspiration, Biomimetics, and Bioreplication* (Vol. 10162, p. 1016206). International Society for Optics and Photonics. [Conference proceeding]

Each article contributed to my scientific formation, giving me the possibility to collaborate with different groups from either the Italian Institute of Technology or the University of Pisa.

Thanks to the work on "A purely bioinformatic pipeline for the prediction of mammalian odorant receptor gene enhancers, *BMC Bioinformatics*" (Degl'Innocenti et al. 2019), I could learn more in depth the use of bioinformatic tools that might be implemented in the context of my future thesis outcomes.

Within the work done for "Chlorophyll derivatives enhance invertebrate red-light and ultraviolet phototaxis. *Scientific Reports*" (Degl'Innocenti et al. 2017), I had the possibility to use a different animal model performing behavioral tests, that even gave me new ideas on my future steps on research. I also have been trained for the histological analysis that I then utilized during my main thesis project.

Thanks to "Can a robot grow? Plants give us the answer. *Bioinspiration, Biomimetics, and Bioreplication*" (Mazzolai, Meloni, and Degl'Innocenti 2017), I could learn how actually the Italian Institute of Technology here in Pontedera operates, also learning about previous works on PLANTOID.

7.2 BMC Bioinformatics

A purely bioinformatic pipeline for the prediction of mammalian odorant receptor gene enhancers

Andrea Degl'Innocenti, Gabriella Meloni, Barbara Mazzolai, Gianni Ciofani

In most mammals, a vast array of genes coding for chemosensory receptors mediates olfaction. Odorant receptor (OR) genes generally constitute the largest multifamily (> 1100 intact members in the mouse). From the whole pool, each olfactory neuron expresses a single OR allele following poorly characterized mechanisms termed *OR gene choice*. OR genes are found in genomic aggregations known as *clusters*. Nearby enhancers (named *elements*) are crucial regulators of OR gene choice. Despite their importance, searching for new elements is burdensome. Other chemosensory receptor genes responsible for smell adhere to expression modalities resembling OR gene choice, and are arranged in genomic clusters — often with chromosomal linkage to OR genes. Still, no elements are known for them.

Here we present an inexpensive framework aimed at predicting elements. We redefine cluster identity by focusing on multiple receptor gene families at once, and exemplify thirty — not necessarily OR-exclusive — novel candidate enhancers.

The pipeline we introduce could guide future *in vivo* work aimed at discovering/validating new elements. In addition, our study provides an updated and comprehensive classification of all genomic *loci* responsible for the transduction of olfactory signals in mammals.

7.3 Scientific Reports

Chlorophyll derivatives enhance invertebrate red-light and ultraviolet phototaxis

Andrea Degl'Innocenti, Leonardo Rossi, Alessandra Salvetti, Attilio Marino, Gabriella Meloni, Barbara Mazzolai & Gianni Ciofani

Chlorophyll derivatives are known to enhance vision in vertebrates. They are thought to bind visual pigments (i.e., opsins apoproteins bound to retinal chromophores) directly within the retina. Consistent with previous findings in vertebrates, here we show that chlorin e6 — a chlorophyll derivative — enhances photophobicity in a flatworm (Dugesia japonica), specifically when exposed to UV radiation ($\lambda = 405$ nm) or red light ($\lambda = 660$ nm). This is the first report of chlorophyll derivatives acting as modulators of invertebrate phototaxis, and in general the first account demonstrating that they can artificially alter animal response to light at a behavioral level. Our findings show that the interaction between chlorophyll derivatives and opsins virtually concerns the vast majority of bilaterian animals, and also occurs in visual systems based on rhabdomeric (rather than ciliary) opsins.

7.4 SPIE proceedings

Can a robot grow? Plants give us the answer

Barbara Mazzolai, Gabriella Meloni, Andrea Degl'Innocenti

Plants have a sessile lifestyle, and, as a consequence of this primordial decision, they must efficiently use the resources available in their surroundings and exhibit a well-

organized sensing system that allows them to explore the environment and react rapidly to potentially dangerous circumstances. Below ground, roots can sense a multitude of abiotic and biotic signals, enabling the appropriate responses while they grow searching nutrients and water to feed the whole plant body. Plant roots show efficient exploration capabilities, adapting themselves morphologically to the environment to explore. Interestingly, movement, evolved sensing systems and distributed control are among the most important topics of contemporary robotics. Plants, which we have recently considered as a new model in bioinspired and soft robotics, must address "problems" that are common also in animals, such as, for example, squid, cuttlefish, and, especially, octopus, which include distributed control to manage the infinite DOF of their body, high flexibility, the capability of growing and/or elongating their extremities, and distributed sensing capabilities. Starting from the study and imitation of these plant features, we developed innovative inspired robots and technologies, named PLANTOIDS, which move by growing, coordinating their artificial roots and showing efficient penetration strategies and high actuation forces. Applications for such technologies include soil monitoring and exploration for contamination or mineral deposits, as well as medical and surgical applications, like new flexible endoscopes, able to steer and grow in delicate human organs.

Literature

1. Albertin, Caroline B., Oleg Simakov, Therese Mitros, Z. Yan Wang, Judit R. Pungor, Eric Edsinger-Gonzales, Sydney Brenner, Clifton W. Ragsdale, and Daniel S. Rokhsar. 2015. “The Octopus Genome and the Evolution of Cephalopod Neural and Morphological Novelties.” *Nature* 524(7564):220.
2. Andrews, Hayley G. and Jas Pal S. Badyal. 2014. “Bioinspired Hook Surfaces Based upon a Ubiquitous Weed (Galium Aparine) for Dry Adhesion.” *Journal of Adhesion Science and Technology* 28(13):1243–55.
3. Baik, Sangyul, Da Wan Kim, Youngjin Park, Tae Jin Lee, Suk Ho Bhang, and Changhyun Pang. 2017. “A Wet-Tolerant Adhesive Patch Inspired by Protuberances in Suction Cups of Octopi.” *Nature* 546(7658):396–400.
4. Baik, Sangyul, Jiwon Kim, Heon Joon Lee, Tae Hoon Lee, and Changhyun Pang. 2018. “Highly Adaptable and Biocompatible Octopus-Like Adhesive Patches with Meniscus-Controlled Unfoldable 3D Microtips for Underwater Surface and Hairy Skin.” *Advanced Science* 5(8).
5. Baldascino, Elena, Giulia Di Cristina, Perla Tedesco, Carl Hobbs, Tanya J. Shaw, Giovanna Ponte, and Paul L. R. Andrews. 2017. “The Gastric Ganglion of Octopus Vulgaris: Preliminary Characterization of Gene-and Putative Neurochemical-Complexity, and the Effect of Aggregata Octopiana Digestive Tract Infection on Gene Expression.” *Frontiers in Physiology* 8:1001.
6. Bhattacharya, Shantanu, Arindom Datta, Jordan M. Berg, and Shubhra Gangopadhyay. 2005. “Studies on Surface Wettability of Poly (Dimethyl) Siloxane (PDMS) and Glass under Oxygen-Plasma Treatment and Correlation

with Bond Strength." *Journal of Microelectromechanical Systems* 14(3):590–97.

7. Bhushan, Bharat. 2009. "Biomimetics: Lessons from Nature–an Overview."
8. Boßelmann, F., P. Romano, H. Fabritius, D. Raabe, and M. Epple. 2007. "The Composition of the Exoskeleton of Two Crustacea: The American Lobster Homarus Americanus and the Edible Crab Cancer Pagurus." *Thermochimica Acta* 463(1–2):65–68.
9. Budelmann, B. U. 1995. "The Cephalopod Nervous System: What Evolution Has Made of the Molluscan Design." Pp. 115–38 in *The nervous systems of invertebrates: An evolutionary and comparative approach*. Springer.
10. Casini, A., R. Vaccaro, L. D'Este, Y. Sakaue, J. P. Bellier, H. Kimura, and T. G. Renda. 2012. "Immunolocalization of Choline Acetyltransferase of Common Type in the Central Brain Mass of Octopus Vulgaris." *European Journal of Histochemistry: EJH* 56(3).
11. Chapman, Garth. 1958. "The Hydrostatic Skeleton in the Invertebrates." *Biological Reviews* 33(3):338–71.
12. Chen, Ying Chu and Hongta Yang. 2017. "Octopus-Inspired Assembly of Nanosucker Arrays for Dry/Wet Adhesion." *ACS Nano* 11(6):5332–38.
13. Chu, Baeksuk, Kyungmo Jung, Chang-Soo Han, and Daehie Hong. 2010. "A Survey of Climbing Robots: Locomotion and Adhesion." *International Journal of Precision Engineering and Manufacturing* 11(4):633–47.
14. Chun, Sungwoo, Wonkyeong Son, Da Wan Kim, Jihyun Lee, Hyeongho Min, Hachul Jung, Dahye Kwon, A. Hee Kim, Young Jin Kim, Sang Kyoo Lim, Changhyun Pang, and Changsoon Choi. 2019. "Water-Resistant and Skin-Adhesive Wearable Electronics Using Graphene Fabric Sensor with Octopus-

Inspired Microsuckers." *ACS Applied Materials and Interfaces* 11(18):16951–57.

15. Cianchetti, Matteo, Maurizio Follador, Barbara Mazzolai, Paolo Dario, and Cecilia Laschi. 2012. "Design and Development of a Soft Robotic Octopus Arm Exploiting Embodied Intelligence." Pp. 5271–76 in *2012 IEEE International Conference on Robotics and Automation*. IEEE.
16. Cianchetti, Matteo, Tommaso Ranzani, Giada Gerboni, Iris De Falco, Cecilia Laschi, and Arianna Menciassi. 2013. "STIFF-FLOP Surgical Manipulator: Mechanical Design and Experimental Characterization of the Single Module." Pp. 3576–81 in *2013 IEEE/RSJ International Conference on Intelligent Robots and Systems*. IEEE.
17. Cianchetti, Matteo, Tommaso Ranzani, Giada Gerboni, Thrishantha Nanayakkara, Kaspar Althoefer, Prokar Dasgupta, and Arianna Menciassi. 2014. "Soft Robotics Technologies to Address Shortcomings in Today's Minimally Invasive Surgery: The STIFF-FLOP Approach." *Soft Robotics* 1(2):122–31.
18. Di Cristo, Carlo, Marina Paolucci, Josè Iglesias, Javier Sanchez, and Anna Di Cosmo. 2002. "Presence of Two Neuropeptides in the Fusiform Ganglion and Reproductive Ducts of Octopus Vulgaris: FMRFamide and Gonadotropin-releasing Hormone (GnRH)." *Journal of Experimental Zoology* 292(3):267–76.
19. Degl'Innocenti, A., L. Rossi, A. Salvetti, A. Marino, G. Meloni, B. Mazzolai, and G. Ciofani. 2017. "Chlorophyll Derivatives Enhance Invertebrate Red-Light and Ultraviolet Phototaxis." *Scientific Reports* 7(1).
20. Degl'Innocenti, Andrea, Gabriella Meloni, Barbara Mazzolai, and Gianni Ciofani. 2019. "A Purely Bioinformatic Pipeline for the Prediction of Mammalian Odorant Receptor Gene Enhancers." *BMC Bioinformatics* 20(1):474.

21. Dejeu, Jérôme, Michaël Gauthier, Patrick Rougeot, and Wilfrid Boireau. 2009. "Adhesion Forces Controlled by Chemical Self-Assembly and Ph: Application to Robotic Microhandling." *ACS Applied Materials & Interfaces* 1(9):1966–73.
22. Denton, Eric James and M. F. Land. 1971. "Mechanism of Reflexion in Silvery Layers of Fish and Cephalopods." *Proceedings of the Royal Society of London. Series B. Biological Sciences* 178(1050):43–61.
23. Emery, Dennis G. 1975. "THE HISTOLOGY AND ULTRASTRUCTURE OF SOME CILIATED SENSORY NEURONS OF CEPHALOPOD MOLLUSKS."
24. Fiorello, Isabella, Omar Tricinci, and Anand Kumar Mishra. 2012. *Biomimetic and Biohybrid Systems*. Vol. 7375. Springer International Publishing.
25. Follador, M., F. Tramacere, and B. Mazzolai. 2014. "Dielectric Elastomer Actuators for Octopus Inspired Suction Cups." *Bioinspiration and Biomimetics* 9(4).
26. Follador, Maurizio, Francesca Tramacere, Lucie Viry, Matteo Cianchetti, Lucia Beccai, Cecila Laschi, and Barbara Mazzolai. 2013. "Octopus-Inspired Innovative Suction Cups BT - Biomimetic and Biohybrid Systems." 368–70.
27. Fossati, Sara Maria, Simona Candiani, Marie-Therese Nödl, Luca Maragliano, Maria Pennuto, Pedro Domingues, Fabio Benfenati, Mario Pestarino, and Letizia Zullo. 2015. "Identification and Expression of Acetylcholinesterase in Octopus Vulgaris Arm Development and Regeneration: A Conserved Role for ACHE?" *Molecular Neurobiology* 52(1):45–56.
28. Fraś, J., Jan Czarnowski, M. Maciaś, J. Główka, Matteo Cianchetti, and Arianna Menciassi. 2015. "New STIFF-FLOP Module Construction Idea for Improved Actuation and Sensing." Pp. 2901–6 in *2015 IEEE International Conference on*

Robotics and Automation (ICRA). IEEE.

29. Fukuda, Toshio, Fei Chen, and Qing Shi. 2018. *Bio-Inspired Robotics*. MDPI - Multidisciplinary Digital Publishing Institute.
30. Gauthier, Michael and Stéphane Régnier. 2011. *Robotic Microassembly*. John Wiley & Sons.
31. Girod, Paul. 1884. "Recherches Sur La Peau Des Céphalopodes. La Ventouse." *Arch. Zool. Exp. Gén* 2:379–401.
32. Gorb, Stanislav N. 2008. "Biological Attachment Devices: Exploring Nature's Diversity for Biomimetics." *Philosophical Transactions of the Royal Society A: Mathematical, Physical and Engineering Sciences* 366(1870):1557–74.
33. Grasso, Frank W., Thomas R. Consi, David C. Mountain, and Jelle Atema. 2000. "Biomimetic Robot Lobster Performs Chemo-Orientation in Turbulence Using a Pair of Spatially Separated Sensors: Progress and Challenges." *Robotics and Autonomous Systems* 30(1–2):115–31.
34. Graziadei, P. 1964. "Electron Microscopy of Some Primary Receptors in the Sucker OfOctopus Vulgaris." *Zeitschrift Für Zellforschung Und Mikroskopische Anatomie* 64(4):510–22.
35. Graziadei, P. 1965. "Muscle Receptors in Cephalopods." *Proceedings of the Royal Society of London. Series B. Biological Sciences* 161(984):392–402.
36. Graziadei, P. 1971. "The Nervous System of the Arms." *The Anatomy of the Nervous System of Octopus Vulgaris. Young JZ Pp44-61, Clarendon Press, Oxford*.
37. Graziadei, P. P. C. and H. T. Gagne. 1976. "Sensory Innervation in the Rim of the Octopus Sucker." *Journal of Morphology* 150(3):639–79.

38. Grieco, Juan Carlos, Manuel Prieto, Manuel Armada, and P. Gonzalez De Santos. 1998. “A Six-Legged Climbing Robot for High Payloads.” Pp. 446–50 in *Proceedings of the 1998 IEEE International Conference on Control Applications (Cat. No. 98CH36104)*. Vol. 1. IEEE.

39. Gutfreund, Yoram, Tamar Flash, Graziano Fiorito, and Binyamin Hochner. 1998. “Patterns of Arm Muscle Activation Involved in Octopus Reaching Movements.” *Journal of Neuroscience* 18(15):5976–87.

40. Gutfreund, Yoram, Tamar Flash, Yosef Yarom, Graziano Fiorito, Idan Segev, and Binyamin Hochner. 1996. “Organization of Octopus Arm Movements: A Model System for Studying the Control of Flexible Arms.” *Journal of Neuroscience* 16(22):7297–7307.

41. Gutfreund, Yoram, Henry Matzner, Tamar Flash, and Binyamin Hochner. 2006. “Patterns of Motor Activity in the Isolated Nerve Cord of the Octopus Arm.” *The Biological Bulletin* 211(3):212–22.

42. Hadley, Neil F. 1986. “The Arthropod Cuticle.” *Scientific American* 255(1):104–13.

43. Hennebert, Elise, Barbara Maldonado, Peter Ladurner, Patrick Flammang, and Romana Santos. 2015. “Experimental Strategies for the Identification and Characterization of Adhesive Proteins in Animals: A Review.” *Interface Focus* 5(1):20140064.

44. Holten-Andersen, Niels, Matthew J. Harrington, Henrik Birkedal, Bruce P. Lee, Phillip B. Messersmith, Ka Yee C. Lee, and J. Herbert Waite. 2011. “PH-Induced Metal-Ligand Cross-Links Inspired by Mussel Yield Self-Healing Polymer Networks with near-Covalent Elastic Moduli.” *Proceedings of the National*

Academy of Sciences 108(7):2651–55.

45. Hwang, Dong Soo, Youngsoo Gim, and Hyung Joon Cha. 2008. "Expression of Functional Recombinant Mussel Adhesive Protein Type 3A in Escherichia Coli." *Biotechnology Progress* 21(3):965–70.
46. Ijspeert, Auke Jan. 2008. "Central Pattern Generators for Locomotion Control in Animals and Robots: A Review." *Neural Networks* 21(4):642–53.
47. Ijspeert, Auke Jan, Alessandro Crespi, and Jean-Marie Cabelguen. 2005. "Simulation and Robotics Studies of Salamander Locomotion." *Neuroinformatics* 3(3):171–95.
48. Ijspeert, Auke Jan, Alessandro Crespi, Dimitri Ryczko, and Jean-Marie Cabelguen. 2007. "From Swimming to Walking with a Salamander Robot Driven by a Spinal Cord Model." *Science* 315(5817):1416–20.
49. Immega, Guy and Keith Antonelli. 1995. "The KSI Tentacle Manipulator." Pp. 3149–54 in *Proceedings of 1995 IEEE International Conference on Robotics and Automation*. Vol. 3. IEEE.
50. Imperadore, Pamela, Sameer B. Shah, Helen P. Makarenkova, and Graziano Fiorito. 2017. "Nerve Degeneration and Regeneration in the Cephalopod Mollusc Octopus Vulgaris: The Case of the Pallial Nerve." *Scientific Reports* 7:46564.
51. Iwakoshi-Ukena, Eiko, Kazuyoshi Ukena, Kyoko Takuwa-Kuroda, Atshuhiro Kanda, Kazuyoshi Tsutsui, and Hiroyuki Minakata. 2004. "Expression and Distribution of Octopus Gonadotropin-releasing Hormone in the Central Nervous System and Peripheral Organs of the Octopus (Octopus Vulgaris) by in Situ Hybridization and Immunohistochemistry." *Journal of Comparative Neurology* 477(3):310–23.

52. Kanda, Atsuhiro, Honoo Satake, Tsuyoshi Kawada, and Hiroyuki Minakata. 2005. “Novel Evolutionary Lineages of the Invertebrate Oxytocin/Vasopressin Superfamily Peptides and Their Receptors in the Common Octopus (Octopus Vulgaris).” *Biochemical Journal* 387(1):85–91.
53. Kanda, Atsuhiro, Toshio Takahashi, Honoo Satake, and Hiroyuki Minakata. 2006. “Molecular and Functional Characterization of a Novel Gonadotropin-Releasing-Hormone Receptor Isolated from the Common Octopus (Octopus Vulgaris).” *Biochemical Journal* 395(1):125–35.
54. Keay, June, Jamie T. Bridgham, and Joseph W. Thornton. 2006. “The Octopus Vulgaris Estrogen Receptor Is a Constitutive Transcriptional Activator: Evolutionary and Functional Implications.” *Endocrinology* 147(8):3861–69.
55. Khorasani, M. T., HAMID Mirzadeh, and P. G. Sammes. 1999. “Laser Surface Modification of Polymers to Improve Biocompatibility: HEMA Grafted PDMS, in Vitro Assay—III.” *Radiation Physics and Chemistry* 55(5–6):685–89.
56. Kier, William M. 1992. “Hydrostatic Skeletons and Muscular Hydrostats.” *Nautilus* 8(11).
57. Kier, WILLIAM M. 1988. “The Arrangement and Function of Molluscan Muscle.” *The Mollusca, Form and Function* 11(21):211–52.
58. Kier, William M. and Andrew M. Smith. 1990. “The Morphology and Mechanics of Octopus Suckers.” *The Biological Bulletin* 178(2):126–36.
59. Kier, William M. and Andrew M. Smith. 2002. “The Structure and Adhesive Mechanism of Octopus Suckers.” *Integrative and Comparative Biology* 42(6):1146–53.
60. Kier, William M. and Kathleen K. Smith. 1985. “Tongues, Tentacles and Trunks:

The Biomechanics of Movement in Muscular-Hydrostats." *Zoological Journal of the Linnean Society* 83(4):307–24.

61. Kier, William M. and Michael P. Stella. 2007. "The Arrangement and Function of Octopus Arm Musculature and Connective Tissue." *Journal of Morphology* 268(10):831–43.
62. Kim, Joong Hyun, HyeungWoo Park, and Soo Won Seo. 2017. "In Situ Synthesis of Silver Nanoparticles on the Surface of PDMS with High Antibacterial Activity and Biosafety toward an Implantable Medical Device." *Nano Convergence* 4(1):33.
63. Kim, Sangbae, Cecilia Laschi, and Barry Trimmer. 2013. "Soft Robotics: A Bioinspired Evolution in Robotics." *Trends in Biotechnology* 31(5):287–94.
64. Kim, Sangsik, Hee Young Yoo, Jun Huang, Yongjin Lee, Sohee Park, Yeonju Park, Sila Jin, Young Mee Jung, Hongbo Zeng, Dong Soo Hwang, and Yongseok Jho. 2017. "Salt Triggers the Simple Coacervation of an Underwater Adhesive When Cations Meet Aromatic π Electrons in Seawater." *ACS Nano* 11(7):6764–72.
65. Kim, Sung Hwan, Jin-Hee Moon, Jeong Hun Kim, Sung Min Jeong, and Sang-Hoon Lee. 2011. "Flexible, Stretchable and Implantable PDMS Encapsulated Cable for Implantable Medical Device." *Biomedical Engineering Letters* 1(3):199.
66. Kingston, Alexandra C. N. and Thomas W. Cronin. 2016. "Diverse Distributions of Extraocular Opsins in Crustaceans, Cephalopods, and Fish."
67. Kong, Tiantian, Guanyi Luo, Yuanjin Zhao, and Zhou Liu. 2019. "Bioinspired Superwettability Micro/Nanoarchitectures: Fabrications and Applications."

Advanced Functional Materials 29(11):1–32.

68. Laschi, Cecilia, Matteo Cianchetti, Barbara Mazzolai, Laura Margheri, Maurizio Follador, and Paolo Dario. 2012. "Soft Robot Arm Inspired by the Octopus." *Advanced Robotics* 26(7):709–27.
69. Lee, H., N. F. Scherer, and P. B. Messersmith. 2006. "Single-Molecule Mechanics of Mussel Adhesion." *Proceedings of the National Academy of Sciences* 103(35):12999–3.
70. Lee, Haeshin, Bruce P. Lee, and Phillip B. Messersmith. 2007. "A Reversible Wet/Dry Adhesive Inspired by Mussels and Geckos." *Nature* 448(7151):338–41.
71. Lin, Q., D. Gourdon, C. Sun, N. Holten-Andersen, T. H. Anderson, J. H. Waite, and J. N. Israelachvili. 2007. "Adhesion Mechanisms of the Mussel Foot Proteins Mfp-1 and Mfp-3." *Proceedings of the National Academy of Sciences* 104(10):3782–86.
72. Liu, Hui, Li-Hsin Chang, Younguk Sun, Xiaochen Lu, and Lisa Stubbs. 2014. "Deep Vertebrate Roots for Mammalian Zinc Finger Transcription Factor Subfamilies." *Genome Biology and Evolution* 6(3):510–25.
73. Mahdavi, Alborz, Lino Ferreira, Cathryn Sundback, Jason W. Nichol, Edwin P. Chan, David J. D. Carter, Chris J. Bettinger, Siamrut Patanavanich, Loice Chignozha, and Eli Ben-Joseph. 2008. "A Biodegradable and Biocompatible Gecko-Inspired Tissue Adhesive." *Proceedings of the National Academy of Sciences* 105(7):2307–12.
74. Martinez, Ramses V, Jamie L. Branch, Carina R. Fish, Lihua Jin, Robert F. Shepherd, Rui M. D. Nunes, Zhigang Suo, and George M. Whitesides. 2013. "Robotic Tentacles with Three-dimensional Mobility Based on Flexible

Elastomers." *Advanced Materials* 25(2):205–12.

75. Mazzolai, B., G. Meloni, and A. Degl'Innocenti. 2017. "Can a Robot Grow Plants Give Us the Answer." in *Proceedings of SPIE - The International Society for Optical Engineering*. Vol. 10162.
76. McMahan, William, Bryan A. Jones, and Ian D. Walker. 2005. "Design and Implementation of a Multi-Section Continuum Robot: Air-Octor." Pp. 2578–85 in *2005 IEEE/RSJ International Conference on Intelligent Robots and Systems*. IEEE.
77. Menon, Carlo, Michael Murphy, and Metin Sitti. 2004. "Gecko Inspired Surface Climbing Robots." Pp. 431–36 in *2004 IEEE International Conference on Robotics and Biomimetics*. IEEE.
78. Mirow, Susan. 1972. "Skin Color in the Squids Loligo Pealii and Loligo Opalescens." *Zeitschrift Für Zellforschung Und Mikroskopische Anatomie* 125(2):143–75.
79. Mishra, Anand Kumar, Emanuela Del Dottore, Ali Sadeghi, Alessio Mondini, and Barbara Mazzolai. 2017. "SIMBA: Tendon-Driven Modular Continuum Arm with Soft Reconfigurable Gripper." *Frontiers in Robotics and AI* 4:4.
80. Montell, Craig. 2005. "TRP Channels in Drosophila Photoreceptor Cells." *The Journal of Physiology* 567(1):45–51.
81. Murphy, Michael P., Burak Aksak, and Metin Sitti. 2009. "Gecko-inspired Directional and Controllable Adhesion." *Small* 5(2):170–75.
82. Nixon, Marion and P. N. Dilly. 1977. "Sucker Surfaces and Prey Capture." Pp. 447–511 in *Symp. Zool. Soc. Lond*. Vol. 38.
83. Packard, Andrew and Geoffrey D. Sanders. 1971. "Body Patterns of Octopus

Vulgaris and Maturation of the Response to Disturbance." *Animal Behaviour* 19(4):780–90.

84. Packard, Andrew, E. R. Trueman, and M. R. Clarke. 1988. "The Skin of Cephalopods (Coleoids): General and Special Adaptations." *The Mollusca* 11:37–67.
85. Ponte, Giovanna and Graziano Fiorito. 2015. "Immunohistochemical Analysis of Neuronal Networks in the Nervous System of Octopus Vulgaris." Pp. 63–79 in *Immunocytochemistry and Related Techniques*. Springer.
86. Potts, W. T. W. 1967. "Excretion in the Molluscs." *Biological Reviews* 42(1):1–41.
87. Ramirez, M. Desmond and Todd H. Oakley. 2015. "Eye-Independent, Light-Activated Chromatophore Expansion (LACE) and Expression of Phototransduction Genes in the Skin of Octopus Bimaculoides." *Journal of Experimental Biology* 218(10):1513–20.
88. Ravindran, Sandeep. 2012. "Barbara McClintock and the Discovery of Jumping Genes." *Proceedings of the National Academy of Sciences* 109(50):20198–99.
89. Rowell, C. H. FRASER. 1963. "Excitatory and Inhibitory Pathways in the Arm of Octopus." *Journal of Experimental Biology* 40(2):257–70.
90. Sakaue, Yuko, Jean-Pierre Bellier, Shin Kimura, Loredana D'Este, Yoshihiro Takeuchi, and Hiroshi Kimura. 2014. "Immunohistochemical Localization of Two Types of Choline Acetyltransferase in Neurons and Sensory Cells of the Octopus Arm." *Brain Structure and Function* 219(1):323–41.
91. Sareh, Sina, Kaspar Althoefer, Min Li, Yohan Noh, Francesca Tramacere, Pooya Sareh, Barbara Mazzolai, and Mirko Kovac. 2017. "Anchoring like Octopus:

Sensory-Physical Soft Artificial Sucker." *Journal of the Royal Society Interface* 14.

92. Smith, Andrew M. 1991. "Negative Pressure Generated by Octopus Suckers: A Study of the Tensile Strength of Water in Nature." *Journal of Experimental Biology* 157(1):257–71.
93. Sumbre, German, Yoram Gutfreund, Graziano Fiorito, Tamar Flash, and Binyamin Hochner. 2001. "Control of Octopus Arm Extension by a Peripheral Motor Program." *Science* 293(5536):1845–48.
94. Suzuki, Hirohumi, Tomofusa Muraoka, and Toshiharu Yamamoto. 2003. "Localization of Corticotropin-Releasing Factor-Immunoreactive Nervous Tissue and Colocalization with Neuropeptide Y-like Substance in the Optic Lobe and Peduncle Complex of the Octopus (Octopus Vulgaris)." *Cell and Tissue Research* 313(1):129–38.
95. Tomokazu, T., S. Kikuchi, M. Suzuki, and S. Aoyagi. 2015. "Vacuum Gripper Imitated Octopus Sucker-Effect of Liquid Membrane for Absorption." *IEEE International Conference on Intelligent Robots and Systems* 2015-Decem:2929–36.
96. Tramacere, F., M. Follador, N. M. Pugno, and B. Mazzolai. 2015. "Octopus-like Suction Cups: From Natural to Artificial Solutions." *Bioinspiration and Biomimetics* 10(3):1–8.
97. Tramacere, Francesca, Lucia Beccai, Michael Kuba, Alessandro Gozzi, Angelo Bifone, and Barbara Mazzolai. 2013. "The Morphology and Adhesion Mechanism of Octopus Vulgaris Suckers." *PLoS One* 8(6):e65074.
98. Tramacere, Francesca, Lucia Beccai, Michael J. Kuba, and Barbara Mazzolai.

2013. “Octopus Suckers Identification Code (OSIC).” *Marine and Freshwater Behaviour and Physiology* 46(6):447–53.

99. Tramacere, Francesca, Lucia Beccai, Fabio Mattioli, Edoardo Sinibaldi, and Barbara Mazzolai. 2012. “Artificial Adhesion Mechanisms Inspired by Octopus Suckers.” Pp. 3846–51 in *2012 IEEE International Conference on Robotics and Automation*. IEEE.

100. Trivedi, Deepak, Christopher D. Rahn, William M. Kier, and Ian D. Walker. 2008. “Soft Robotics: Biological Inspiration, State of the Art, and Future Research.” *Applied Bionics and Biomechanics* 5(3):99–117.

101. Trujillo-de Santiago, Grissel, Roholah Sharifi, Kan Yue, Ehsan Shrizaei Sani, Sara Saheb Kashaf, Mario Moisés Alvarez, Jeroen Leijten, Ali Khademhosseini, Reza Dana, and Nasim Annabi. 2019. “Ocular Adhesives: Design, Chemistry, Crosslinking Mechanisms, and Applications.” *Biomaterials* 197(December 2018):345–67.

102. Tsagarakis, Nikolaos G., Giorgio Metta, Giulio Sandini, David Vernon, Ricardo Beira, Francesco Becchi, Ludovic Righetti, Jose Santos-Victor, Auke Jan Ijspeert, and Maria Chiara Carrozza. 2007. “ICub: The Design and Realization of an Open Humanoid Platform for Cognitive and Neuroscience Research.” *Advanced Robotics* 21(10):1151–75.

103. Umedachi, T., V. Vikas, and B. A. Trimmer. 2016. “Softworms: The Design and Control of Non-Pneumatic, 3D-Printed, Deformable Robots.” *Bioinspiration & Biomimetics* 11(2):25001.

104. Villaseñor, Carlos, Jorge Rios, Nancy Arana-Daniel, Alma Alanis, Carlos Lopez-Franco, and Esteban Hernandez-Vargas. 2018. “Germinal Center

Optimization Applied to Neural Inverse Optimal Control for an All-Terrain Tracked Robot." *Applied Sciences* 8(1):31.

105. Waite, J. Herbert and Xiaoxia Qin. 2001. "Polyphosphoprotein from the Adhesive Pads of Mytilus Edulis." *Biochemistry* 40(9):2887–93.

106. Wang, Jin-hai and Xiao-dong Zheng. 2017. "Comparison of the Genetic Relationship between Nine Cephalopod Species Based on Cluster Analysis of Karyotype Evolutionary Distance." *Comparative Cytogenetics* 11(3):477.

107. Wells, Martin John. 2013. *Octopus: Physiology and Behaviour of an Advanced Invertebrate*. Springer Science & Business Media.

108. Woodhams, P. L. and J. B. Messenger. 1974. "A Note on the Ultrastructure of the Octopus Olfactory Organ." *Cell and Tissue Research* 152(2):253–58.

109. Young, John Zachary. 1971. "Anatomy of the Nervous System of Octopus Vulgaris."

110. Zesch, Wolfgang, Markus Brunner, and Ariel Weber. 1997. "Vacuum Tool for Handling Microobjects with a Nanorobot." Pp. 1761–66 in *Proceedings of International Conference on Robotics and Automation*. Vol. 2. IEEE.

111. Zhu, Yaguang, Long Chen, Qiong Liu, Rui Qin, and Bo Jin. 2018. "Omnidirectional Jump of a Legged Robot Based on the Behavior Mechanism of a Jumping Spider." *Applied Sciences* 8(1):51.